Reviewed Preprint
v1 • October 6, 2025
Not revised

Reviewed Preprint
v2 • December 15, 2025
Revised by authors

For correspondence:
sstowers@montana.edu

Competing interests: No competing interests declared

Funding: See page 64

Reviewing editor: Jimena Berni, University of Sussex, United Kingdom

Two classes of amine/glutamate multi-transmitter neurons innervate Drosophila internal male reproductive organs

Martha Chaverra[1], John Paul Toney[1], Lizetta D Dardenne-Ankringa[1], Jace Tolleson Knee[1], Ann R Morris[1], Joseph B Wadhams[1], Sarah J Certel[2], R Steven Stowers[1]

[1]Montana State University, Department of Microbiology and Cell Biology, Bozeman, United States • [2]The University of Montana, Division of Biological Sciences, Missoula, United States

eLife Assessment

This **important** study characterizes with rigorous methodology anatomical and functional aspects of the peripheral innervation of the Drosophila male reproductive tract. The **convincing** analysis reveals two distinct types of glutamatergic neurons that co-release either serotonin or octopamine. While serotonergic neurons are required for male fertility, octopaminergic neurons are dispensable. The work is providing invaluable insight into neurochemical control of insemination, peripheral motor control and neuromodulation in the male reproductive tract.

https://doi.org/10.7554/eLife.108225.2.sa4

Abstract

The essential outcome of a successful mating is the transfer of genetic material from males to females in sexually reproducing animals from insects to mammals. In males, this culminates in ejaculation, a precisely timed sequence of organ contractions driven by the concerted activity of interneurons, sensory neurons, and motor neurons. Although central command circuits that trigger copulation have been mapped, the motor architecture and the chemical logic that couple specific neuronal subclasses to organ specific contractility, seminal fluid secretion, and sperm emission remain largely uncharted. This gap in knowledge limits our ability to explain how neural circuits adapt to varying contexts and how their failure contributes to infertility. Here we present an in-depth anatomical and functional analysis of the motor neurons that innervate the internal male reproductive tract of Drosophila melanogaster. We identify two classes of multi-transmitter motor neurons based on neurotransmitter usage, namely octopamine and glutamate neurons (OGNs) and serotonin and glutamate neurons (SGNs), each with a biased pattern of innervation: SGNs predominate in the accessory glands, OGNs in the ejaculatory duct, with equal contributions of each to the seminal vesicles. Both classes co-express vesicular transporters for glutamate (vGlut) and amines (vMAT), confirming their dual chemical identity. Their target organs differentially express receptors for glutamate, octopamine, and serotonin, suggesting combinatorial neuromodulation of contractility. Functional manipulations show that SGNs are essential for male fertility but OGNs are dispensable. Glutamatergic transmission from both classes is also dispensable for fertility. These findings provide the first high-resolution map linking multi-transmitter motor neurons to specific reproductive organs, reveal an unexpected division of labor between serotonergic and octopaminergic signaling pathways, and establish a framework for dissecting conserved neural principles that govern ejaculation and male fertility.

Introduction

Reproduction is a biological imperative of all species. For most sexually reproducing animal species, this involves locating a mate, courtship, and most essentially, the transfer of genetic material via copulation. The endpoint of copulation, ejaculation, consists of two coordinated phases, emission and expulsion (Alwaal et al. 2015; Soni et al. 2022). During the emission phase, sperm and seminal fluid are relocated from their site of origin to a central canal for transfer to the female during the subsequent expulsion phase. The series of events that culminate in ejaculation are regulated by a spinal ejaculation generator located in the lumbar L3-L4 region of the spinal cord of mammals that executes a motor program coordinating a series of muscle contractions and relaxations of the internal and external male genitalia (Truitt and Coolen 2002; Carro-Juarez et al. 2003; Chehensse et al. 2017).

While male external genitalia exhibit remarkable evolutionary variation (Eberhard 1985), internal male reproductive organs exhibit remarkable evolutionary conservation over the last 600 million years since the last common ancestor of insects and mammals (Guerrero et al. 2004; Gomes et al. 2012; Beguelini et al. 2013; Tomas et al. 2019; Fromme et al. 2021; Oliveira et al. 2021; Yartsev and Evseeva 2021; Maciel et al. 2024). These evolutionarily conserved structures of the male reproductive system include paired testes, seminal vesicles (SVs), and semen producing organs (prostate glands in humans, accessory glands (AGs) in insects), as well as a singular duct (urethra in humans, ejaculatory duct (ED) in insects) through which sperm and seminal fluid flow during mating.

Drosophila melanogaster has been instrumental in revealing fundamental principles of male reproductive behavior and physiology that extend beyond insects, including how neural circuits control mating drive, courtship, and the mechanics and duration of copulation (Acebes et al. 2004; Billeter et al. 2006a; Villella and Hall 2008; Tayler et al. 2012; Crickmore and Vosshall 2013; Pavlou et al. 2016; Jois et al. 2018; Baker et al. 2024). Among the findings of these studies is the existence of neural circuitry in the ventral nerve cord that regulates ejaculation similar to the spinal ejaculation generator circuitry of mammals, suggesting an ancient evolutionary origin. How the motor neurons directly innervating the internal male reproductive organs control the events leading to ejaculation is less well understood. It is also known in Drosophila and other species, including humans, that male ejaculate quality is plastic and can be adapted to environmental conditions, especially the level of male-male competition (Gage and Baker 1991; Wedell and Cook 1999; Pizzari et al. 2003; Pound and Gage 2004; Bretman et al. 2009; Garbaczewska et al. 2013; Hopkins et al. 2019; Delecce et al. 2025), but the neural mechanisms underlying these adaptations remain to be identified.

Previous studies have determined there are at least three types of motor neurons innervating the Drosophila internal male reproductive system distinguished by neurotransmitter usage including serotonergic (Lee and Hall 2001), octopaminergic (Pauls et al. 2018), and glutamatergic (Pavlou et al. 2016) motor neurons, although there may be at least some overlap in neurotransmitter usage as serotonin/glutamate multi-transmitter motor neurons have been reported in the seminal vesicle (Castellanos et al. 2013). How these neurons coordinate the motor program to elicit ejaculation is an open question, as is their anatomical organization relative to each other. Clarifying the targets and anatomy of these motor neuron classes will uncover critical principles for how neuronal coordination of internal male reproductive organ function contributes to male fertility. To address these questions, we performed a comprehensive analysis of the neurons innervating each internal organ, defined their neurotransmitter complements and receptor profiles, and tested their necessity for successful sperm transfer and fecundity.

Results

Drosophila male reproductive system anatomy

The Drosophila male reproductive system consists of paired testes, SVs, and AGs, as well as a singular ED and ejaculatory bulb (Figure 1) (Demerec 1950). The testes are surrounded by smooth muscle with no neuronal innervation, while the SVs, AGs, and ED are ensheathed by neuronally innervated skeletal muscles (Lee and Hall 2001; Billeter *et al*. 2006b; Susic-Jung *et al*. 2012). The ejaculatory bulb also possesses neuronally innervated skeletal muscle for pumping sperm out of the ED to the female. The SVs fuse just prior to termination in the ED where they form a narrow sphincter that opens during mating to allow sperm to flow. The AGs, insect equivalent of mammalian prostate glands, produce the bulk of seminal fluid (Wolfner 1997; Majane et al. 2022) and remain separate before terminating in the ED (Bairati 1968). Underlying the muscles of the internal male reproductive system organs are a layer of secretory epithelial cells (Bairati 1968) that are the cellular source of the seminal fluid components (Sepil et al. 2019; Wigby et al. 2020).

Neurotransmitter identity of neurons innervating internal male reproductive organs

To confirm previous reports of innervation of the Drosophila male reproductive system by octopaminergic, serotonergic, and glutamatergic neurons, GAL4 drivers for the octopamine (OA) neurotransmitter synthesis enzyme tyrosine decarboxylase 2 (Tdc2), the serotonin (5-Hydroxytryptamine, 5-HT) neurotransmitter synthesis enzyme tryptophan hydroxylase (TRH) and the vesicular glutamate transporter (vGlut) were used to drive expression of a *UAS-CD8-mCherry* plasma membrane reporter. As expected, all three drivers exhibited expression in neurons of the male reproductive system, but with distinguishable differences in expression patterns. *Tdc2-GAL4* exhibited dense innervation of the SV and ED with sparse innervation of the AG (Figure 2, A). *TRH-GAL4* exhibited dense innervation of the SV and AGs, with modest innervation of the ED (Figure 2, B), and *vGlut-GAL4* exhibited dense innervation of all three organs (Figure 2, C).

OA/glutamate neurons are distinct from 5-HT/glutamate neurons

To determine if the observed neuronal expression of the GAL4 drivers for Tdc2, TRH, and vGlut are coincident or exclusive, two separate approaches were implemented. In the first approach, split-GAL4 drivers specific for each neurotransmitter were tested in pairwise combinations. Both *Tdc2-AD* paired with *vGlut-GAL4-DBD* (Figure 2, D) and *vGlut-AD* paired with *Tdc2-GAL4-DBD* (Figure 2, E) exhibited expression patterns very similar to *Tdc2-GAL4* with dense innervation of the SV and ED, and sparse innervation of the AGs. These results suggest that all the Tdc2 neurons innervating the male reproductive system are OA/glutamate dual neurotransmitter neurons (OGNs). Similarly, both *TRH-AD* paired with *vGlut-GAL4-DBD* (Figure 2, F) and *vGlut-AD* paired with *TRH-GAL4-DBD* (Figure 2, G) exhibited expression patterns very similar to *TRH-GAL4* with dense innervation of the SVs and AGs with modest innervation of the ED. These results suggest that all the serotonergic neurons innervating the male reproductive system are 5-HT/glutamate dual neurotransmitter neurons (SGNs). To determine if there is overlap between the OGNs and SGNs, *Tdc2-AD* was paired with *TRH-GAL4-DBD* with the result that no neuronal expression was observed (Figure 2, H). This result suggests the OGNs and SGNs are exclusive and non-overlapping.

A second approach to assess overlap between octopaminergic, serotonergic, and glutamatergic neurons of the male reproductive system utilized pairwise combinations of GAL4 and LexA drivers specific for each neurotransmitter. Pairing *TRH-GAL4* and *Tdc2-LexA* together with *UAS-6XGFP* and *LexAop-6XmCherry* reporters revealed no overlap in either the SVs (Figure 3, A-F), ED (Figure 3, G-L), or AGs (Figure 3, M-R). These results are consistent with the split-GAL4 result above of no intersection between octopaminergic and serotonergic neurons of the male reproductive system, although both neuron types are often tightly fasciculated, especially in the

Figure 1. The Drosophila male reproductive system.

A) Schematic diagram showing paired testes (uncolored), SVs (green), and AGs (purple), Sph (red), ED (gray), and EB (uncolored). B) Actual male reproductive system. Te-testes, SV-seminal vesicle, AG-accessory gland, Sph-sphincter, ED-ejaculatory duct, EB-ejaculatory bulb. Scale bar: 200μm.

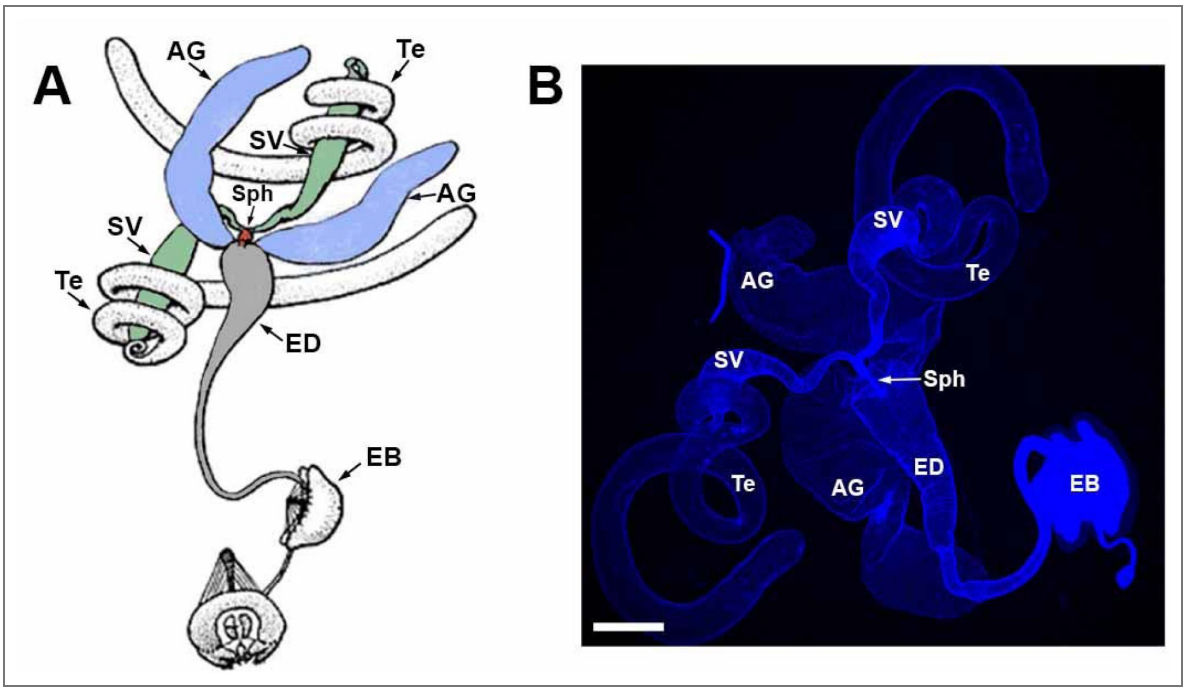

Figure 2. Gal4 and Split-GAL4 expression patterns in the Drosophila male reproductive system.

A) *Tdc2-GAL4*; B) *TRH-GAL4*; C) vGlut-GAL4; D) Tdc2-AD ∩ *vGlut-GAL4-DBD*; E) *vGlut-AD* ∩ *Tdc2-GAL4-DBD*; F) *TRH-AD* ∩ *vGlut-GAL4-DBD*; G) *vGlut-AD* ∩ *TRH-GAL4-DBD*; H) *Tdc2-AD* ∩ *TRH-GAL4-DBD*. Scale bar: 200μm.

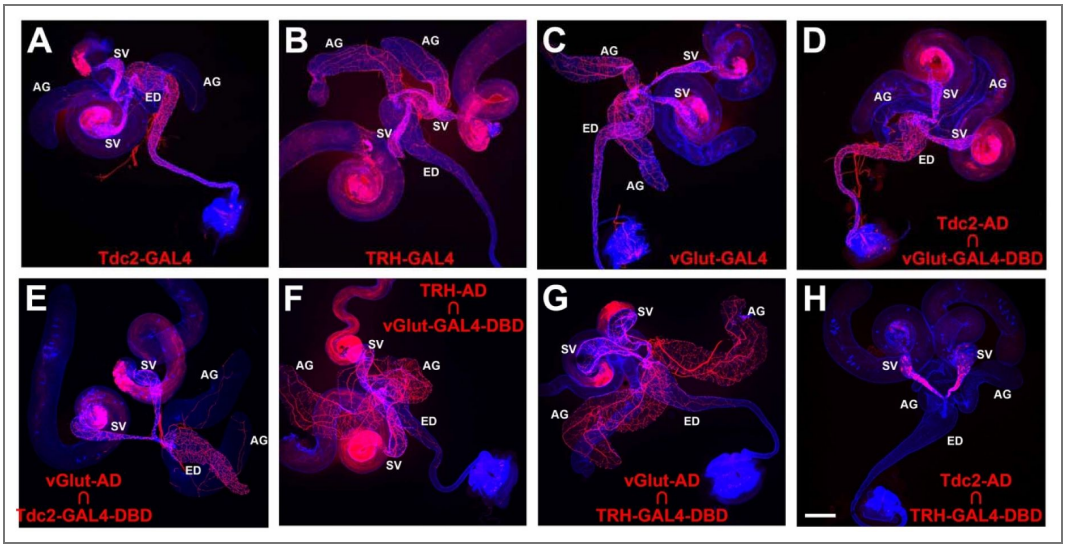

SVs. Pairing *vGlut-LexA* with *TRH-GAL4* revealed a high degree of overlap in the SVs (Figures 3S1, A-F), partial overlap in the ED (Figures 3S1, G-L), and near complete overlap in the AGs (Figures 3S1, M-R). Pairing *vGlut-LexA* with *Tdc2-GAL4* revealed significant overlap in the SVs (Figures 3S2, A-F), majority overlap in the ED (Figures 3S2, G-L), and limited overlap in the AGs (Figures 3S2, M-R). The results of the split-GAL4 intersectional strategy and the GAL4/LexA overlap strategy are entirely consistent with each other. Taken together, they demonstrate that the Drosophila internal male reproductive system receives input from two distinct and nonoverlapping motor-neuron populations, one population that co-expresses octopamine and glutamate (OGNs) and another distinct population that co-expresses serotonin and glutamate (SGNs). The SV receives roughly equal innervation from both classes, the AG is innervated more extensively by SGNs, and the ED is innervated more extensively by OGNs.

OGNs are *fru* +/*dsx* + while SGNs are *fru*+/*dsx* -

Neurons that innervate the male reproductive tract are expected to be sexually dimorphic (Billeter and Goodwin 2004; Yamamoto 2007; Siwicki and Kravitz 2009; Verhulst and van de Zande 2015). To determine whether they express the canonical sex-determination genes *fruitless* (*fru*) and/or *doublesex* (*dsx*), *fru-GAL4* and *vGlut-LexA* were paired with *UAS-6XGFP* and *LexAop-6XmCherry*. This experiment revealed complete overlap: every vGlut-positive neuron in the reproductive system—both OGNs and SGNs—was also *fru*-positive (Fig. 3S3, A–C). To examine *dsx* expression, the octopaminergic driver *Tdc2-AD* was combined with *dsx-GAL4-DBD*. The resulting pattern (dense terminals in the SVs and ED, sparse arbors in the AGs; Fig. 3S3, D) matched that of *Tdc2-GAL4* alone, indicating that all OGNs are *dsx*-positive. In contrast, pairing the serotonergic *TRH-AD* with *dsx-GAL4-DBD* produced no signal in the reproductive tract (Fig. 3S3, E), showing that SGNs are *dsx*-negative. Together, these experiments establish that OGNs are *fru*+/*dsx*+, whereas SGNs are *fru*+/*dsx*–, underscoring a molecular distinction between the two neuromodulatory inputs to the male reproductive system.

Non-overlapping expression of TβH and Tdc2 with 5-HT confirms exclusivity of OGNs and SGNs

Several predictions follow from the finding that non-overlapping sets of OGNs and SGNs innervate the male reproductive system. Among these are that the neurotransmitter synthesis enzymes for OA, Tyramine-β-hydroxylase (TβH), and Tyrosine decarboxylase 2 (Tdc2) should be exclusively expressed in the OGNs along with the sole Drosophila vesicular glutamate transporter (vGlut), while 5-HT should be exclusively expressed in the SGNs along with vGlut-40XV5. To test these predictions, vGlut-40XV5 expression was separately assessed in combination with TβH or Tdc2. 5-HT expression, visualized with an anti-5-HT antibody, was also included in this analysis to distinguish SGNs. As predicted, extensive vGlut-40XV5 expression was observed throughout the male reproductive system except for the testes (Figures 4, A and G) with a sharp boundary of neuronal innervation at the testicular duct (arrows, Figure 4, A). Also as predicted, TβH-GFP and Tdc2 were observed in the male reproductive system with expression patterns similar to that of *Tdc2-GAL4* (Figures 4, B and H, respectively). Pairwise combinations of overlapping expression of vGlut-40XV5, 5-HT, and either TβH (Figures 4, D-F) or Tdc2 (Figures 4, J-L) are also shown.

Higher resolution images of vGlut-40XV5, TβH-GFP, Tdc2, and 5-HT in the male reproductive system allow an assessment of overlapping expression. In the SV, broad robust expression was observed for vGlut-40XV5 (Figures 4S1, A, G, M, and S) and 5-HT (Figures 4S1, C, I, O, and U), with somewhat more restricted expression for TβH-GFP (Figure 4S1, B and H) and Tdc2 (Figure 4S1, N, T). Pairwise overlapping expression is also shown for vGlut-40XV5 and 5-HT with TβH-GFP (Figures 4S1, D-F and J-L) and Tdc2 (Figures 4S1, P-R and V-X). In the highest resolution images, coincident expression is evident between vGlut-40XV5 with TβH-GFP (Figure 4S1, J) and vGlut-40XV5 with Tdc2 (Figure 4WS1, V). Consistent with results above, exclusivity of expression is apparent between TβH-GFP and 5-HT (Figure 4S1, L) and between Tdc2 and 5-HT (Figure 4S1, X), although the tight fasciculation of OGNs and SGNs is evident.

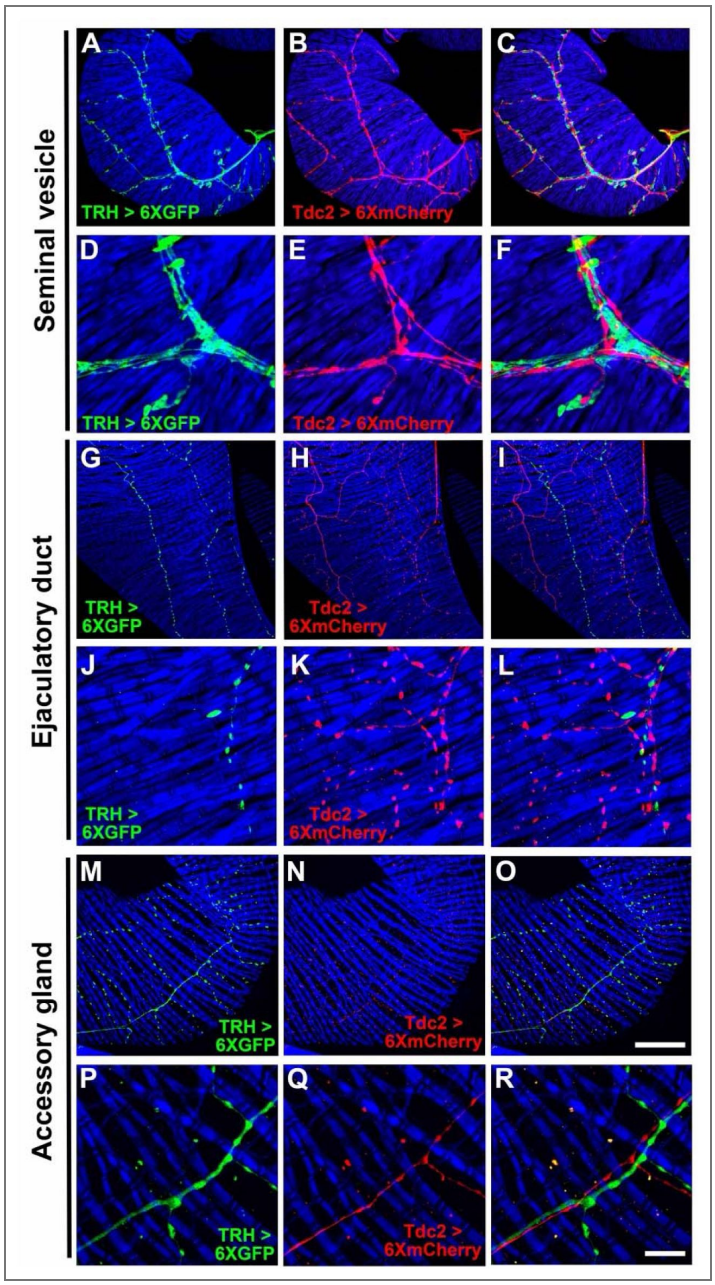

Figure 3. **Expression of *TRH-GAL4* and *Tdc2-LexA* in the Drosophila male reproductive system.**

A, D, G, J, M, P) *TRH-GAL4*, *UAS-6XGFP*; B, E, H, K, N, Q) *Tdc2-LexA*, *LexAop-6XmCherry*. C, F, I, L, O, R) overlay. Scale bars: O-50μm; R-10μm.

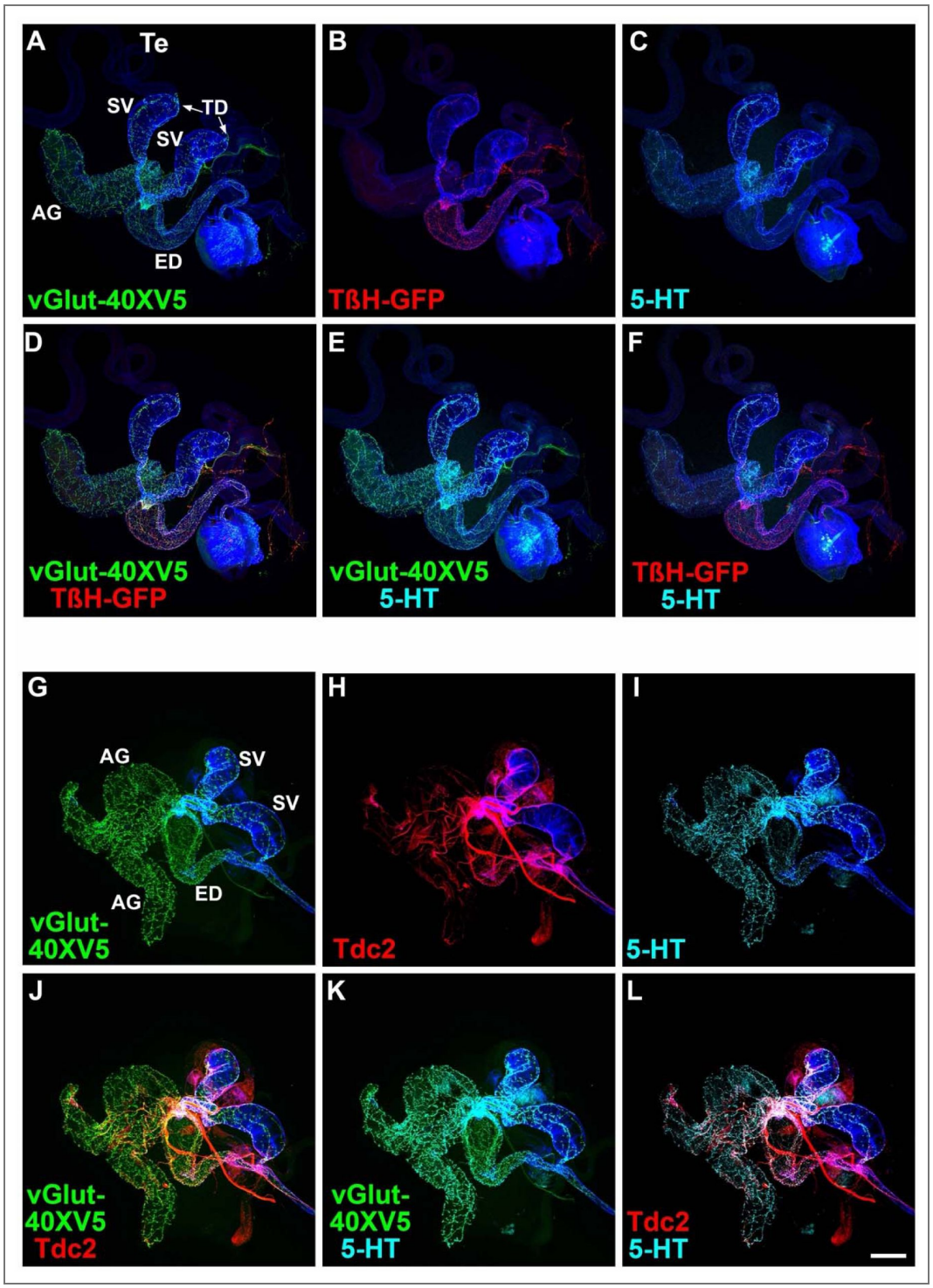

Figure 4. Expression of vGlut, TβH-GFP, Tdc2, and 5-HT in the Drosophila male reproductive system.

A) vGlut-40XV5; B) TβH-GFP; C) 5-HT; D) vGlut-40XV5, TβH-GFP overlay; E) vGlut-40XV5, 5-HT overlay; F) TβH-GFP, 5-HT overlay. G) vGlut-40XV5; H) Tdc2; I) 5-HT; J) vGlut-40XV5, Tdc2 overlay; K) vGlut-40XV5, 5-HT overlay; L) Tdc2, 5-HT overlay. Scale bar: 200μm.

Similar results were obtained in higher resolution images of the ED and AGs although the extent of innervation of the different amines varies between these tissues with more OGNs than SGNs in the ED and the reciprocal in the AGs. In higher resolution images of the ED, strong extensive expression was observed for vGlut-40XV5 (Figures 4S2, A, G, M, and S) with moderately less expression for TβH-GFP (Figure 4S2, B and H) and Tdc2 (Figure 4S2, N, T), with noticeably less expression of 5-HT (Figures 4S2, C, I, O, and U. Pairwise overlapping expression is also shown for vGlut-40XV5 and 5-HT with TβH-GFP (Figures 4S2, D-F and J-L) and Tdc2 (Figures 4S2, P-R and V-X). In the highest resolution images, coincident expression is evident between vGlut-40XV5 with TβH-GFP (Figure 4S2, J) and vGlut-40XV5 with Tdc2 (Figure 4S2, V). As in the SV, exclusivity of expression is apparent between TβH-GFP and 5-HT (Figure 4S2, L) and between Tdc2 and 5-HT (Figure 4S2, X), also with tight fasciculation of the OGNs and SGNs.

In higher resolution images of the AGs, robust widespread expression was observed for vGlut-40XV5 (Figures 4S3, A, G, M, and S) and 5-HT (Figures 4S3, C, I, O, and U, with no expression of TβH-GFP (Figure 4S3, B and H), and sparse expression of Tdc2 (Figure 4S3, N, T). Pairwise overlapping expression is also shown for vGlut-40XV5 and 5-HT with TβH-GFP (Figures 4S3, D-F and J-L) and Tdc2 (Figures 4S3, P-R and V-X). In the highest resolution images, coincident expression is evident between vGlut-40XV5 and Tdc2 (Figure 4S3, V). As in the SV and ED, exclusivity of expression is apparent between Tdc2 and 5-HT (Figure 4S3, X).

The expression of vGlut-40XV5, TβH-GFP, and 5-HT was also assessed at the junction of the SVs and AGs with the ED. vGlut-40XV5 innervation of both the SV and AG is particularly dense (Figure 4S4, A). Significant expression of TβH-GFP and 5-HT was also observed (Figure 4S4, B and C, respectively). Pairwise overlapping expression for vGlut-40XV5, TβH-GFP, and 5-HT is also shown (Figure 4S4, D-F). These experiments showing no overlap in expression of TβH-GFP and Tdc2 with 5-HT provide additional support to the exclusivity of OGNs and SGNs. Collectively, these findings confirm that octopaminergic vGlut-positive and serotonergic vGlut-positive motor neurons form distinct, nonoverlapping populations that differentially innervate the Drosophila male reproductive tract, underscoring strict transmitter exclusivity within this circuit.

Expression of vGlut and vMAT in both OGNs and SGNs further confirms multi-neurotransmitter usage

Co-labeling of vGlut-40XV5 with TβH / Tdc2 in OGNs and with 5-HT in SGNs implies both neuron types are multi-transmitter and predicts they will express not only vGlut but also the sole Drosophila monoamine vesicular transporter vMAT known to package both OA and 5-HT (Deshpande *et al*. 2020). Since OGNs and SGNs often fasciculate tightly together, co-conditional expression of vGlut and vMAT was implemented to visualize expression separately in each population. This was achieved using either the *TRH-GAL4* or *Tdc2-GAL4* drivers in combination with the *B2RT-STOP-B2RT-vGlut-40XMYC*, *RSRT-STOP-RSRT-6XV5-vMAT*, *UAS-B2* and *UAS-R* recombinase transgenes. Using the *TRH-GAL4* driver to restrict conditional expression to SGNs, as predicted, both vGlut-40XMYC (Figures 5, A, E) and 6XV5-vMAT (Figures 5, B, F) were detected in the SV. Tdc2 expression was also included in this experiment (Figures 5, C and G) as was a *UAS-CD8-mCherry* reporter to outline SGNs (Figures 5, D and H). A high degree of overlap was observed between vGlut-40XMYC and 6XV5-vMAT (Figure5, I) with no overlap between Tdc2 and the other markers (Figures 5, J-L).

In a reciprocal experiment in the SV using the *Tdc2-GAL4* driver and 5-HT immunostaining, both vGlut-40XMYC (Figure 5, M and Q) and 6XV5-vMAT (Figure 5, N and R) were detected with a mostly overlapping distribution (Figure 5, U). 5-HT immunostaining was in close proximity but did not overlap with any of the other markers (Figure 5, V-X). It is also notable that the morphology of the SGNs is distinct from the OGNs with the SGNs being larger and more extensively branched compared to the OGNs (SGNs-Figures 5, D and H; OGNs-Figures 5, P and T), suggesting SGNs may assert more regulatory control of SV muscle activity than OGNs.

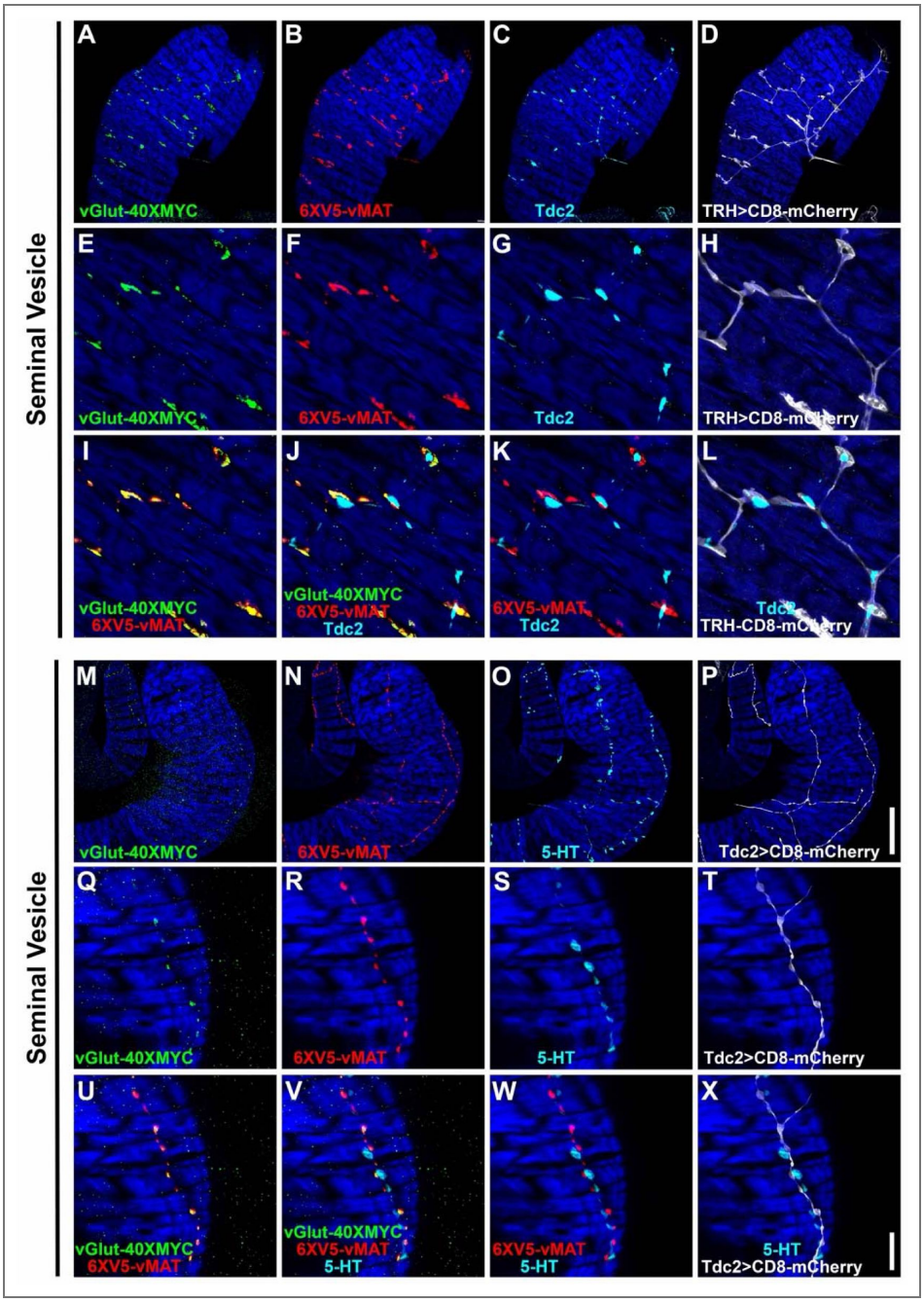

Figure 5. Co-conditional expression of vGlut-40XMYC and 6XV5-vMAT in the SV of serotonergic (TRH) or octopaminergic (Tdc2) neurons of the Drosophila male reproductive system.

A-D) 63X. A) vGlut-40XMYC; B) 6XV5-vMAT; C) Tdc2; D) TRH>CD8-mCherry. E-L) 63X zoom 4X. E) vGlut-40XMYC; F) 6XV5-vMAT; G) Tdc2; H) TRH>CD8-mCherry; I) vGlut-40XMYC, 6XV5-vMAT overlay; J) vGlut-40XMYC, 6XV5-vMAT, Tdc2 overlay; K) 6XV5-vMAT, Tdc2 overlay; L) Tdc2, TRH>CD8-mCherry overlay. M-P) 63X. M) vGlut-40XMYC; N) 6XV5-vMAT; O) 5-HT; P) Tdc2>CD8-mCherry. Q-X) 63X zoom 4X. Q) vGlut-40XMYC; R) 6XV5-vMAT; S) 5-HT; T) Tdc2>CD8-mCherry; U) vGlut-40XMYC, 6XV5-vMAT overlay; V) vGlut-40XMYC, 6XV5-vMAT, 5-HT overlay; W) 6XV5-vMAT, 5-HT overlay; X) 5-HT, Tdc2>CD8-mCherry overlay. Scale bars: P-50μm; X-10μm.

Similar results were obtained in these co-conditional experiments for the ED and AGs. With the *TRH-GAL4* experiment in the ED, vGlut-40XMYC (Figure 5S1, A and E) and 6XV5-vMAT (Figure 5S1, B and F) were both present with a highly overlapping distribution (Figure 5S1, I). Tdc2 did not overlap with any of the other markers (Figure 5S1, J-L). With the *Tdc2-GAL4* experiment in the ED, vGlut-40XMYC (Figure 5S1, M and Q) and 6XV5-vMAT (Figure 5S1, N and R) were both observed in a highly overlapping distribution (Figures 5S1, U). 5-HT immunostaining did not overlap with any of the other markers (Figures 5S1, V-X). Note that morphological differences between the SGNs and OGNs in the ED are not as easily distinguished as in the SV.

With the *TRH-GAL4* experiment in the AGs, both vGlut-40XMYC (Figures 5S2, A and E) and 6XV5-vMAT (Figures 5S2, B and F) are present in a largely overlapping distribution (Figure 5S2, I). As with the SV and ED, Tdc2 expression did not overlap with any of the other markers (Figures 5S2, J-L). With the *Tdc2-GAL4* experiment in the AG, both vGlut-40XMYC (Figures 5S2, M and Q) and 6XV5-vMAT (Figures 5S2, N and R) are present in an overlapping configuration (Figure 5S2, U). The distribution of 5-HT is distinct from any of the other markers (Figure 5S2, V-X). In the AGs the morphology of the SGNs (Figures 5S2, D and H) is distinct from that of the OGNs (Figures 5S2, P and T).

Since OGNs and SGNs are intermingled in tightly fasciculated neuron bundles, we used intersectional labeling to visualize the glutamate transporter vGlut-40XV5 and the monoamine transporter 6XV5-vMAT in each class separately. Together, the results show that both vesicular transporters are expressed in OGNs and SGNs in an overlapping distribution while the OGNs and SGNs remain anatomically distinct throughout the male reproductive tract.

Expansion microscopy reveals prominent co-occurrence of vGlut and vMAT on ED synaptic vesicles of both OGNs and SGNs

Although there is apparent overlap between vGlut-40XMYC and 6XV5-vMAT in both SGNs and OGNs it is not possible to resolve whether they reside on the same or different synaptic vesicles using standard microscopy methods. This constraint is due to the ~250nm diffraction limit of light at visible wavelengths (Abbe 1873). To overcome this limitation, expansion microscopy was performed on EDs using co-conditional expression of vGlut-40XMYC and 6XV5-vMAT separately in SGNs and OGNs as above. The protocol utilized in these experiments reported 10X expansion in a single round (Damstra et al. 2023) and this agreed well with our empirically determined expansion factor of 10.47X based on the size comparison of nuclei area in muscles of the unexpanded and expanded EDs (Figure 5S5, A and B, respectively). In a representative example of expanded SGNs, 6XV5-vMAT (Figure 5S3, A) and vGlut-40XMYC (Figure 5S3, B) revealed a significantly overlapping distribution (Figure 5S3, C). To quantify the co-occurrence of vGlut-40XMYC and 6XV5-vMAT the BIOP JACop ImageJ plug-in was used to calculate a Mander's co-efficient, a metric that calculates the fraction of one signal that co-occurs with another. The output of the BIOP JACop plug-in revealed substantial co-occurrence of 6XV5-vMAT and vGlut-40XMYC (Figures 5S3, D-I) including a graphical representation (Figure 5S3, J). For the SGNs, the numerical Mander's coefficients for 6XV5-vMAT co-occurrence with vGlut-40XMYC were 67.9% and vGlut-40XMYC co-occurrence with 6XV5-vMAT were 57.2% (Figure 5S3, K).

Expanded OGNs yielded similar results. In a representative example, 6XV5-vMAT (Figure 5S4, A) and vGlut-40XMYC (Figure 5S4, B) exhibited substantial overlap (Figure 5S4, C). The output of the BIOP JACop plug-in also revealed majority co-occurrence in image (Figure 5S4, D-I) and graphical form (Figure 5S4, J). For the OGNs, the numerical values of the Mander's coefficients were 67.4% for 6XV5-vMAT co-occurrence with vGlut-40XMYC and 75.6% for vGlut-40XMYC co-occurrence with 6XV5vMAT (Figure 5S4, K).

The results of the expansion microscopy experiments indicate that in both SGNs and OGNs the majority of ED synaptic vesicles are positive for both vGlut-40XMYC and 6XV5-vMAT and thereby they co-release glutamate and either OA (OGNs) or 5-HT (SGNs). This demonstration of a

neurotransmitter co-release mechanism may be a conserved strategy for synchronizing rapid gland and muscle activity during copulation that has general implications across species for how co-transmitter neurons mediate complex motor behaviors.

OGNs and SGNs express synaptic markers common to other neuromuscular junctions

In addition to providing information on whether a given synapse is primarily excitatory or modulatory, identifying vesicular transporters and synaptic markers allows mapping of active release sites to determine how pre- and post-synaptic specializations align. Such information is essential for (i) elucidating how each neurotransmitter influences muscle contractility and secretory function, and (ii) predicting how synaptic efficacy might change during prolonged copulation or in response to neuromodulatory feedback. To further characterize the synapses of the neurons innervating the male reproductive system immunostaining was performed with vGlut-40XMYC, 6XV5-vMAT, and either of three well-established Drosophila synaptic markers including Synapsin (Syn)-synaptic vesicles, Bruchpilot (Brp)-active zones, and Discs-large (Dlg-Drosophila homolog of mammalian PSD-95)-post-synaptic density. In the SV, strong Syn staining was observed (Figures 6, C and F) that exhibited extensive co-localization with vGlut-40XMYC (Figure 6, H) and 6XV5-vMAT (Figure 6, I). Similar results were obtained in the ED and AGs. Abundant Syn expression was observed (Figure 6, C′ and F′) that exhibited near precise overlap with vGlut-40XMYC (Figure 6, H′) and 6XV5-vMAT (Figure 6H, I′). For the AG, robust Syn expression was observed (Figures 6A, C′′ and F′′) that co-localized strongly with vGlut-40XMYC (Figure 6A, H′′) and 6XV5-vMAT (Figure 6A, I′′). It is notable that a visibly higher density of Syn expression was observed in the SV (Figure 6A, F) compared with the AGs (Figure 6A, F′) and ED (Figure 6A. F”), presumably indicating greater neurotransmitter output.

The active zone marker Brp exhibited strong expression in the SV (Figure 6S1, C and G) that overlapped almost entirely with 6XV5-vMAT. Brp expression in the ED and AG was noticeably sparser as compared to the SV. The sparse Brp expression in the ED (Figure 6S1, K and O) overlapped with 6XV5-vMAT. Similarly, in the AGs, Brp expression was sparse and overlapped with 6XV5-vMAT (Figure 6S1, S and W).

The post-synaptic density marker Dlg was expressed broadly throughout the male reproductive system (Figure 6S2, C). In the SV, the bulk of Dlg expression is predominantly in the epithelial cells with lower levels of expression in the muscles (Figure 6S2, G and K) and no preferential post-synaptic accumulation (Figures 6S2, H and L). Similar results were observed in the ED and AGs. In the ED at the level of the muscle Dlg expression is diffuse (Figure 6S2, O) and does not accumulate post-synaptically opposite synapses in the muscles (Figure 6S2, P). In the AGs, Dlg expression is also diffuse in the muscles (Figure 6S2, T) and does not accumulate post-synaptically opposite synapses in the muscle (Figure 6C, U). Images of Dlg expression in the epithelial layer of the ED (Figure 6C, Q) and AG (Figure 6C, V) reveal apparent membrane localization in a honeycomb pattern. The lack of post-synaptic accumulation of Dlg opposite the synapses of SGNs and OGNs in the male reproductive system is reminiscent of larval type II OGNs and distinct from larval type I glutamatergic neurons that exhibit prominent post-synaptic concentration of Dlg (Parnas et al. 2001). It is also notable that there is no vGlut-40XMYC that does not co-localize with 6XV5-vMAT, indicating there are no neurons innervating the SVs, AGs, or ED that uses glutamate as their sole small molecule neurotransmitter. The absence of synapses with post-synaptic Dlg accumulation, a characteristic of type I glutamate-only larval neurons, also supports this assertion. Defining the molecular architecture of these synapses is critical for understanding how they package, release, and receive neurotransmitters to shape the strength and specificity of communication between motor neurons and target organs.

LDCVs are present in OGNs and SGNs

In addition to synaptic transmission via synaptic vesicles, neurons are also known to communicate using neuropeptides released via Large Dense Core Vesicles (LDCVs). To determine whether neurons innervating the male reproductive system contain LDCVs, immunostaining was

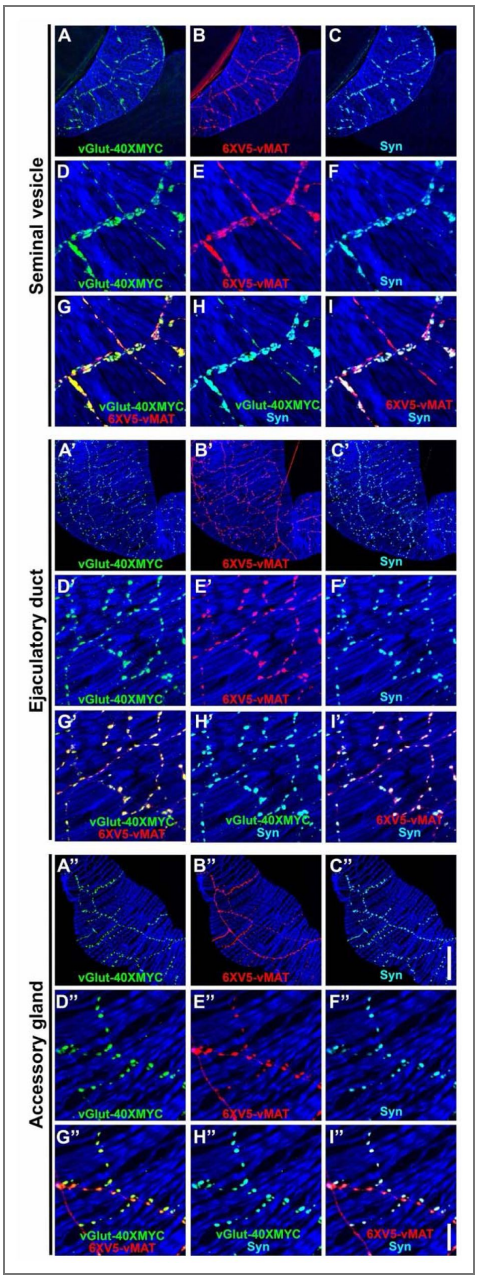

Figure 6. Expression of the synaptic vesicle marker Synapsin in combination with vGlut-40XMYC and 6XV5-vMAT in the SV, ED, and AG of the Drosophila male reproductive system.

A-I) SV. A) vGlut-40XMYC; B) 6XV5-vMAT; C) Synapsin; D) vGlut-40XMYC; E) 6XV5-vMAT; F) Synapsin; G) vGlut-40XMYC, 6XV5-vMAT overlay; H) vGlut-40XMYC, Synapsin overlay; I) 6XV5-vMAT, Synapsin overlay. A'-I') ED. A') vGlut-40XMYC; B') 6XV5-vMAT; C') Synapsin; D') vGlut-40XMYC; E') 6XV5-vMAT; F') Synapsin; G') vGlut-40XMYC, 6XV5-vMAT overlay; H') vGlut-40XMYC, Synapsin overlay; I') 6XV5-vMAT, Synapsin overlay. A''-I'') AG. A'') vGlut-40XMYC; B'') 6XV5-vMAT; C'') Synapsin; D'') vGlut-40XMYC; E'') 6XV5-vMAT; F'') Synapsin; G'') vGlut-40XMYC, 6XV5-vMAT overlay; H'') vGlut-40XMYC, Synapsin overlay; I'') 6XV5-vMAT, Synapsin overlay. Scale bars: C''-50µm; I''-10µm.

performed with the LDCV marker IA2-GFP (Yu et al. 2025) in combination with vGlut-40XMYC and 6XV5-vMAT. Abundant IA2-GFP expression was observed throughout the male reproductive system (Figure 6S3, C). In the SVs, IA2-GFP (Figure 6S3, F and L) localizes to the same pre-synaptic regions of the neurons as vGlut-40XMYC (Figures 6S3, D and J) and 6XV5-vMAT (Figures 6S3, E and K). In the highest resolution images, there appears to be some overlap between IA2-GFP and vGlut-40XMYC (Figure 6S3, N) as well as between IA2-GFP and 6XV5-vMAT (Figure 6S3, O), but a substantial fraction of IA2-GFP distributes in close proximity to, but is distinct from, vGlut-40XMYC and 6XV5-vMAT. This distribution pattern is not entirely surprising as it is consistent with the prior observation that vesicular neurotransmitter transporters have been detected on LDCVs (Yu et al. 2025).

Similar results were observed in the ED and AGs. In the ED, prominent IA2-GFP expression was evident (Figures 6S4, C and I) that partially co-localized with vGlut-40XMYC (Figures 6S4, E and K) and 6XV5-vMAT (Figures 6S4, F and L). Considerable IA2-GFP expression was also apparent in the AGs (Figures 6S4, O and U) that partially overlapped with vGlut-40XMYC (Figures 6S4, Q and W) and 6XV5-vMAT (Figures 6S4, R and X). This finding of pronounced expression of IA2-GFP throughout the pre-synaptic terminals of neurons innervating the male reproductive system suggest substantial LDCVs are present in both SGNs and OGNs, and that these neurons are thus communicating not just via small molecule neurotransmitters inside synaptic vesicles but also by neuropeptides contained within LDCVs.

No cholinergic or GABAergic transmission at OGN or SGN synapses

Although to our knowledge there have been no motor neurons reported in Drosophila that use acetylcholine or GABA as a neurotransmitter, to rule out these possibilities for the male reproductive system, Drosophila containing genome-edited 7XMYC-vAChT and 9XV5-vGAT were immunostained for their corresponding epitope tags. Not unexpectedly, no expression of 7XMYC-vAChT was observed in the SVs, ED, or AGs (Figures 6S5, C, G, and K, respectively). Similarly, no expression of 9XV5-vGAT was observed in the SVs, ED, or AGs (Figures 6S5, D, H, and L, respectively), indicating that neither acetylcholine nor GABA are used as neurotransmitters in the OGNs and SGNs of the Drosophila internal male reproductive system.

GAL4 drivers for OA, 5-HT, and glutamate receptors express in the muscles of male reproductive organs

Given that OGNs and SGNs innervate the male reproductive system, an obvious prediction that follows is that neurotransmitter receptors for glutamate, OA, and 5-HT should be expressed in the muscles of the male reproductive system. As a first step in testing this prediction, GAL4 drivers for each of these neurotransmitters were paired with the *UAS-CD8-mCherry* reporter and assessed for expression. As it is well established that the GluRIIA-E/kainate type glutamate receptors mediate synaptic transmission at Drosophila NMJs (Diantonio 2006; He and Dickman 2025), GAL4 drivers for all five were assessed. GAL4 drivers for GluRIIA, GluRIID, and GluRIIE showed no expression in the male reproductive system, but they also exhibited no expression in other adult or larval muscles where they are known to be expressed. These results suggest that the GAL4 drivers for these three GluRII receptors are simply non-functional and are therefore non-informative. However, GluRIIB-GAL4 and GluRIIC-GAL4 exhibited broad expression in the musculature of the male reproductive system (Figures 7, A and B, respectively). This suggests glutamate is used for signaling throughout the male reproductive system, consistent with the widespread expression of vGlut in pre-synaptic terminals.

OA receptor GAL4 drivers for OAMB, OAα2R, Oct-TyrR, OAβ1R, OAβ2R, and OAβ3R were assessed for expression in the male reproductive system. OAMB-GAL4 exhibited expression in the muscles of the SVs and ED, as well as epithelial cells of the AGs (Figure 7S1, A). OAα2R-GAL4 displayed strong expression in the muscles of the SVs, weak expression in the muscles of the AGs, and no expression in the ED (Figure 7S1, B). Oct-TyrR-GAL4 showed strong expression in non-muscle cells of the distal AG, muscle expression in the AGs, ED, and ejaculatory bulb, expression in the testes, but no expression in the muscles of the SVs (Figure 7S1, C). OAβ2R-GAL4 exhibited strong

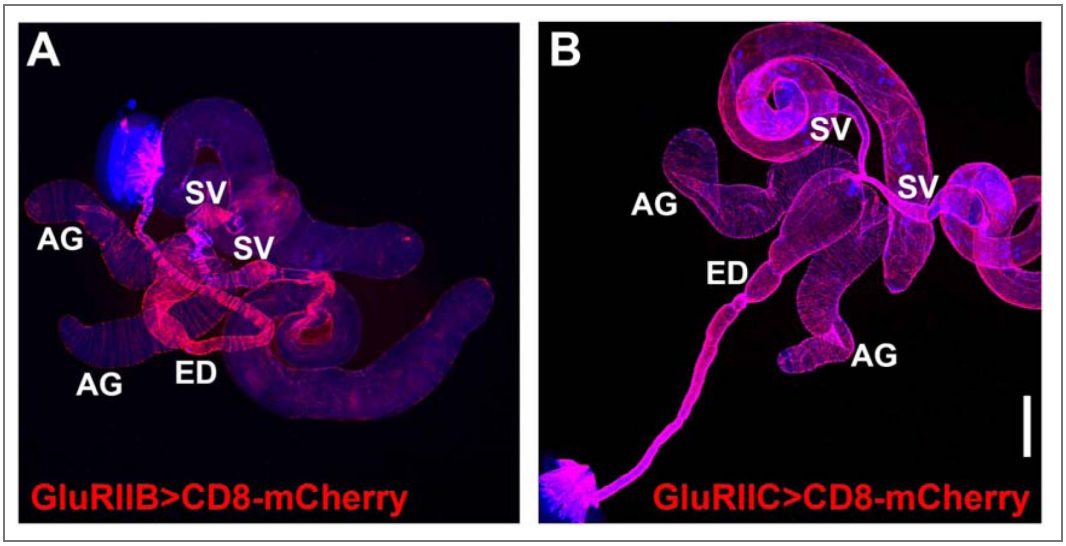

Figure 7. Glutamate receptor GAL4 expression patterns in Drosophila male reproductive system.

A) GluRIIB; B) GluRIIC. Scale bar: 200μm.

expression in the epithelial cells of the ED, muscle expression in the SVs, ED, and ejaculatory bulb, expression in the testes, but no muscle expression in the AGs (Figure 7S1, E). OAβ1R-GAL4 and OAβ3R-GAL4 exhibited broad expression in the neurons innervating the male reproductive system (Figures 7S1, D and F, respectively) but no muscle expression, suggesting they are not mediating OA signaling in the muscles. OAβ3R-GAL4 also displayed expression in the testes. These results suggest OA receptors play a prominent role in the functioning of the male reproductive system and differentially mediate OA signaling in specific parts of the male reproductive system based on their restricted, non-uniform expression patterns.

5-HT receptor GAL4 drivers for 5-HT1A, 5-HT2A, 5-HT-1B, 5-HT2B, and 5-HT7 were also assessed for expression in the male reproductive system. 5-HT1A-GAL4, 5-HT1B-GAL4, and 5-HT2B-GAL4 exhibited broad expression in the neurons innervating the male reproductive system, but no muscle expression (Figures 7S2, A, C, and D, respectively), suggesting these receptors are not mediating 5-HT signaling in the muscles. 5-HT2A exhibited expression specifically in the epithelial cells of the SVs (Figure 7S2, B). 5-HT7 showed substantial expression in neurons, but most strikingly, strong expression in the muscles of the distal SVs, including the sphincter region, with a discrete boundary of expression (arrows, Figure 7S2, E).

GluRIIA is expressed in the SVs and AGs, but not the ED

While informative for determining cellular expression, GAL4 driven reporters for genes of interest do not provide critical mechanistic information about the subcellular distribution of the corresponding proteins. To gain further insight into the role of OA, 5-HT, and glutamate receptors in the function of the male reproductive system the expression patterns of several receptors were assessed using epitope-tagging. To determine the subcellular distribution of the ionotropic GluRII/kainate-type glutamate receptors known to mediate fast excitatory glutamatergic transmission at other Drosophila NMJs (Diantonio 2006; He and Dickman 2025), the expression of a previously characterized genome-edited GluRIIA-GFP fly strain in which GFP has been inserted near the carboxy-terminus of GluRIIA at its endogenous genomic location was evaluated in the male reproductive system. In the SV, GluRIIA-GFP (Figure 8, B and E) exhibited punctate expression that paralleled, but was complementary to, that of the glutamatergic synaptic vesicle marker vGlut-40XV5 (Figure 8, A and D). This distribution of GluRIIA-GFP is not unlike its distribution at the NMJ of third instar larva, optimally localized post-synaptically to bind glutamate released from pre-synaptic terminals (Beckers *et al*. 2024). Surprisingly, no GluRIIA-GFP was observed in the ED (Figures 8, H and K) despite abundant expression of vGlut-40XV5 (Figures 8, G and J). Expression of GluRIIA-GFP in the AGs (Figures 8, N and Q) was similar to that in the SVs in that it closely paralleled vGlut-40XV5 expression (Figure 8, M and P) but was complementary to it. Finding GluRIIA-GFP expression in the SVs and AGs, but not the ED, and the expression of GluRIIB in all three tissues based on the *GluRIIB-GAL4* expression pattern, suggest the SVs and AGs use a mixture of glutamate receptors containing one or the other of the mutually exclusive GluRIIA or GluRIIB subunits in combination with the common GluRIIC, D, and E subunits, while all glutamate receptors in the ED solely utilize GluRIIB. As GluRII receptors containing GluRIIA generate higher currents than those that contain GluRIIB (Diantonio et al. 1999), the lower GluRIIB currents are apparently sufficient for a functional ED.

OA receptors exhibit distinct expression patterns in the muscles, neurons, and epithelial cells of the male reproductive system

OA receptors are modulatory G-protein coupled receptors (GPCRs) that mediate slower-acting but longer-lasting effects than ionotropic receptors. To visualize expression of the OA receptors OAMB, OAα2R, and OAβ2R, CRISPR/Cas9 genome editing was used to create conditional alleles of each receptor fused at their carboxy termini to a multimerized epitope tag for enhanced detection sensitivity. These genome edits are at the endogenous genomic location of each gene and their expression is thus under the control of their complete endogenous regulatory regions. For visualizing expression in the male reproductive system, germline inversion or excision variants were generated that converted conditional expression to constitutive expression.

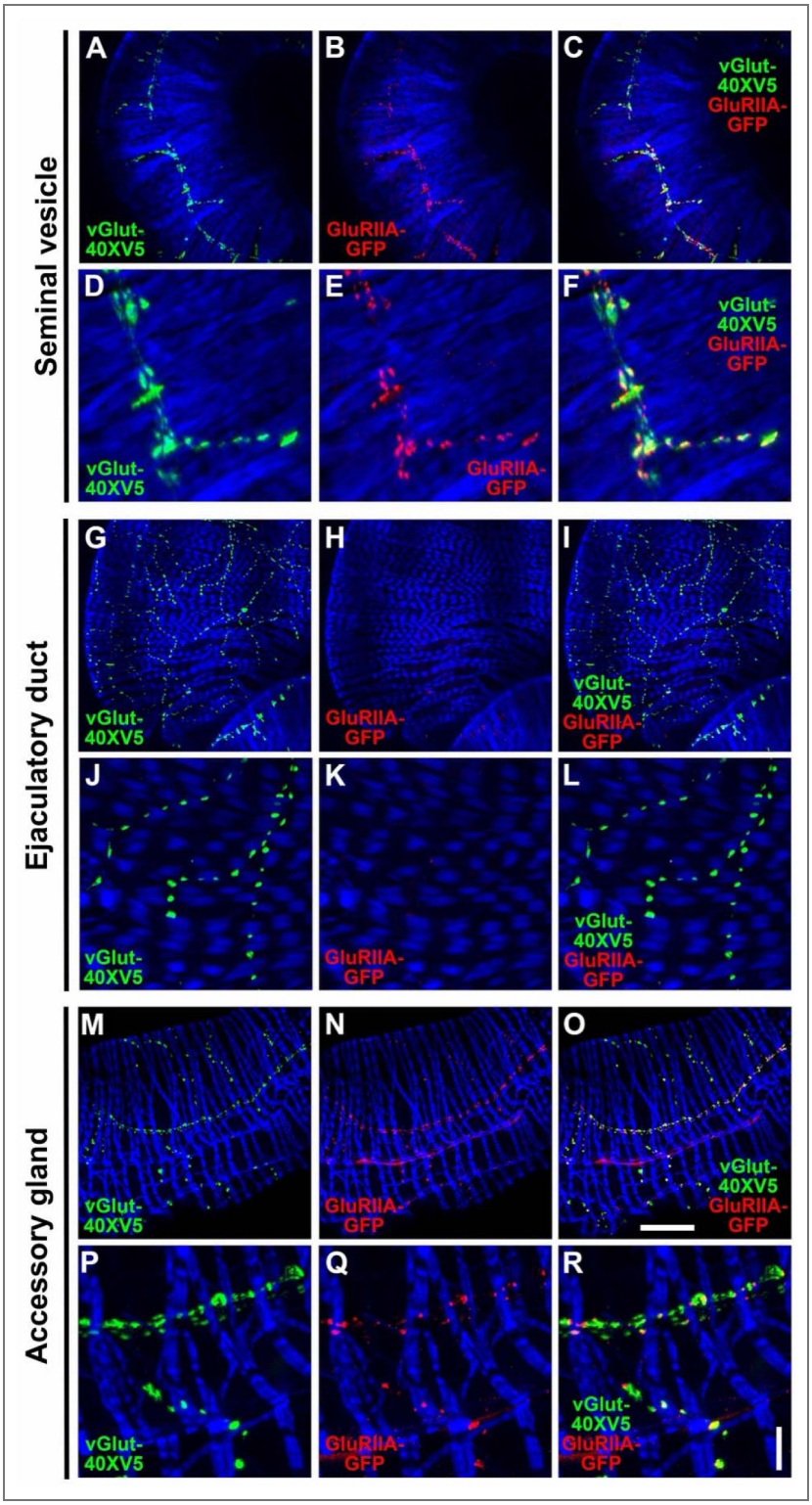

Figure 8. **GluRIIA-GFP expression in the SV, ED, and AG of the Drosophila male reproductive system.**

A-F) SV. A, D) vGlut-40XV5; B,E) GluRIIA-GFP; C, F) vGlut-40XV5, GluRIIA-GFP overlay. G-L) ED. G, J) vGlut-40XV5; H, K) GluRIIA-GFP; I, L) vGlut-40XV5, GluRIIA-GFP overlay. M-R) AG. M, P) vGlut-40XV5; N, Q) GluRIIA-GFP; O, R) vGlut-40XV5, GluRIIA-GFP overlay. Scale bars: O-50μm; R-10μm.

OAMB-10XV5 exhibited strong expression in the epithelial cells of the ED and AGs with limited expression in muscles (Figure 8S1, A). Co-immunostaining with the synaptic vesicle marker Synapsin was conducted to visualize pre-synaptic terminals (Figure 8S1, B). In the SVs, higher resolution images revealed low level expression of OAMB-10XV5 in muscles as well as obvious expression in pre-synaptic neurons (Figures 8S1, D and G) that largely overlapped with Syn (Figures 8S1, F and I). OAMB-10XV5 was similarly distributed in the ED with low-level expression in muscle and clearly discernible expression in pre-synaptic neurons (Figure 8S1, J) based on substantial overlap with Syn (Figure 8S1, L).

Strong OAMB-10XV5 expression was also observed in the epithelial cells of the ED in a honeycomb pattern (Figure 8S1, M and P) reminiscent of Dlg and presumably associated with the plasma membrane. OAMB-10XV5 expression in the epithelial cells of the AGs was similar to its expression in the epithelial cells of the ED with prominent signal in a honeycomb pattern (Figure 8S2, A and D). OAMB-10XV5 also exhibited low-level expression in the muscles of the AG and expression in the pre-synaptic neurons (Figure 8S2, G) by virtue of significant overlap with Syn (Figure 8S2, I). Prominent OAMB-10XV5 expression was also observed in the ejaculatory bulb. Low-level expression of OAMB-10XV5 was detected in the muscles of the ejaculatory bulb as was expression in the pre-synaptic neurons (Figure 8S2, J and M) as evidenced by mostly overlapping expression with Syn (Figure 8S2, L and O). In the non-muscular portion of the ejaculatory bulb, OAMB-10XV5 expression was readily discernable in the epithelial cells in a honeycomb pattern (Figure 8S2, J and P).

OAα2R-20XV5 exhibited strong expression in the muscles of both the SVs and more distal regions of the proximal ED near where it connects with the ejaculatory bulb, as well as lower-level expression in the AGs (Figure 8S3, A). Higher resolution images of OAα2R-20XV5 in the SV indicate expression is restricted to the muscle (Figure 8S3, G) as there is no apparent overlap with Syn (Figure 8S3, I). A cross-section of the SV muscle reveals OAα2R-20XV5 is localized to the membrane of the muscle (Figure 8S3, J), as would be expected for a GPCR. In the AGs, OAα2R-20XV5 is expressed in the muscles (Figure 8S3, M and P) as well as in the pre-synaptic neurons as evidenced by co-localization with Syn (Figure 8S3, O and R). OAα2R-20XV5 expression ends abruptly just after the SVs fuse into the sphincter that regulates the movement of sperm into the ED (Figure 8S4, A and D). OAα2R is expressed in the pre-synaptic neurons innervating the sphincter with little to no expression in the sphincter muscles (Figure 8S4, C and F). In the proximal region of the anterior ED prominent OAα2R-20XV5 expression is observed throughout the innervating neurons with little to no OAα2R-20XV5 in the muscles (Figures 8S4, G, I, J, and L). In contrast, in the distal region of the anterior ED, robust expression of OAα2R-20XV5 is detected in the muscles (Figures 8S4, M, P, and S) but not in the pre-synaptic neurons (Figures 8S4 O, R, and U). This complementary pattern of OAα2R-20XV5 in neurons but not muscles in the proximal ED and muscles but not neurons in the distal ED suggests these different regions of the ED are exhibiting a differential response to OA. As in the SV, OAα2R-20XV5 localizes to the membrane of the muscles as evident in a cross-sectional image (Figure 8S4 S).

Interestingly in this region, Syn expression is inside the muscles of the ED (Figure 8S4 T), potentially suggesting the muscles are being stimulated from the inside, or alternatively, that the neurons are stimulating the underlying epithelial cells. As pre-synaptic neuronal expression of adrenoreceptors in mammals has been shown to be release-inhibiting (Brown and Gillespie 1957; Starke 1972), including in the urinary bladder (Somogyi and de Groat 1990) and vas deferens (O'Connor et al. 1999; Scheibner et al. 2001), OAα2R expression in the pre-synaptic neurons of the internal male reproductive system may also function via inhibitory auto-reception.

OAβ2R-40XV5 exhibits strong expression in the epithelial cells of the ED, the muscles of the ejaculatory bulb, the muscles of the SVs near the point of fusion, the testes, with lower-level muscle expression in the SVs, ED, and AGs (Figure 8S5, A). Higher resolution images of the SV reveal obvious expression in the muscle (Figure 8S5, D and G) but not in the pre-synaptic neurons as there is no apparent overlap with Syn (Figures 8S5, F and I). A cross-sectional image of the SV reveals OAβ2R-40XV5 is localized to the plasma membrane of muscle cells (Figure

8S5, J). In higher resolution images of the ED, moderate levels of OAβ2R-40XV5 are present in the muscles (Figures 8S5, M and P) but not in the innervating pre-synaptic neurons as there is no obvious overlap with Syn (Figures 8S5, O and R). At the junction where the SVs fuse into a single duct, OAβ2R-40XV5 expression is strong prior to fusion but drops off abruptly at the point of full fusion (arrow, Figure 8S6, A). The strongest levels of OAβ2R-40XV5 expression throughout the entire male reproductive system is in what appears to be the epithelial cells that line the ED (Figure 8S6, A). A cross-section of the ED reveals the distribution of OAβ2R-40XV5 in epithelial cells is exclusively at the apical surface (Figure 8S6, D). Also notable, there is another boundary of OAβ2R-40XV5 expression in the SVs somewhat prior to fusion (solid arrow, Figure 8S6, G).

Higher resolution images of OAβ2R-40XV5 expression at the point of SV fusion shows the sharp dip in expression at the point of full fusion (arrow, Figure 8S6, J). A cross-sectional image also reveals the drop in expression and membrane localization of OAβ2R-40XV5 in the muscle (Figure 8S6, M). Similar to the proximal anterior ED, the more distal region of the anterior ED exhibits strong expression in the muscles, and especially the underlying epithelial cells (Figures 8S7, A and D), In the AGs, OAβ2R-40XV5 expression is manifest in the muscles (Figures 8S7, G and J) but does not overlap with the pre-synaptic neurons as evidenced by the lack of overlap with Syn (Figures 8S7, I and L). Prominent OAβ2R-40XV5 expression was also observed in the ejaculatory bulb (Figure 8S7, M and P). As β2 adrenoreceptors relax bladder muscles in mice (Wuest et al. 2009), OAβ2R may relax muscles in the male reproductive system.

Octopamine receptor expression in the internal organs of the male reproductive tract was predicted based on the dense OGN innervation of these tissues. Although OA receptor presence in these muscles aligns with their role in modulating contractile strength and rhythm, the organ-specific differences in receptor subtype abundance could only be established empirically. Epithelial expression implies that octopamine influences non-neuronal functions such as protein secretion or barrier permeability, but the precise cellular responses remain to be defined. Mapping OAMB, OAα2R, and OAβ2R to discrete muscle, neuronal, and epithelial compartments provides mechanistic information about how octopamine fine-tunes contraction, secretion, and presynaptic feedback across the male reproductive tract, offering an evolutionary framework for adrenergic control of fertility and pinpointing cell-specific targets for modulating reproductive output.

5-HT7 is widely expressed in the male reproductive system but most prominently in the sphincter region

Since the *5-HT7-GAL4* reporter delineates a sharp posterior boundary in the SV, endogenous 5-HT7 receptor expression was evaluated to pinpoint where 5-HT may directly modulate reproductive tract motility. To assess the expression pattern of the 5-HT7 receptor, a 20XV5 tag was added to the carboxy-terminus by CRISPR/Cas9 genome editing at its endogenous genomic location. 5-HT7-20XV5 localizes to the muscles of the SV just before and after the junction, the epithelial cells of the AGs, and the ejaculatory bulb (Figures 8S8, A). Higher resolution images of the SV reveal low level expression in muscles (Figures 8S8, D and G), as well as expression in the pre-synaptic neurons innervating the male reproductive system as evidenced by co-localization with Syn (Figures 8S8, F and I). In the ED, 5-HT7-20XV5 is expressed in the muscles (Figures 8S8, J and M), but unlike the SV, it is not expressed the pre-synaptic neurons as it does not appear to co-localize with Syn (Figures 8S8, L and O). Expression levels of 5-HT7-20XV5 increase in the SV near the point of fusion and are maximal from just before the junction all the way to the terminus in the ED (Figure 8S9, A). Expression levels of 5-HT7-20XV5 appear to increase at a discrete boundary point on the SVs prior to fusion (arrow, Figure 8S9, D). This boundary of increasing expression at this same region of the SV is highly reminiscent of OAβ2R-40XV5 (Figure 8S6, G). A higher resolution image of the sphincter region of the SV post-fusion reveals high levels of 5-HT7-20XV5 expression (Figure 8S9, G) but not in the innervating pre-synaptic neurons based on the absence of co-localization with Syn (Figure 8S9, I). A cross-section of this same region reveals the 5-HT7-20XV5 protein localizes to muscle membranes (Figure 8S9, J). A high-resolution image of the terminus of the sphincter confirms 5-HT7-20XV5 expression extends

all the way to the end (Figure 8S9, M). This observation of 5-HT7-20XV5 expression throughout the fused sphincter region of the SV contrasts with that of OAα2R-20XV5 (Figure 8S4, D) and OAβ2R-40XV5 (Figure 8S6, A), both of which end at the point of full SV fusion and suggests 5-HT plays a more important role than OA in sphincter regulation. 5-HT7-20XV5 expression is also elevated in the muscles at the terminus of the AGs (Figure 8S9, P). In the AGs, 5-HT7-20XV5 is most prominently expressed in the underlying epithelial cells (Figures 8S10, A and D). An AG cross-section reveals 5-HT7-20XV5 localizes exclusively to the apical surface of the epithelial cells (Figure 8S10, G), highly reminiscent of OAβ2R-40XV5 localization to the apical surface of epithelial cells of the ED (Figure 8S6, D). Nearer the surface of the AGs, low-level expression of 5-HT7-20XV5 is detected in the muscle (Figure 8S10, J) and obvious expression is observed in the innervating pre-synaptic neurons based on overlapping expression with Syn (Figure 8S10, L). 5-HT7-20XV5 expression was also observed in the ejaculatory bulb (Figures 8S10, M). Interestingly, none of the OA or serotonin receptors exhibited preferential accumulation in the post-synaptic muscle opposite the pre-synaptic terminals, as observed for GluRIIA. This observation implies volume transmission may play a significant role in modulating muscle activity in the male reproductive system. Neurotransmitter signaling via volume transmission has previously been proposed for the Drosophila female reproductive system based on expression patterns of OA receptors(Rohrbach *et al*. 2024a).

SGNs are essential for male fertility but OGNs are dispensable

Having established that both OGNs and SGNs innervate the male reproductive system an obvious question follows: what are their roles in male fertility? It has previously been reported that OA-deficient flies are male fertile and female sterile (Monastirioti et al. 1996; Cole et al. 2005). However, in Tβh and Tdc2 mutant flies that fail to synthesize OA, glutamate signaling in the OGNs innervating the male reproductive system is still intact. To determine if simultaneously silencing the OGNs innervating the male reproductive system for both glutamate and OA signaling causes sterility, *Tdc2-GAL4-DBD* was combined with *AbdB-AD* and *UAS-BONT-C* to block all synaptic transmission in these neurons (BONT-C cleaves the SNARE protein syntaxin) (Han *et al*. 2022)). This intersectional combination results in the silencing of only the Tdc2 neurons in the posterior VNC by virtue of the restricted expression of the AbdB-AD hemidriver to the posterior few segments of the VNC. The result was the same as eliminating OA signaling alone, males were fertile, and females were sterile (Table 1), thus establishing that neither OA nor glutamate signaling is required for fertility in the OGNs innervating the male reproductive system. The observed female sterility validates the silencing function of the UAS-BONT-C transgene.

To assess the requirement of the SGNs innervating the male reproductive system for fertility, flies containing TRH-DBD, AbdB-AD, and UAS-BONT-C were generated. Both males and females of this genotype were sterile (Table 1). The observation that females were also sterile, while no serotonergic innervation of the female reproductive system has been reported, suggests the male sterility is due to 5-HT neurons common to both males and females, and thus the male sterility cannot be unambiguously attributed to the SGNs innervating the male reproductive system.

In an attempt to identify a split-GAL4 combination that more specifically targets SGNs innervating the male reproductive system, several dozen hemi-drivers that express in neurons whose cell bodies are located in the most posterior region of the VNC were screened for male sterility in combination with UAS-BONT-C and either *TRH-AD* or *TRH-GAL4-DBD*, as appropriate. One line, *VT019028-GAL4-DBD* was identified that resulted in male sterility and female fertility, suggesting silencing of male-specific sexually dimorphic neurons, and not neurons common to both males and females, were responsible for the male sterility. The *TRH-AD*/*VT019028-GAL4-DBD* driver in combination with a *UAS-His2A-GFP* nuclear reporter results in expression in sparse neurons in the brain and VNC as well as around two dozen neurons at the posterior tip of the VNC (Figure 9, A). Female flies of the same genotype exhibited a similar sparse pattern of expression in the brain and VNC with the exception that there were noticeably fewer His2A-GFP expressing neurons at the tip of the VNC (Figure 9, B). The neurons most likely responsible for male sterility are those unique to males. The *VT019028-GAL4-DBD* driver was also assessed for fertility in combination with *AbdB-*

Genotype	Male Fertile	Female Fertile
yw; TRH-GAL4DBD/AbdB-AD, UAS-BONT-C	No	No
yw; Tdc2-GAL4DBD/AbdB-AD, UAS-BONT-C	Yes	No
yw; VT019028-GAL4-DBD/AbdB-AD, UAS-BONT-C	No	Yes
yw; TRH-AD; UAS-BONT-C/VT019028-GAL4-DBD	No	Yes
yw; AbdB-AD/UAS-BONT-C	Yes	Yes
yw; UAS-BONT-C	Yes	Yes
Canton-S wildtype	Yes	Yes

Table 1. **Male and female fertility phenotypes.**

AD and *UAS-BONT-C* with the same result of male sterility and female fertility (Table 1). The expression patterns of *VT019028-GAL4-DBD* with *AbdB-AD* in combination with *UAS-His2A-GFP* reveals restricted expression to the tip of the ventral nerve cord with noticeably more neurons in the male (Figure 9A, C and D). These results with *AbdB-AD* narrow the neurons responsible for the male sterility to the tip of the VNC. The expression patterns of 5-HT and Tdc2 in these immunostains are also shown (Figures 9, E-H, and I-L, respectively).

To determine if any of the *VT019028-GAL4-DBD* neurons intersecting with *TRH-AD* or *AbdB-AD* are serotonergic or octopaminergic, higher resolution images of the tip of the VNC were examined. In the full confocal stack image, Three His2A-GFP neurons are clearly visible that overlap with 5-HT (Figure 9S1, D). However, it has previously been shown that there are both dorsal (~10 neurons) and ventral (~9 neurons) clusters of serotonergic neurons innervating the male reproductive system (Billeter et al. 2006b) and some neurons may thus be obscured from a dorsal perspective. A partial stack containing the dorsal cluster reveals the same three neurons (Figure 9S1, I).

However, a ventral view of these neurons shows a fourth neuron overlapping with 5-HT (Figure 9S1, K). A partial stack of the ventral cluster reveals three His2A-GFP neurons overlapping with 5-HT (Figure 9S1, O). There also appears to be one or two Tdc2 neurons overlapping with His2A-GFP. However, examination of three-dimensional images revealed they are only in close proximity but not overlapping.

Similar results were obtained with *VT019028-GAL4-DBD* neurons intersecting with *AbdB-AD*. Four His2A-GFP neurons overlap with 5-HT in a full confocal stack view (Figure 9S2, D). These four neurons are visible in the dorsal serotonergic cluster (Figure 9S2, I), while three additional His2A-GFP neurons overlapping with 5-HT are apparent in the ventral serotonergic neuron cluster (Figure 9S2, N). One His2A-GFP neuron appears to overlap with Tdc2 (Figure 9S2, E), but this apparent overlap is not reproduced in the dorsal (Figure 9S2, J) or ventral (Figure 9S2. O) partial stacks. The innervation of *VT019028-GAL4-DBD* neurons with *TRH-AD* and *AbdB-AD* visualized with the *UAS-CD8-mCherry* reporter is similarly broad in the SVs, ED, and AGs (Figure 9S3, A and B, respectively). Taken together, these results strongly suggest synaptic transmission in the SGNs included in the *VT019028-GAL4-DBD* intersections with *TRH-AD* and *AbdB-AD* that innervate the male reproductive organs are required for male fertility, although a role for the small number of other interneurons at the tip of the VNC in common between both combinations cannot be excluded.

To rule out the possibility that the male sterility observed in the *VT019028-GAL4-DBD* intersections with *UAS-BONT-C* and either *TRH-AD* and *AbdB-AD* is due to failure to mate, mating assays were performed where single males and single females of the different genotypes were placed together in a well of a 12-well plate and videotaped. The mating success rates of *VT019028-GAL4-DBD*/*TRH-AD* and *VT019028-GAL4-DBD*/*AbdB-AD* were 81.25% (n=16) and 57.9% (n=28), respectively. These results demonstrate the observed male sterility is not due to failure to copulate.

In these mating assays, mating duration was also assessed along with several control genotypes. Mean mating durations for *VT019028-GAL4-DBD*/*TRH-AD* and *VT019028-GAL4-DBD*/*AbdB-AD* were 28.74 and 24.75 minutes, respectively (Figure 10, A). This was not significantly different from *Canton-S* wildtype controls (26.91), and other controls missing one or more of the components necessary for silencing *AbdB-AD*, *UAS-BONT-C* (27.07) and *UAS-BONT-C* alone (28.75) (Figures 10, B and C). These results are in line with previously reported mating durations for Drosophila (Crickmore and Vosshall 2013). Interestingly, silencing all 5-HT neurons (*TRH-GAL4-DBD* ∩ *AbdB-AD*) or all OA neurons (*Tdc2-GAL4-DBD* ∩ *AbdB-AD*) innervating the male reproductive system resulted in statistically significant reductions in mating duration, 19.11 (Figure 10D) and 21.8 (Figure 10E), respectively.

To assess the distribution of sperm in the reproductive system during mating by *VT019028-GAL4-DBD*/*TRH-AD* > *UAS-BONT-C* sterile males, a Protamine-GFP (Prot-GFP) reporter that fluorescently labels sperm nuclei was incorporated into the genotype. For this experiment, control and experimental males were placed in petri dishes with virgin females, separated 10 minutes after the initiation of mating, immediately dissected, and the isolated male reproductive systems video

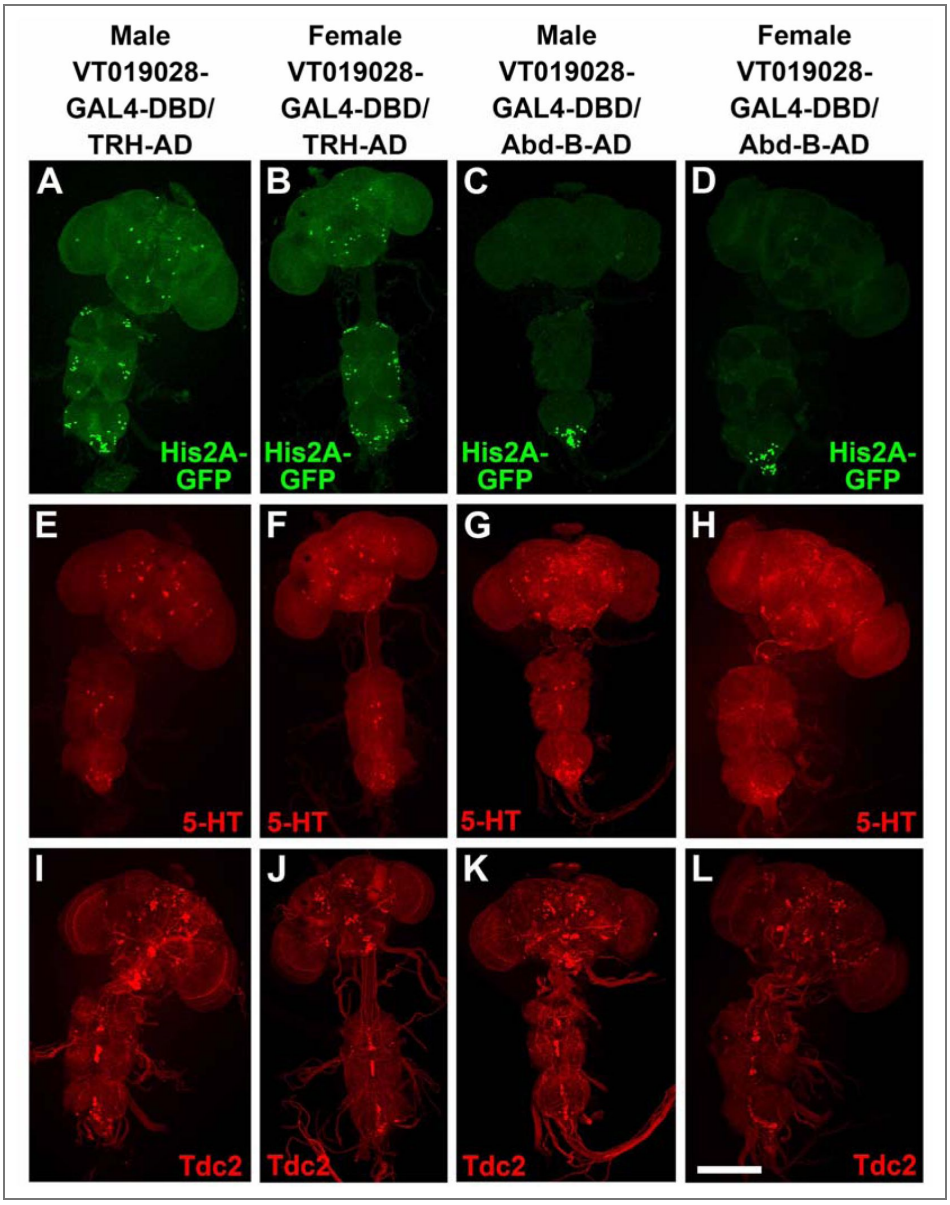

Figure 9. Low resolution images of nuclear expression of *VT019028-GAL4-DBD* in combination with *TRH-AD* and *AbdB-AD* in Drosophila male and female adult nervous system relative to 5-HT and Tdc2.

A-D) nuclear expression using HIS2A-GFP marker. A) male *VT019028-GAL4-DBD*/*TRH-AD*; B) female *VT019028-GAL4-DBD*/*TRH-AD*; C) male *VT019028-GAL4-DBD*/*AbdB-AD*; B) female *VT019028-GAL4-DBD*/*AbdB-AD*. E-H) 5-HT expression. E) male *VT019028-GAL4-DBD*/TRH-AD; F) female *VT019028-GAL4-DBD*/*TRH-AD*; G) male *VT019028-GAL4-DBD*/*AbdB-AD*; H) female *VT019028-GAL4-DBD*/*AbdB-AD*. Tdc2 expression. I) male *VT019028-GAL4-DBD*/*TRH-AD*; J) female *VT019028-GAL4-DBD*/*TRH-AD*; K) male *VT019028-GAL4-DBD*/*AbdB-AD*; L) female *VT019028-GAL4-DBD*/*AbdB-AD*. Scale bar: 200μm.

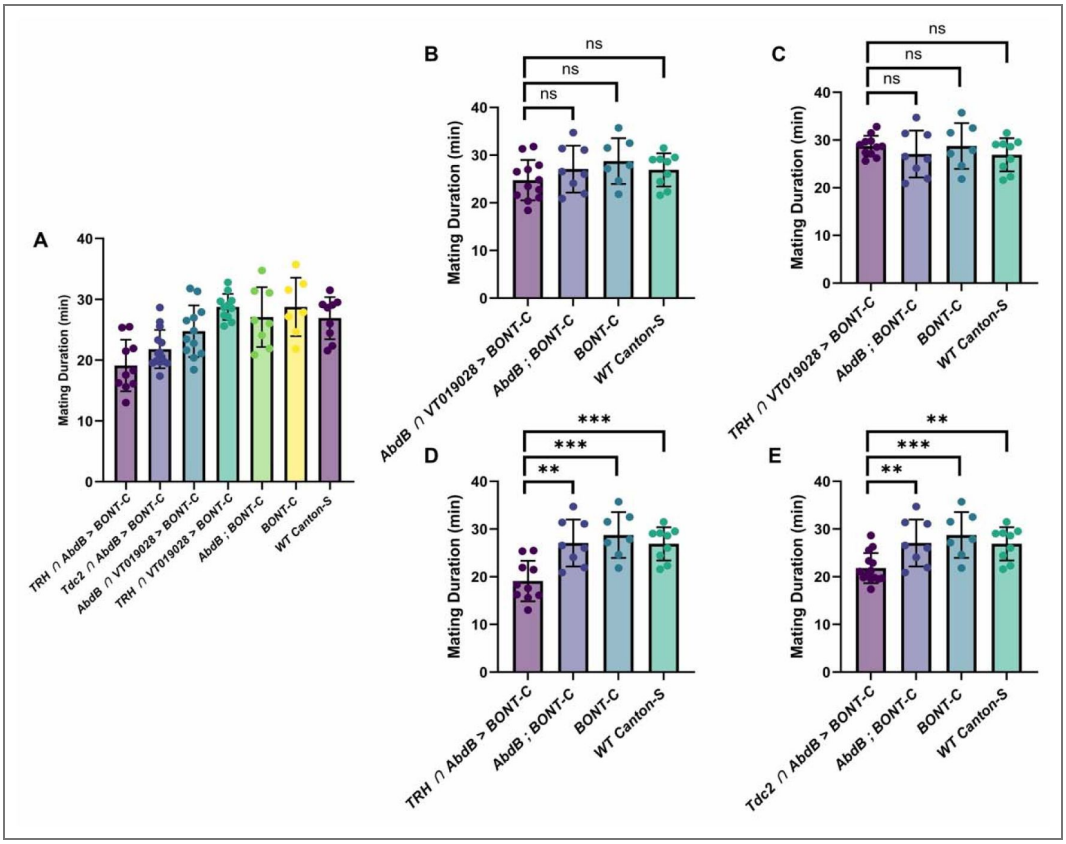

Figure 10. Comparison of mating duration between genotypes.

Bar plots show the mean ± SD for each group with individual data points overlaid on each bar. Statistical comparisons were made using unpaired two-tailed t tests where appropriate. Asterisks above indicate significance levels: $p < 0.001$ (**), $p < 0.0001$ (***), ns = not significant. (A) Columns from left to right: TRH ∩ AbdB > BONT-C: n= 10, mean= 19.11, SD=4.251. Tdc2 ∩ AbdB > BONT-C: n=14, mean=21.80, SD= 3.155. AbdB ∩ VT019028 > BONT-C: n=12, mean=24.75, SD=4.247. TRH ∩ VT019028 > BONT-C: n=11, mean=28.74, SD=2.155. AbdB; BONT-C: n=8, mean=27.07, SD=4.907. BONT-C: n=7, mean=28.75, SD=4.809. WT Canton-S: n=9, mean=26.91, SD=3.473.

recorded using a stereofluorescent microscope. In the control males, Prot-GFP sperm were readily visible in the ED (Figure 10S1, A, Video 1). In contrast, in the experimental males, no Prot-GFP sperm were observed (Figure 10S1, B, Video 2). ProtB-GFP expression in the reproductive systems of wildtype Canton-S females mated to these same male genotypes was also assessed. In this experiment matings were allowed to go to completion and the female reproductive systems were dissected immediately thereafter. An abundance of Prot-GFP sperm were observed in females mated to the control males (Figure 10S1,C), while no Prot-GFP sperm were observed in females mated to *VT019028-GAL4-DBD/TRH-AD > UAS-BONT-C* males (Figure 10S1, D). These results demonstrate that the male sterility is due to a failure of the sphincter that regulates the flow of sperm between the SV and ED to open and thus the defect is with the emission phase of ejaculation.

Glutamate signaling in OGNs and SGNs is dispensable for male fertility

In the *VT019028-GAL4-DBD/TRH-AD > UAS-BONT-C* sterile males, 5-HT and glutamate signaling are both abolished due to the BONT-C blockade of synaptic transmission. To determine if glutamate signaling alone is required in these neurons, a conditional allele of vGlut in which the vGlut coding sequence is excised by recombination (Sherer *et al*. 2020), was incorporated into this genotype such that specifically glutamate signaling was eliminated while serotonergic signaling remained intact. These males were determined to be fertile. To ascertain whether there were changes in the level of fertility, fertility assays were conducted on 5-day post-eclosion males. No changes in fertility as compared to controls were observed (Figure 10S2, A). Immunostaining the AGs of control and experimental flies confirmed the effectiveness of the conditional vGlut allele by the presence of vGlut in control flies and its absence in experimental flies (Figure 10S3, A and D, respectively). As glutamate has been shown to promote neuron survival as neurons age (Shen et al. 2018; Buck et al. 2023), to determine if fertility might be altered in older males, the same 5-day old males used in the previous fertility experiment were held in isolation from females until they were 30 days post-eclosion and the experiment was repeated. While there was not unexpectedly a modest decrease in fertility with age, no differences in fertility were apparent between the control and experimental genotypes (Figure 10S2, B). These results establish that glutamatergic signaling is not required in *VT019028-GAL4-DBD/TRH-AD* neurons for fertility. To determine if more extensive elimination of glutamate signaling in the OGNs and SGNs would alter fertility, glutamate was specifically eliminated in both classes of neurons. No reductions in fertility were observed in 5-day post-eclosion males (Figure 10S2, A). These results indicate glutamate is not required in either OGNs or SGNs for fertility.

The sphincter region of the SV initiates ED peristaltic waves

Neuron-independent peristaltic waves are known to occur spontaneously in the male ED of Drosophila that persist even when all nerves innervating the male reproductive system have been severed (Norville et al. 2010). To gain a better understanding of the muscle activity occurring during these waves in both the ED and throughout the rest of the male reproductive system, a fly strain was generated that expressed the Ca++ sensor GCAMP8m specifically in muscles under control of the myosin heavy chain promoter (*MHC-GCAMP8m*). This fly strain allows visualization of the changes in Ca++ levels that occur in the muscles during these peristaltic waves. As expected, waves of fluorescence are visualizable coincident with peristaltic waves of muscle contractions in the ED (video 3). These peristaltic waves originate not in the ED but in the sphincter region of the SV just prior to and after the point of SV fusion (video 4), although the region of the SV prior to the fusion point that is involved in initiation varies (video 5).

Muscle contractions in other regions of the male reproductive system are also apparent. These contractions are weak and seemingly random in the SV (video 6), AG (video 7), and testes (video 8), but occasionally in the AG strong coordinated contractions are observed (video 9). Together, these imaging data reveal that the seminal-vesicle sphincter acts as an autonomous pacemaker, launching neuron-independent peristaltic waves that drive ejaculatory-duct motility.

Discussion

The male reproductive tract of flies and mammals have obvious morphological differences, yet they share many essential anatomical features and a common organizational logic. During copulation Drosophila males deliver seminal fluid and ~4000-6000 sperm to females during a tightly choreographed ~20-minute window (Kaufman 1942; Gilbert 1981). This involves the emission of sperm and seminal fluid from their sites of origin into the ED where they mix and are subsequently expelled into the female reproductive tract. Despite the critical importance of ejaculation, its neuronal mechanisms have remained poorly defined, hindering broader insights into the neural logic of male fertility. Here we close this gap by demonstrating that two distinct yet intermingled classes of amine/glutamate neurons, OGNs and SGNs, coordinate the ejaculatory sequence that ensures successful reproduction. Their transmitter pairs confer the capacity to co-release both fast excitatory and slower acting aminergic modulatory neurotransmitters. Differential expression of ionotropic glutamate receptors and aminergic metabotropic neurotransmitter receptors combine in post-synaptic muscle across the male reproductive system to confer an additional level of complexity to coordinately regulate fluid secretion, organ contractility, and directional sperm movement, to the end of optimizing male fertility.

This system can serve as a genetically tractable model to gain general insights into how multi-transmitter neurons coordinate and modulate interrelated action sequences critical for complex organ function. Lessons learned from this system may have implications for understanding how males of Drosophila and other species adapt their reproductive strategies to a dynamic environment. Additionally, understanding the mechanisms by which this system operates has the potential to identify neuromodulation strategies for male infertility and prostate cancer as multi-transmitter sympathetic and parasympathetic neurons innervating human male reproductive organs have been implicated in these conditions (Burnstock 2009; Magnon *et al*. 2013; Burnstock 2014; Drobnis and Nangia 2017; Dwivedi *et al*. 2021).

Mechanisms of multi-transmitter neuron-mediated transfer of sperm and seminal fluid

Movement of sperm and seminal fluid through the male reproductive tract requires an alternating series of coordinated muscle contractions and relaxations. Based on the observed co-packaging of vMAT and vGlut in the majority of synaptic vesicles in the ED of both the OGNs and SGNs, combined with the observed non-uniform distribution of neurotransmitter receptors for OA, 5-HT, and glutamate in neurons and muscles, potential pre- and post-synaptic mechanisms for regulating the activity of the muscles of the internal male reproductive system are possible.

Pre-synaptic expression of the α-type OA receptors OAMB and OAα2R may facilitate alternating bursts of action potential-dependent neurotransmitter release by diminishing pre-synaptic neurotransmitter release via an auto-receptive mechanism. As α-type adrenergic and noradrenergic receptors have been consistently shown to inhibit neurotransmitter release in multiple rodent species in both the peripheral and central nervous system including the vas deferens, heart, and brain when expressed in pre-synaptic neurons (Starke 1972; Trendelenburg et al. 1994; Miyazaki et al. 1998; Scheibner et al. 2001; Trendelenburg et al. 2003), the presence of OAMB and OAα2R in the pre-synaptic terminals of neurons innervating the internal male reproductive organs may have the effect of suppressing neurotransmitter output from pre-synaptic terminals and shortening the duration of muscle contractions. Thus, pre-synaptic expression of OAMB and OAα2R may have the effect of increasing the cycling frequency of muscle contractions and relaxations.

As glutamate is acting via post-synaptic GluRII-type receptors, its effect will almost certainly be excitatory with the result of eliciting fast muscle contractions. In contrast, the functional consequences of OA and 5-HT are not so clear cut. Either of these amines could enhance muscle contractions or facilitate muscle relaxation, depending on the neurotransmitter receptor(s) receiving the signal. In muscles of the mammalian prostate and lower urinary tract, α-type adrenergic and noradrenergic receptors have been demonstrated to augment muscle contractions

while β-type receptors have been found to facilitate muscle relaxation (Honda et al. 1985; Michel and Vrydag 2006; Wuest et al. 2009). In contrast, OAMB and OAβ2R have been shown to enhance muscle relaxation and contraction, respectively in the Drosophila female reproductive system (Deshpande et al. 2022).

5-HT7 receptors are known to promote smooth muscle relaxation in the urinary tract, gut, oviduct, and blood vessels of mammals (Carter et al. 1995; Leung et al. 1996; Prins et al. 1999; Inoue et al. 2003; Recio et al. 2009; Chang Chien et al. 2015; Matsumoto-Miyai et al. 2015). Although muscle contraction receives preferential focus, muscle relaxation is also critically important for the execution of motor programs (Goulding et al. 2014; Wong and Lange 2014; Gowda et al. 2018; Hiramoto et al. 2021) and 5-HT7 most likely plays a role in mediating muscle relaxation in the internal male reproductive system. An additional confounding factor is that OAα2R has been shown to respond not just to OA but also to 5-HT (Qi et al. 2017). The observations of the presence of both muscle contraction enhancing, and muscle relaxation promoting, OA and 5-HT receptors in the same muscles of the internal male reproductive organs indicates the mechanisms of neuronal regulation of their activity are complex and may even involve synergistic effects that can only be established empirically.

A potential timing mechanism mediated by multi-transmitter neurons

Pre-synaptic release of glutamate acting on post-synaptic ionotropic GluRII-type glutamate receptors will cause near immediate, short-term, contraction of muscles. At least in the ED, our results show that the majority of synaptic vesicles co-package either OA or 5-HT along with glutamate, and thus simultaneous co-release is being used as a mechanism of neurotransmitter signaling. The amines OA or 5-HT acting on post-synaptic metabotropic OA and 5-HT receptors will have the effect of either prolonging the length of, or augmenting the relaxation of, muscles, dependent on the specific aminergic neurotransmitter receptors involved. These latter effects will be delayed relative to the glutamate-induced fast muscle contractions due to the discrepancy in the time course of action between ionotropic and metabotropic receptors. Thus, co-releasing a fast-acting excitatory neurotransmitter acting through an ionotropic receptor simultaneous with a modulatory aminergic neurotransmitter acting through slower acting GPCRs in the same multi-transmitter neuron may create a sequential timing mechanism whereby fast glutamate-mediated muscle contractions always precede either amine-mediated prolonging of muscle contraction or facilitation of muscle relaxation. A single neuron co-releasing one fast and one slow neurotransmitter may thus have the advantage over two distinct neurons separately releasing these transmitters in that the former can more effectively synchronize, and at the same time, stagger events that require precise timing.

Potential for adaptation to environment

The complexity of neuronal control of male reproductive function revealed in this investigation exposes a variety of possibilities for adaptive regulation to dynamic environmental conditions. Polygynous Drosophila males are well-established to alter the quantity and quality of their ejaculate based on environmental circumstances, especially the level of competition with other males (Bretman et al. 2009; Moatt et al. 2014), but also due to nutrient availability (Macartney et al. 2021) and the presence of pathogens (Liao et al. 2024). The male reproductive system may adapt to environmental conditions by tuning octopamine, serotonin, and glutamate signaling, adjusting the levels of their biosynthetic enzymes, the vesicular glutamate and monoamine transporters vGlut and vMAT, or relevant receptors to alter the amount of sperm and seminal fluid released during copulation. Given that glutamate-deficient SGNs and OGNs, as well as BONT-C-silenced OGNs, show no readily detectable male fertility defects under benign laboratory conditions, the primary role of glutamate and octopamine may be to optimize male reproductive success under fluctuating or adverse environmental conditions.

An additional potential mechanism for altering OA and/or 5-HT levels is extra-synaptic volume transmission whereby the level of OA or 5-HT secreted into the hemolymph in locations anatomically distant from the male reproductive system. Thus, global levels of OA and 5-HT in the hemolymph could be adjusted based on environmental conditions and this signal could then impact the male reproductive system to optimize ejaculate quality and quantity. Finally, the presence of OAMB and 5-HT7 on epithelial cells suggest the potential for the regulation of the quality of seminal fluid as the expression of these receptors implies, they could differentially alter gene expression in the epithelial cells in response to changing levels of OA and 5-HT. The results of this study create a foundation for mechanistic investigations into the molecular basis by which male reproductive resources are adaptively modulated.

Potential for signaling via neuropeptides

The broad abundant expression of the LDCV reporter IA2 in the neurons innervating the internal organs of the male reproductive system suggests a significant role for neuropeptide signaling since neuropeptides are known to be packaged into LDCVs (Pelletier and Leclerc 1979; Kreiner et al. 1986). Bolstering the prospect of this possibility, numerous neuropeptides across evolutionary distant insect species have been shown to alter the frequency and/or amplitude of the spontaneous peristaltic waves in the ED of male insect reproductive systems (Marciniak et al. 2017; Cizmar et al. 2019; Lange et al. 2023). Multiple neuropeptides have also been implicated in the function of the internal male reproductive organs of mammals, including humans, (Segawa et al. 1978; Allen et al. 1982; Tainio 1995). Given these considerations, it thus seems likely that neuropeptides outside the scope of this investigation also play a role in regulating Drosophila male reproduction.

The SV/ED junction is a control center

Immediately proximal to the ED, SVs fuse into a single duct that forms the sphincter regulating sperm flow from the SV to the ED during mating. The differential expression patterns of OAα2R, OAβ2R, and 5-HT7 in this region of the SV is intriguing. The extent of OAα2R and OAβ2R expression ends very shortly after the merge, at precisely the point where full SV fusion occurs and there is no longer a partition separating the ducts (Bairati 1968). Only 5-HT7 expression extends into the fully fused SV that constitutes the sphincter separating the SV from the ED. This expression pattern implies a prominent role for 5-HT7 in sphincter regulation. Previous reports of 5-HT7 mediating relaxation of smooth muscle in the mammalian gut (Carter et al. 1995; Prins et al. 1999), urinary bladder neck (Recio et al. 2009), cardiovascular system (Leung et al. 1996; Chang Chien et al. 2015), lymphatic system (Chan and von der Weid 2003), and oviduct (Inoue et al. 2003) raises the possibility it may function to relax the sphincter muscles during copulation to permit sperm flow, consistent with our observations that silencing a subset of serotonergic neurons results in male fertility due to failure of sperm emission into the ED (Figure 10S1). Additionally, expression of OAβ2R and the likely relaxation-promoting 5-HT7 receptors increases sharply in the SV just prior to the point of fusion. Perhaps not coincidentally, this limit of expression corresponds with the distal-most extent of sperm localization in the SV where relaxation of the SV muscles must also occur for sperm to move along the duct to the ED. It is also notable, as revealed in the Ca++ imaging experiments, that the sphincter region is the site of initiation of the peristaltic waves of muscle contractions that are promulgated through the ED. The SV/ED junction is thus a critical control center for both regulation of sperm flow into the ED during mating and initiating neuron-independent peristaltic waves in the ED.

Molecular continuity of neurotransmitter signaling between males and females?

The expression of 5-HT7 and OAβ2R on the apical surface of the epithelial cells lining the AG and ED, respectively, is surprising because it implies that levels of 5-HT and OA are fluctuating in the lumen of these organs. The origin of these neurotransmitters is not obvious but if OA and 5-HT are present in the lumen of the AG and ED, another intriguing possibility is that these

neurotransmitters are transferred to the female at mating for signaling in order to modulate female behavior and/or reproductive activity. A recent study detailed the molecular continuity of proteins in the seminal fluid of males functionally interacting with proteins in the female reproductive tract (Mccullough et al. 2022). The potential presence of OA and 5-HT in the lumen of the AG and ED raises the possibility that this molecular continuity could extend to neurotransmitters in male seminal fluid signaling to neurotransmitter receptors in the female reproductive tract to convey information such as health, internal state, or environmental conditions to regulate female reproductive output. A detailed examination of the expression patterns of OA receptors in the female reproductive tract indicates this is indeed a possibility, at least for OA signaling (Rohrbach *et al*. 2024b).

Materials and methods

Fly strains

Stocks from the Bloomington Drosophila Stock Center (NIH P40OD018537) were used in this study. *Tdc2-GAL4* (Cole et al. 2005) *RRID:BDSC_9313*, *GluRIIA-GAL4*

RRID:BDSC_84637, *GluRIID-GAL4 RRID:BDSC_84638*, and *TRH-GAL4*

RRID:BDSC_84694 (Deng et al. 2019)

vGlut-GAL4 RRID:BDSC_60312, *vGlut-GAL4-DBD* (Diao et al. 2015)

Tdc2-AD (Dionne et al. 2018) *RRID:BDSC_601902*

TRH-GAL4-DBD RRID:BDSC_70371

TRH-AD RRID:BDSC_70975

GluRIIB-GAL4 RRID:BDSC_60333 and *GluRIIE-GAL4 RRID:BDSC_60332* (Diao et al. 2015)

Oct-TyrR-GAL4 RRID:BDSC_77735 and *GluRIIC-GAL4* RRID_83268 (Lee et al. 2018)

GluRIIA-GFP RRID:BDSC_99517 (Beckers et al. 2024)

5-HT1A-GAL4 RRID:BDSC_84588, *5-HT1B-GAL4 RRID:BDSC_84589*, *5-HT2A-GAL4*

RRID:BDSC_84590, *5-HT2B-GAL4 RRID:BDSC_84591*, and *5-HT7-GAL4*

RRID:BDSC_84592 (Deng et al. 2019)

TβH-GFP RRID:BDSC_80113 (Li-Kroeger et al. 2018)

fru-GAL4 RRID:BDSC_66696

UAS-CD8-mCherry RRID:BDSC_27392

ProtB-GFP (Manier et al. 2010) *RRID:BDSC_58406*

AbdB-AD (Diao et al. 2024)

vGlut-AD (Gao et al. 2008)

IA2-GFP (Yu et al. 2025)

UAS-BONT-C (Han et al. 2022)

dsx-GAL4-DBD (Shirangi et al. 2016)

vGlut-40XV5 and *vGlut-40XMYC* (Stowers 2025)

B2RT-7XMYC-vAChT (Tison et al. 2020)

RSRT-9XV5-vGAT (Certel et al. 2022)

OAMB-GAL4, *OAα2R-GAL4*, *OAβ1R-GAL4*, *OAβ2R-GAL4*, *OAβ3R-GAL4* (Mckinney et al. 2020)

FRT-F3 OAMB-10XV5 (Bakshinska et al. 2025)

B3RT-Tdc2-LexA, *B3RT-vGlut-LexA*, *RSRT-STOP-RSRT-6XV5-vMAT*, *UAS-B3* and *20XUAS-R* (Sherer et al. 2020)

20XUAS-B2 (Williams et al. 2019)

13LexAop-6XmCherry (Shearin et al. 2014)

Stocks original to this report

Tdc2-GAL4-DBD (*JK65C*)

B3RT-Tdc2-LexA germline excision

B3RT-vGlut-LexA germline excision

RSRT-6XV5-vMAT germline excision

FRT-F3-OAα2R-20XV5

FRT-F3-OAα2R-20XV5 germline inversion

B2RT-STOP-B2RT-OAβ2R-40XV5

B2RT-OAβ2R-40XV5 germline excision

5-HT7-20XV5

MHC-GCAMP8m (*VK27*)

Entry clones

The *R4-GAL4-DBD-R3* entry clone contains a 640bp insert encoding the GAL4 DNA binding domain. The *L1-MHC-5'Reg-R5* entry clone contains 5254bp of upstream regulatory sequence from the Drosophila Myosin Heavy Chain (MHC) gene. The *L5-GCAMP8m-L2* entry clone contains a 1276bp insert encoding GCAMP8m (Zhang et al. 2023). Entry clones were generated as previously described (Petersen and Stowers 2011).

Expression clones

Tdc2-GAL4-DBD was constructed by combining entry clones *L1-Tdc2-5'Reg-L4* and *L3-Tdc2-3'Reg-L2* (Shearin et al. 2013) with the *R4-GAL4-DBD-R3* entry clone and the destination vector *pDESTP10* (Shearin et al. 2013). *MHC-GCAMP8m* was assembled by combining entry clones *L1-MHC-5'Reg-R5* and *L5-GCAMP8m-L2* with *pDESTP10-SPEC*. *pDESTP10-Spec* is a derivative of *pDESTP10* in which AmpR was replaced with SpecR.

Donor plasmid assembly

Donor plasmids were assembled starting with gene synthesis of the homology arms (Synbio). The gene synthesis also included recombinase target sites and mutations in the PAM sites associated with the guide RNAs. Homology arms typically extended ~750bp beyond the cut sites of the guide RNAs. STOP cassettes were added via Gibson cloning. Multimerized epitope tags (Stowers 2025) were added via *Asc I*/*Not I* restriction enzyme cloning. The *OAα2R-FRT-F3-20XV5* donor plasmid contained a pair of *FRT-F3* sites appropriately arranged for conditional expression of OAα2R-20XV5 after inversion/excision by FLP recombinase (Fisher *et al*. 2017) with the 20XV5 fused to the carboxy-terminus. The *OAβ2R-B2RT-STOP-B2RT-40XV5* donor plasmid contained B2 recombinase target sites flanking a STOP cassette such that OAβ2R-40XV5 was expressed after excision of the STOP cassette with 40XV5 fused to the carboxy-terminus. The 5-HT7-20XV5 donor plasmid contained a 20XV5 multimerized epitope tag fused to the carboxy-terminus but was not designed for conditional expression.

Guide RNA plasmid assembly

Guide RNAs were assembled in the *pCFD4* double-guide RNA plasmid as previously described (Port *et al*. 2014). Two double guide RNA plasmids were used with each donor construct for genome editing. The guide RNA plasmids and the guide RNAs they contain are as follows: *pCFD4-OAα2RGd12*-TCTAAATCAATATCAGTG and AACATAAACATCCTAAAA; *pCFD4-OAα2R-Gd34*-ACCTGTAACAGCACACAT and GGCATGTATCAGCACTAC; *pCFD4-OAβ2R-Gd56*-ATAAATGAGATTATACTC and CATGCATCTGGAATTTAT; *pCFD4-OAβ2R-Gd78*-

CGGCGGGCGGATCCCGCC and AGGATGGCAGGGAGTCGA; *pCFD4-5-HT7-Gd56-*TGGGCGATGAGAGGCACG and TGGGCGATGAGAGGCACG; *pCFD4-5-HT7-Gd78-*CCACGAGGACCTCCATTC and GGGTCTTCCCTAGGTTTC.

Genome editing

For each genome edit, the donor plasmid was injected together with both *pCFD4* guide RNA plasmids into the *nos-Cas9 attP40* fly strain by Rainbow Transgenic Flies. Adult flies that were injected as embryos were crossed to 3rd chromosome balancer stocks. Candidate progeny males from this first cross containing the *TM6b* balancer chromosome were crossed to yw; n-syb-GAL4, UAS-FLP/TM6c (*OAα2R-FRT-F3-20XV5*, *yw*; *20XUAS-B2*; *n-syb-GAL4* (*OAβ2R-B2RT-STOP-B2RT-40XV5*) or *yw*; *Ly*/*TM6c* (*5-HT7-20XV5*) fly strain and larval progeny were screened by immunostaining. Males whose progeny exhibited positive immunostaining were subsequently crossed to a third chromosome balancer stock to establish stable lines.

Germline excision/inversion

Germline inversion of *OAα2R-FRT-F3-20XV5* was accomplished by crossing to *yw*; *nos-GAL4*; *UAS-FLP*. Males containing all three genetic components were crossed to a third chromosome balancer stock. Individual progeny males from this cross were crossed a second time to the third chromosome balancer stock and non-Tb larva were screened by anti-V5 immunostaining to identify germline excisions. A similar strategy was used with *OAβ2R-B2RT-STOP-B2RT-40XV5* for a germline excision except the initial cross was to *yw*; *nos-GAL4*; *UAS-B2*. *vGlut-LexA* was generated by crossing *B3RT-vGlut-LexA* to *yw*: *nos-GAL4*; *UAS-B3*. Progeny from this cross containing all three genetic components were crossed to a second chromosome balancer stock. Single progeny males were then crossed to a *13XLexAop-6XmCherry* reporter and larva were screened for expression in the ventral nerve cord to identify germline excision positives. A similar strategy was used to create *B3RT-Tdc2-LexA* starting with *B3RT-Tdc2-LexA* (Mckinney et al. 2020). *RSRT-6XV5-vMAT* was generated by crossing *RSRT-STOP-RSRT-6XV5-vMAT* with *yw*; *nos-GAL4*; *UAS-R*. Progeny from this cross containing all three genetic components were crossed to a second chromosome balancer stock. Single progeny males were crossed to the second balancer a second time and larval progeny were subjected to anti-V5 immunostaining to identify germline excisions.

Immunostaining

Male reproductive systems were dissected in PBS and fixed in 4% paraformaldehyde for 30 minutes with rotation. After 2X brief washes with PBS, they were incubated in PBS containing 2% Triton-X 100 and 2% BSA (PBSTB) for at least two hours with rotation. Subsequently, they were incubated in primary antibodies PBSTB for one hour with rotation, followed by overnight incubation at 4°C without rotation to prevent tissue damage. After 3X 5-minute washes in PBSTB, male reproductive systems were incubated for 2-3 hours in PBSTB with secondary antibodies with rotation. After three 5-minute washes in PBS, they were incubated in PBS containing Phalloidin 405 for one hour. After two 5-minute washes in PBSTB and one 5-minute wash in PBS, male reproductive systems were mounted on glass slides in Vectashield Plus (Vector Laboratories, Cat. #H-1900) using a coverslip that was glued on the edges with clear nail polish.

Primary antibodies and dilution factors: The SYN (3C11) mAb 1:20 (Klagges et al. 1996). Brp nc82 mAb 1:40 (deposited at the DSHB by Eric Buchner), Dlg 4F3 mAb 1:40 (Parnas *et al*. 2001), were obtained from the Developmental Studies Hybridoma Bank, created by the NICHD of the NIH and maintained at The University of Iowa, Department of Biology, Iowa City, IA 52242. Mouse anti-V5 SV5-P-K (Novus NBP2-52703) 1:200; rat anti-V5 SV5-P-K (Novus NBP2-81037) 1:200, rabbit anti-V5 SV5-P-K (Novus NBP2-52653) 1:200; Human anti-V5 (Novus NBP2-81035) 1:200; rat anti-MYC 9E10 (Novus NBP2-81020) 1:200, rabbit anti-MYC 9E10 (Novus NBP2-52636), mouse anti-MYC 4A6; (Millipore Sigma) 1:200, mouse anti-vGlut 1:10 (Banerjee et al. 2021), mouse anti-GFP 3E6 (Thermo-Fisher A11120) 1:200; Rabbit anti-GFP (Thermo-Fisher G10362); rat anti-mCherry 16D7 (ThermoFisher-M11217) 1:200, rabbit anti-Tdc2 pab0822-P, Covalab) 1:500; rat anti-5-HT YC5 (Abcam ab6336) 1:300.

Secondary antibodies and dilution factors: Goat anti-Mouse Alexa 405 (Thermo-Fisher A31553) 1:400; Goat anti-Mouse Alexa 488 (Jackson Immunoresearch 115-545-166) 1:400; Donkey anti-Rat Alexa 488 (Jackson Immunoresearch 712-546-153) 1:400, Goat anti-Rabbit Alexa 488 (Thermo-Fisher A32731) 1:400, Goat anti-Mouse Alexa 568 (Thermo Fisher A11031) 1:400, Goat anti-Rabbit Alexa 568 (Thermo Fisher A11036)1:400, Donkey anti-Rat Alexa 568 (Thermo-Fisher A78946) 1:400; Goat anti-Mouse Alexa 647 (Thermo-Fisher A32728) 1:400; Goat anti-Rabbit Alexa 647 (Thermo-Fisher A32733) 1:400; Goat anti-Rat Alexa 647 (Thermo-Fisher A48265 1:400); Donkey anti-Human Alexa 790 (Jackson Immunoresearch 709-655-149) 1:400. Muscles were stained with Phalloidin iFluor405 (Abcam AB176752) 1:800.

Confocal microscopy was performed using a Leica Stellaris DMI8 inverted confocal scanning light microscope in the microscopy facility at the Montana State University Center for Biofilm Engineering.

Expansion microscopy

The Ten-fold Robust Expansion Microscopy (TREx) protocol was used to expand the male ED (ED) (Damstra et al. 2023). Briefly, Drosophila male reproductive systems were dissected and fixed for at least thirty minutes in 4% paraformaldehyde. The ED's were then dissected out and immunostained as described above. Tissues were then incubated in Acryloyl-X solution, 1:100 dilution (Invitrogen, catalog #2604348), overnight, at room temperature and protected from light. The next day, the ED's were rinsed in PBS and incubated in TRex solution at 4 C, for 45-60 minutes. 0.15% ammonium persulfate and 0.15% TEMED was added and the TREx mixture was quickly transferred to chamber slides. TREx mixture with ED's were placed in wells (1 ED per well), coverslipped and allowed to polymerize at 37 C for at least 45 minutes. After gel polymerization, each gel-ED was trimmed to eliminate excess gel. Gel-ED's were incubated in proteinase K (Biolabs, catalog #P81075, 800U/ml) 1:100 solution, overnight at room temperature. Expansion of gel-ED's was done the following day. Three washes in water were performed, at least 20 minutes per wash. DAPI (Thermofisher Scientific, catalog# D1306), 2ug/ml, was added in the first wash to aid in tissue visualization. After the third wash, hydrogel-ED's were trimmed again and placed in chamber slides. 1 hydrogel-ED per well and coverslipped. Imaged expanded ED's in upright confocal (Leica Stellaris 8 DIVE) equipped with a ×40 NA = 0.8 water objective. z Stack-images were deconvoluted using the Lightning confocal function and 3D images were generated for each image. ED's typically expanded approximately tenfold.

Colocalization Analysis

Digitally deconvolved-3D images of expanded EDs were analyzed using ImageJ software (Schindelin et al. 2012). To exclude background in an unbiased manner, we thresholded all images by using the Otsu threshold and calculated Manders' coefficients by using the BIOP JACop.plugin. A scatter plot of green and red pixel intensities (associated with each of the two markers, Vmat and Vglut) was generated by using the colocalization function. Manders' coefficient ranges from 0 to 1, indicating no or complete colocalization. Prior to doing the colocalization analysis of each image, a region of interest (ROI) was traced using the stain from the CD8 marker. This ROI corresponded to an axon terminal.

Mating assays

Mating assays involved placing single 3–7-day old virgin males with single 3-7-day old virgin females in the same well of a 12 well tissue culture plate without anesthesia. The wells of the 12 well plates were half-filled with agarose. Flies were videotaped for three hours. Mating assays were conducted at 25C and 50% humidity in a room dedicated to behavioral assays. Mating was scored by viewing the videos and scorers were blind to the genotypes.

Fertility assays

The fertility assays involved placing single 5 day old or 30-day old virgin males with four 3-7-day old virgin females in fresh vials without anesthesia for six hours. After six hours the males were removed and the four females returned to the vials for 72hrs at which point the females were removed. Six days after removal of the females the pupae on the walls of the vials were counted. The counting was done blind to the genotypes. Fly culturing for all stages of the fertility assays were conducted at 25C and 50% in an incubator.

Animal use

All experiments involving *Drosophila melanogaster* were conducted in accordance with approved protocols and standard laboratory practices. *Drosophila melanogaster* is not considered a vertebrate animal and accordingly does not require Montana State University Institutional Animal Care and Use Committee (IACUC) approval.

Supplementary figures

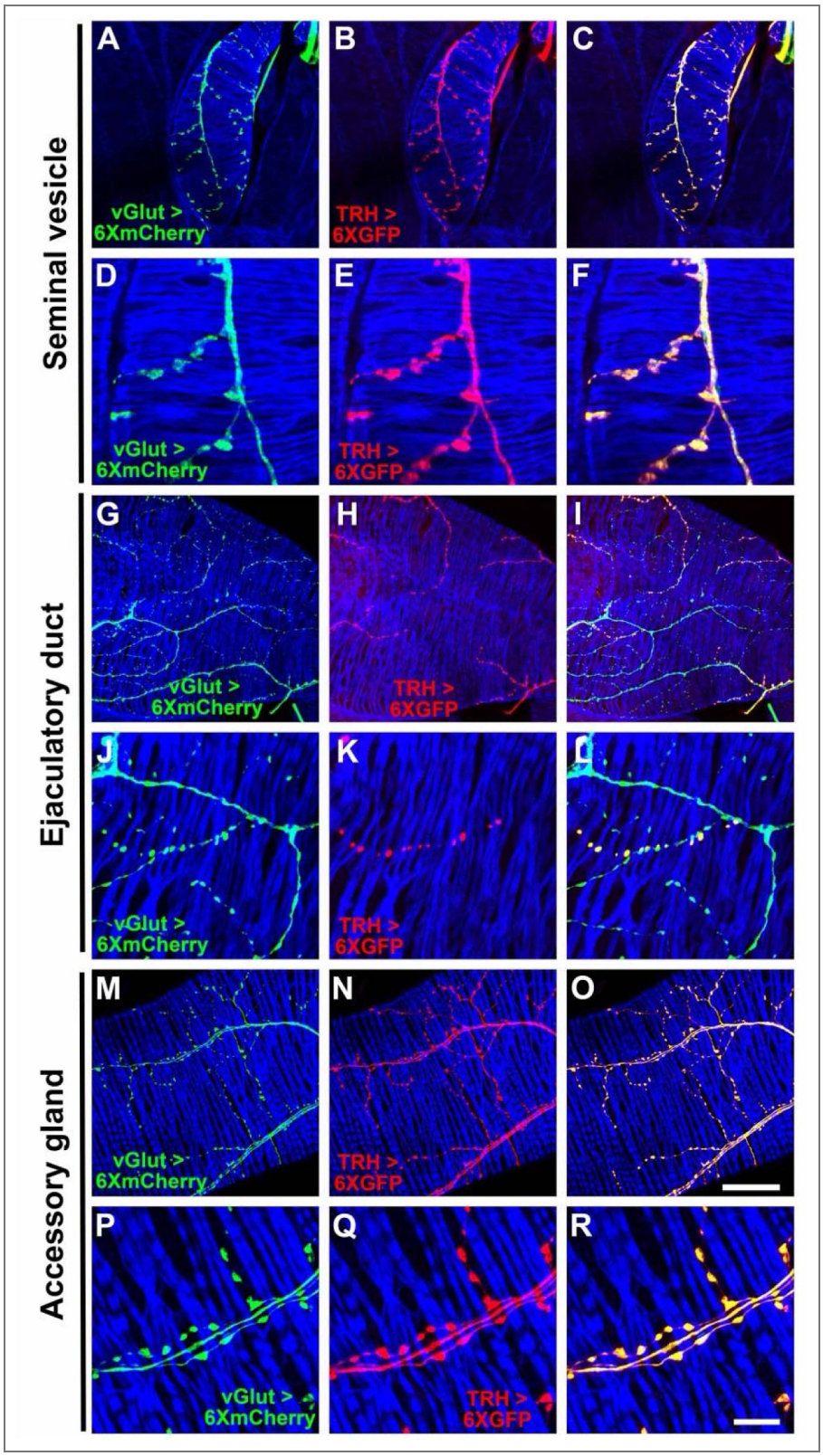

Figure 3S1. Expression of *vGlut-LexA* and *TRH-GAL4* in the Drosophila male reproductive system. A, D, G, J, M, P) *vGlut-LexA*, *LexAop-6XmCherry*; B, E, H, K, N, Q) *TRH-GAL4*, *UAS-6XGFP*. C, F, I, L, O, R) overlay. Scale bars: O-50μm; R-10μm.

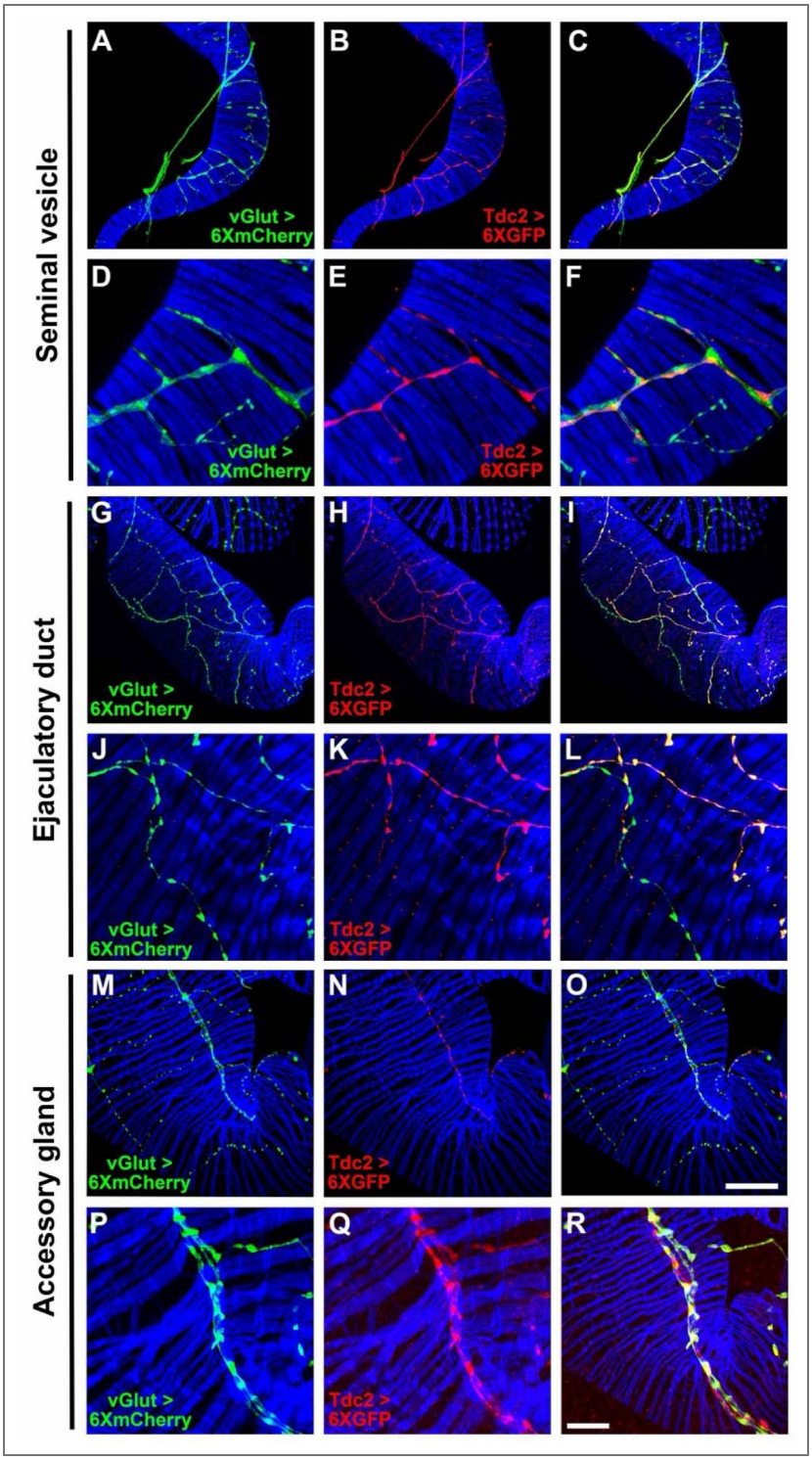

Figure 3S2. Expression of *vGlut-LexA* and *Tdc2-GAL4* in the Drosophila male reproductive system.

A, D, G, J, M, P) *vGlut-LexA, LexAop-6XmCherry*; B, E, H, K, N, Q) *Tdc2-GAL4*, *UAS-6XGFP*. C, F, I, L, O, R) overlay. Scale bars: O-50μm; R-10μm.

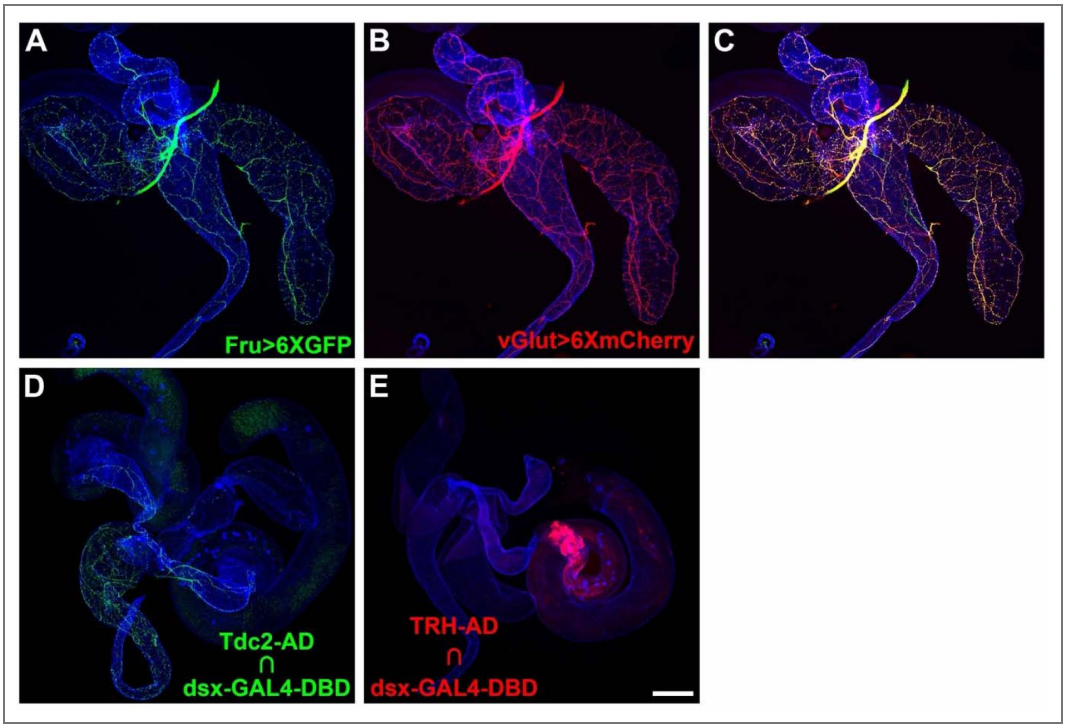

Figure 3S3. Fruitless and Doublesex expression in the Drosophila male reproductive system.

A) *fru-GAL4*, *UAS-6XGFP*; B) *vGlut-LexA*, *LexAop-6XmCherry*; C) overlay; D) Tdc2-AD ∩ dsx-GAL4-DBD; E) TRH-AD ∩ dsx-GAL4-DBD. Scale bar: 200μm.

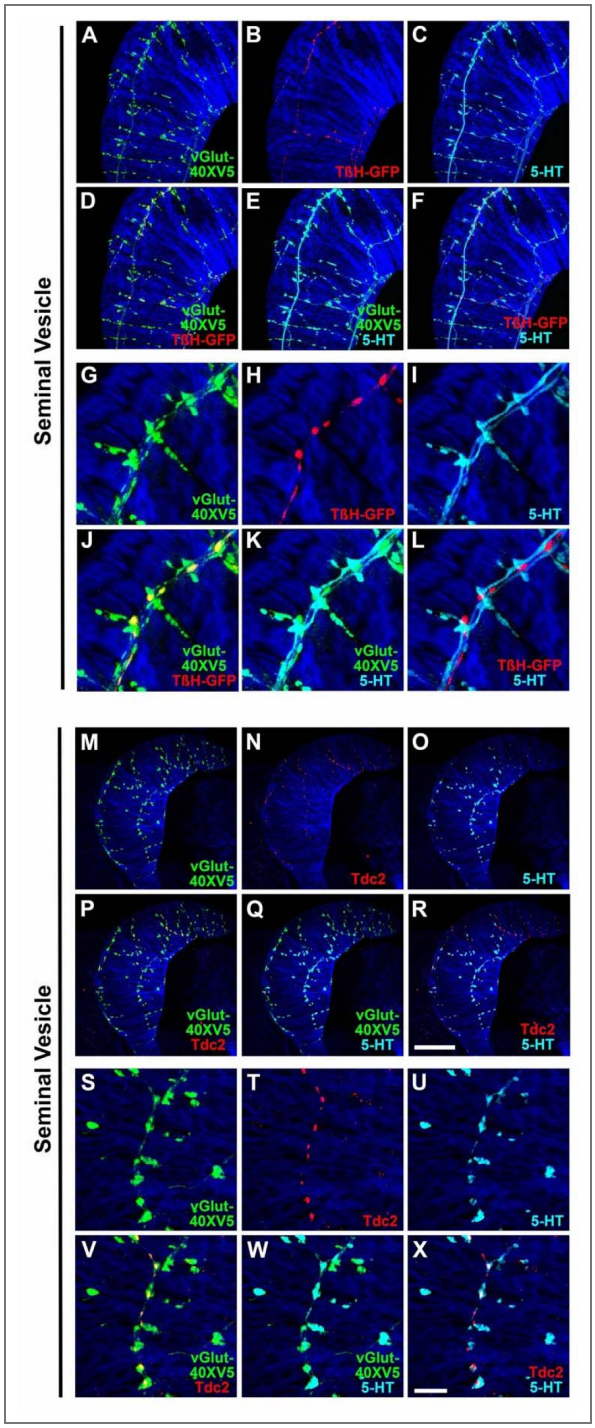

Figure 4S1. Expression of vGlut, TβH-GFP, Tdc2, and 5-HT in the SV of the Drosophila male reproductive system.

A, G) vGlut-40XV5; B, H) TβH-GFP; C, I) 5-HT; D, J) vGlut-40XV5, TβH-GFP overlay; E, K) vGlut-40XV5, 5-HT overlay; F, L) TβH-GFP, 5-HT overlay; M, S) vGlut-40XV5; N, T) Tdc2; O, U) 5-HT; P, V) vGlut-40XV5, Tdc2 overlay; Q, W) vGlut-40XV5, 5-HT overlay; R, X) Tdc2, 5-HT overlay. Scale bars: R-50μm; X-10μm.

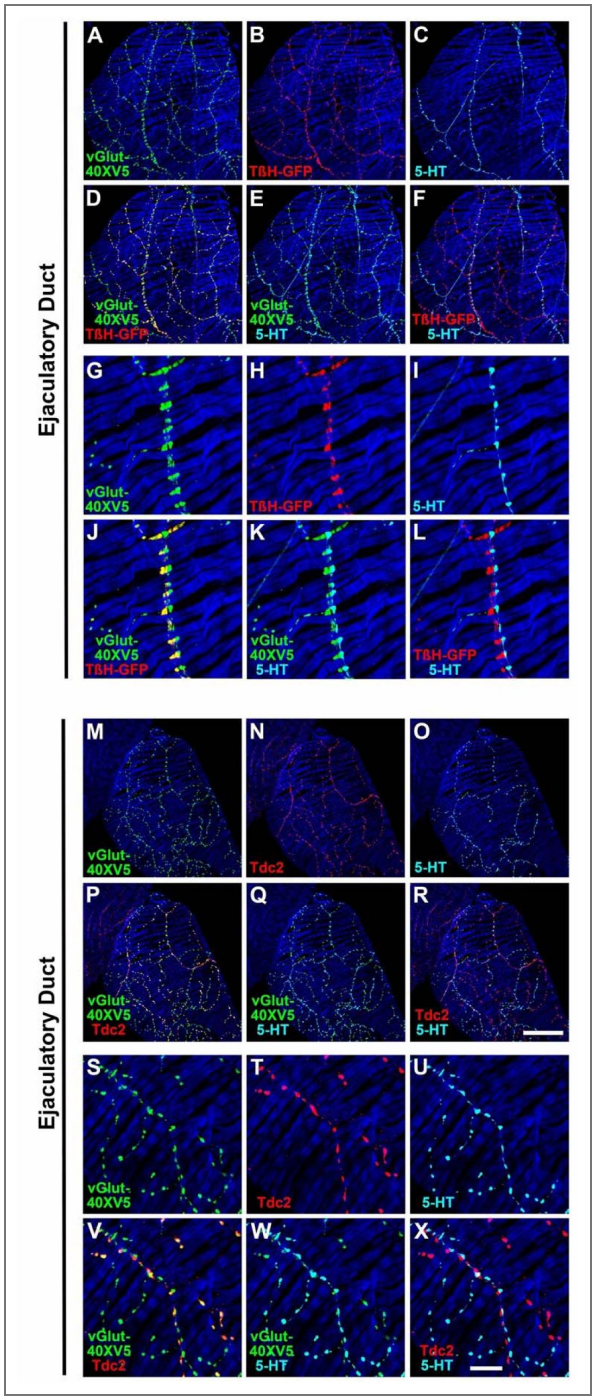

Figure 4S2. Expression of vGlut, TβH-GFP, Tdc2, and 5-HT in the ED of the Drosophila male reproductive system.

A, G) vGlut-40XV5; B, H) TβH-GFP; C, I) 5-HT; D, J) vGlut-40XV5, TβH-GFP overlay; E, K) vGlut-40XV5, 5-HT overlay; F, L) TβH-GFP, 5-HT overlay; M, S) vGlut-40XV5; N, T) Tdc2; O, U) 5-HT; P, V) vGlut-40XV5, Tdc2 overlay; Q, W) vGlut-40XV5, 5-HT overlay; R, X) Tdc2, 5-HT overlay. Scale bars: R-50μm; X-10μm.

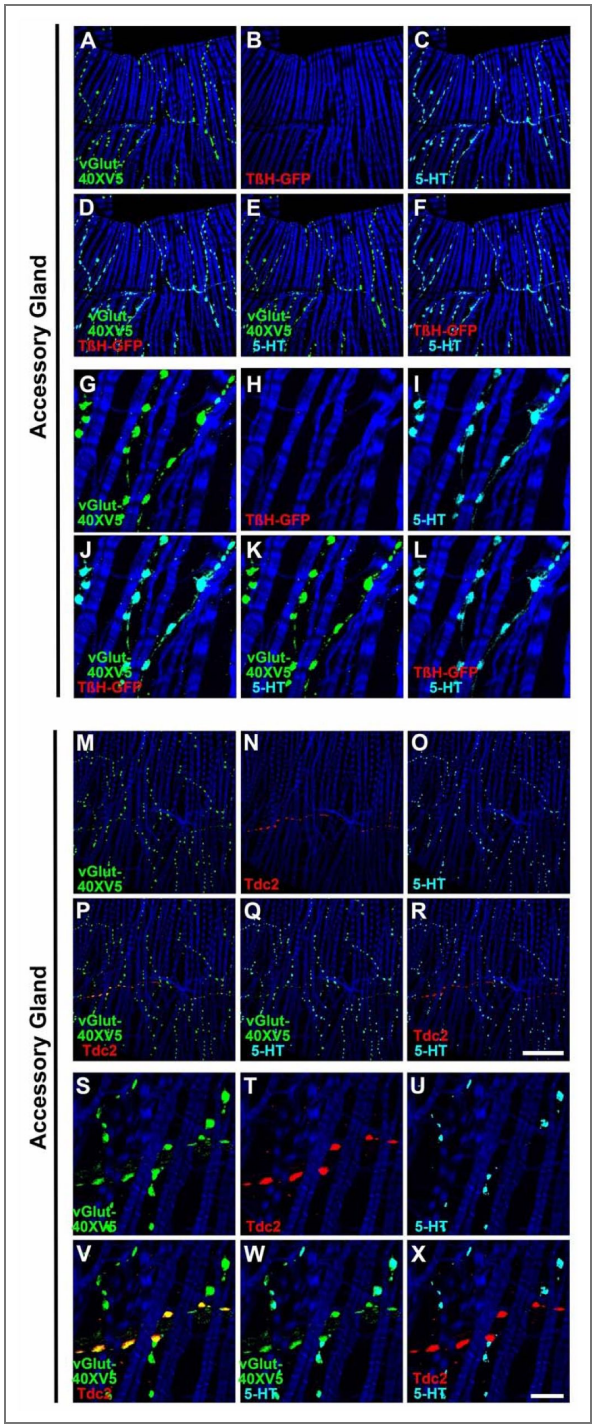

Figure 4S3. Expression of vGlut, TβH-GFP, Tdc2, and 5-HT in the AG of the Drosophila male reproductive system.

A, G) vGlut-40XV5; B, H) TβH-GFP; C, I) 5-HT; D, J) vGlut-40XV5, TβH-GFP overlay; E, K) vGlut-40XV5, 5-HT overlay; F, L) TβH-GFP, 5-HT overlay; M, S) vGlut-40XV5; N, T) Tdc2; O, U) 5-HT; P, V) vGlut-40XV5, Tdc2 overlay; Q, W) vGlut-40XV5, 5-HT overlay; R, X) Tdc2, 5-HT overlay. Scale bars: R-50μm; X-10μm.

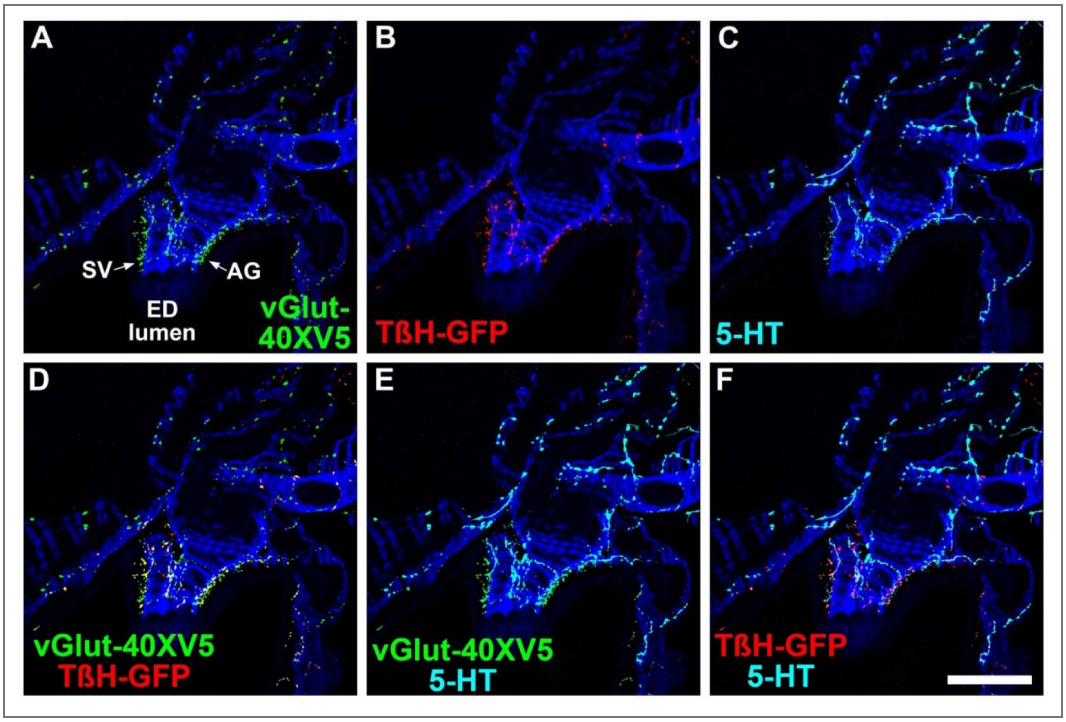

Figure 4S4. Expression of vGlut, TβH-GFP, and 5-HT at the junction of the SV and AGs with the ED of the Drosophila male reproductive system.

A) vGlut-40XV5; B) TβH-GFP; C) 5-HT; D) vGlut-40XV5, TβH-GFP overlay; E) vGlut-40XV5, 5-HT overlay; F) TβH-GFP, 5-HT overlay. Scale bar: 50μm.

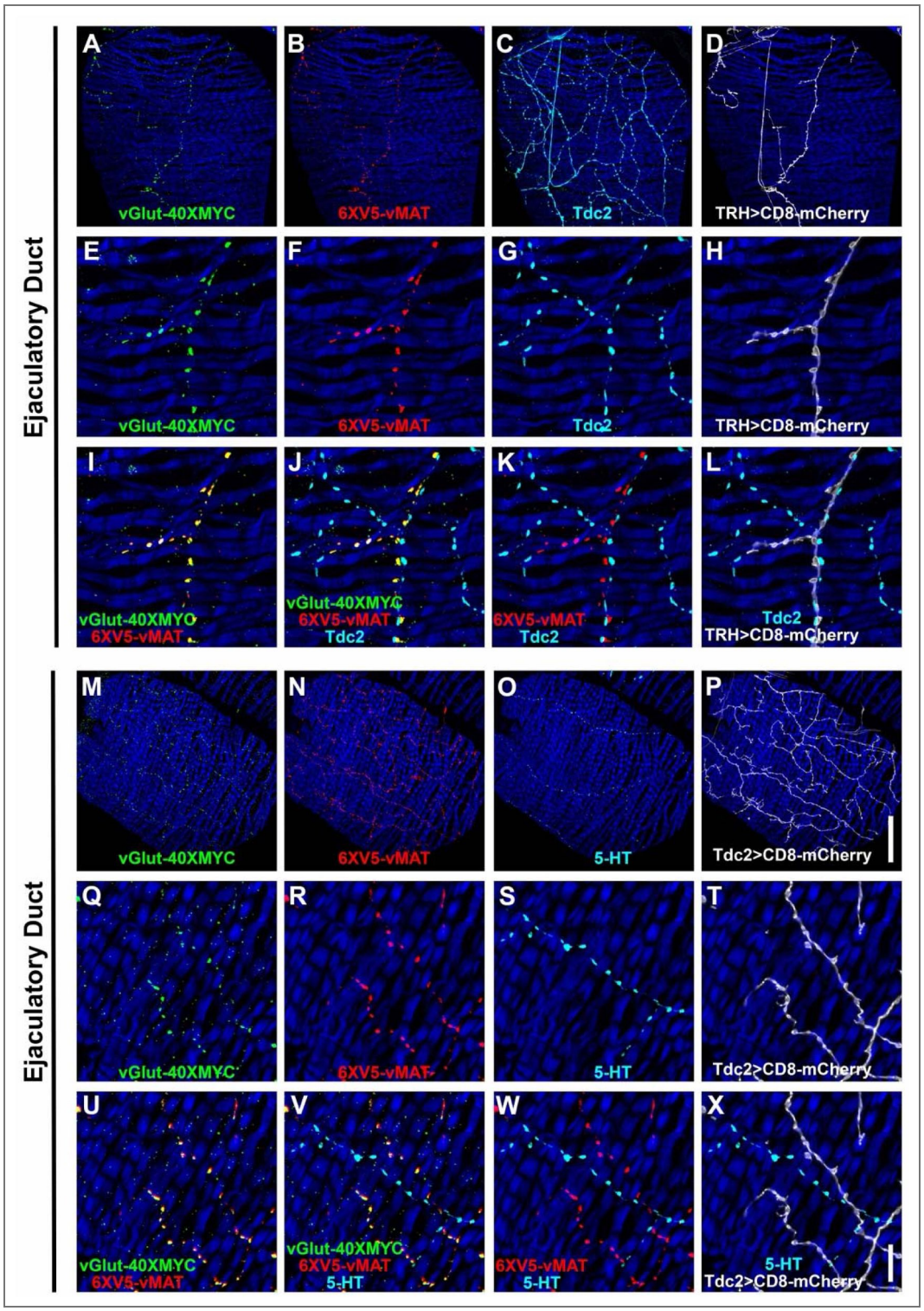

Figure 5S1. Co-conditional expression of vGlut-40XMYC and 6XV5-vMAT in the ED of serotonergic (TRH) or octopaminergic (Tdc2) neurons of the Drosophila male reproductive system.

A-D) 63X. A) vGlut-40XMYC; B) 6XV5-vMAT; C) Tdc2; D) TRH>CD8-mCherry. E-L) 63X zoom 4X. E) vGlut-40XMYC; F) 6XV5-vMAT; G) Tdc2; H) TRH>CD8-mCherry; I) vGlut-40XMYC, 6XV5-vMAT overlay; J) vGlut-40XMYC, 6XV5-vMAT, Tdc2 overlay; K) 6XV5-vMAT, Tdc2 overlay; L) Tdc2, TRH>CD8-mCherry overlay. M-P) 63X. M) vGlut-40XMYC; N) 6XV5-vMAT; O) 5-HT; P) Tdc2>CD8-mCherry. Q-X) 63X zoom 4X. Q) vGlut-40XMYC; R) 6XV5-vMAT; S) 5-HT; T) Tdc2>CD8-mCherry; U) vGlut-40XMYC, 6XV5-vMAT overlay; V) vGlut-40XMYC, 6XV5-vMAT, 5-HT overlay; W) 6XV5-vMAT, 5-HT overlay; X) Tdc2, Tdc2>CD8-mCherry overlay. Scale bars: P-50μm; X-10μm.

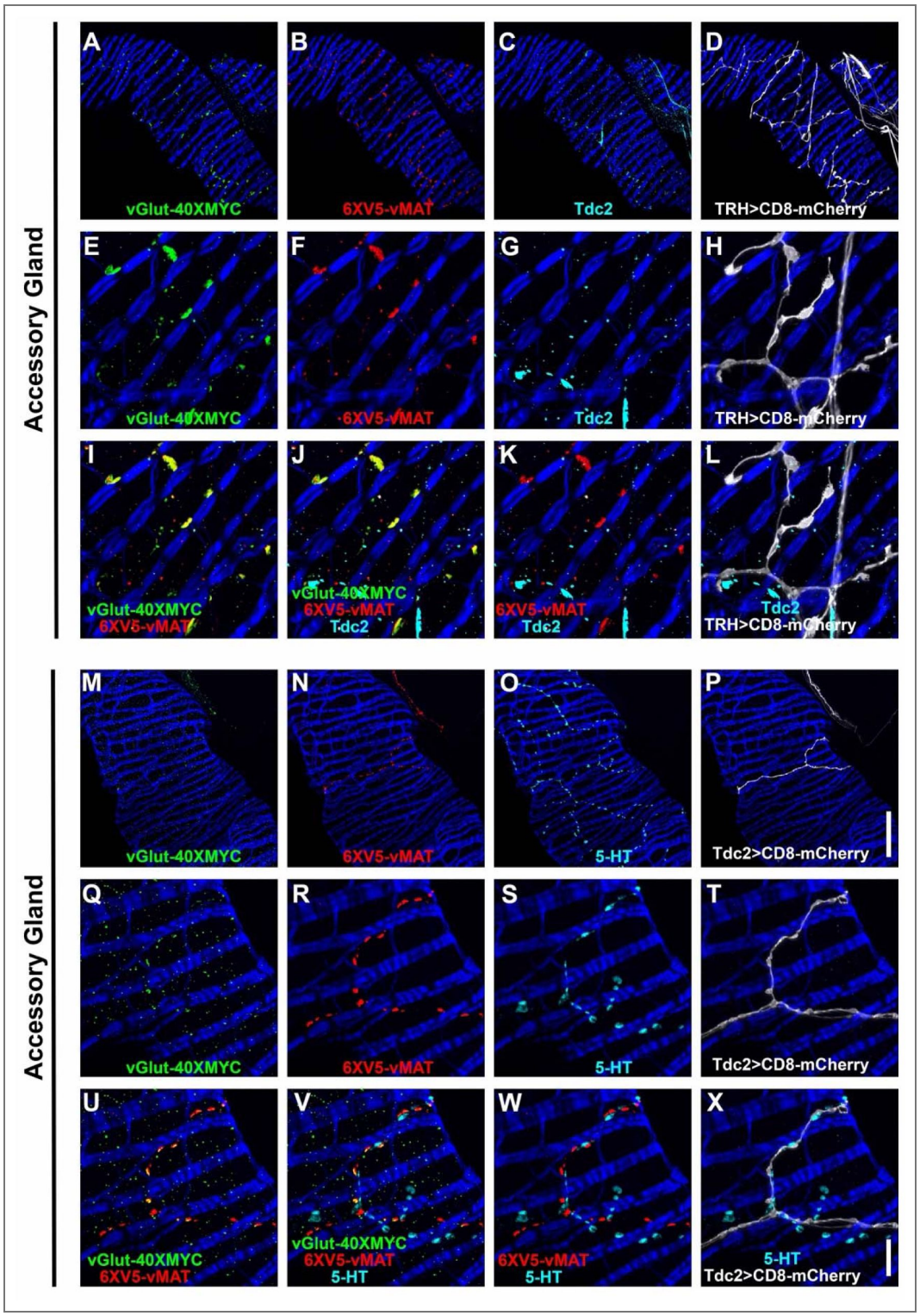

Figure 5S2. Co-conditional expression of vGlut-40XMYC and 6XV5-vMAT in the AG of serotonergic (TRH) or octopaminergic (Tdc2) neurons of the Drosophila male reproductive system.

A-D) 63X. A) vGlut-40XMYC; B) 6XV5-vMAT; C) Tdc2; D) TRH>CD8-mCherry. E-L) 63X zoom 4X. E) vGlut-40XMYC; F) 6XV5-vMAT; G) Tdc2; H) TRH>CD8-mCherry; I) vGlut-40XMYC, 6XV5-vMAT overlay; J) vGlut-40XMYC, 6XV5-vMAT, Tdc2 overlay; K) 6XV5-vMAT, Tdc2 overlay; L) Tdc2, TRH>CD8-mCherry overlay. M-P) 63X. M) vGlut-40XMYC; N) 6XV5-vMAT; O) 5-HT; P) Tdc2>CD8-mCherry. Q-X) 63X zoom 4X. Q) vGlut-40XMYC; R) 6XV5-vMAT; S) 5-HT; T) Tdc2>CD8-mCherry; U) vGlut-40XMYC, 6XV5-vMAT overlay; V) vGlut-40XMYC, 6XV5-vMAT, 5-HT overlay; W) 6XV5-vMAT, 5-HT overlay; X) Tdc2, Tdc2>CD8-mCherry overlay. Scale bars: P-50μm; X-10μm.

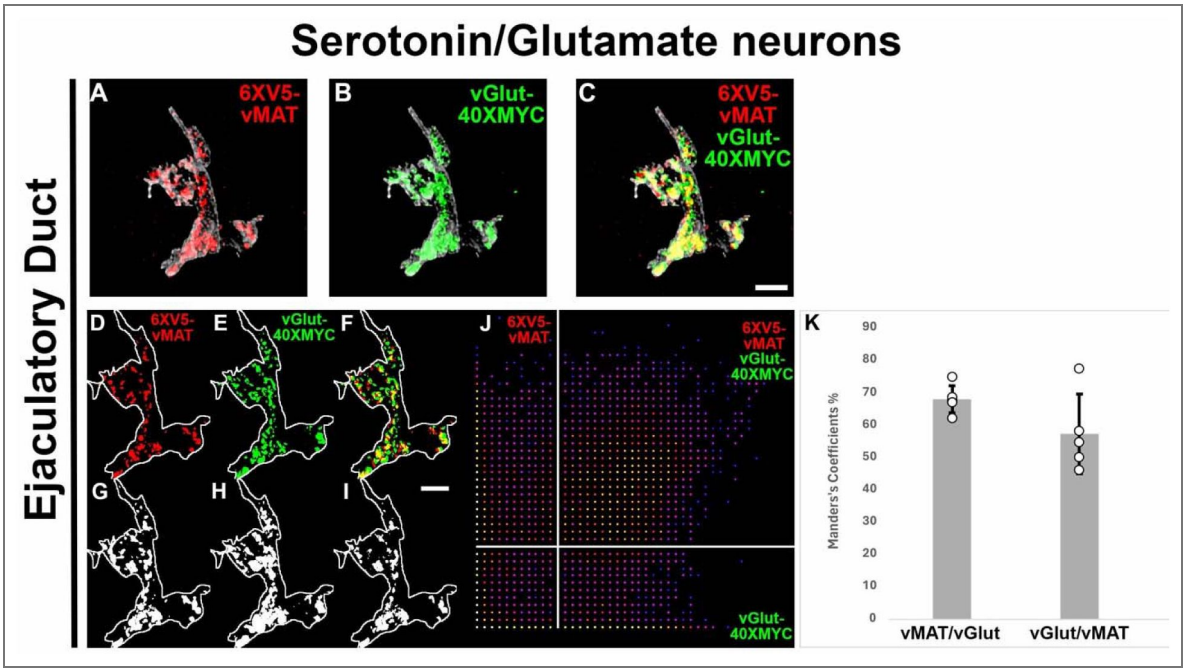

Figure 5S3. Co-conditional expression of vGlut-40XMYC and 6XV5-vMAT in serotonergic neurons of the Drosophila ED using expansion microscopy.

A, D) 6XV5-vMAT; B, E) vGlut-40XMYC; C, F) overlay. A-C) 6XV5-vMAT and vGlut-40XMYC expression above the threshold intensity values. D-F) Complete 6XV5-vMAT and vGlut-40XMYC expression. G) Mander's plot of 6XV5-vMAT and vGlut-40XMYC. Vertical line indicates intensity threshold value for 6XV5-vMAT. Horizontal line indicates intensity threshold value for vGlut-40XMYC. H) Mander's coefficients. Grayscale signal in A-C) denotes the CD8-mCherry plasma membrane marker. Scale bars: 500nm. Scale bars have been corrected by 10X to reflect the empirically determined 10.5X expansion factor.

Figure 5S4. Co-conditional expression of vGlut-40XMYC and 6XV5-vMAT in octopaminergic neurons of the Drosophila ED using expansion microscopy.

A, D) 6XV5-vMAT; B, E) vGlut-40XMYC; C, F) overlay. A-C) 6XV5-vMAT and vGlut-40XMYC expression above the threshold intensity values. D-F) Complete 6XV5-vMAT and vGlut-40XMYC expression. G) Mander's plot of 6XV5-vMAT and vGlut-40XMYC. Vertical line indicates intensity threshold value for 6XV5-vMAT. Horizontal line indicates intensity threshold value for vGlut-40XMYC. H) Mander's coefficients. Grayscale signal in A-C) denotes the CD8-mCherry plasma membrane marker. Scale bars: 500nm. Scale bars have been corrected by 10X to reflect the empirically determined 10.5X expansion factor.

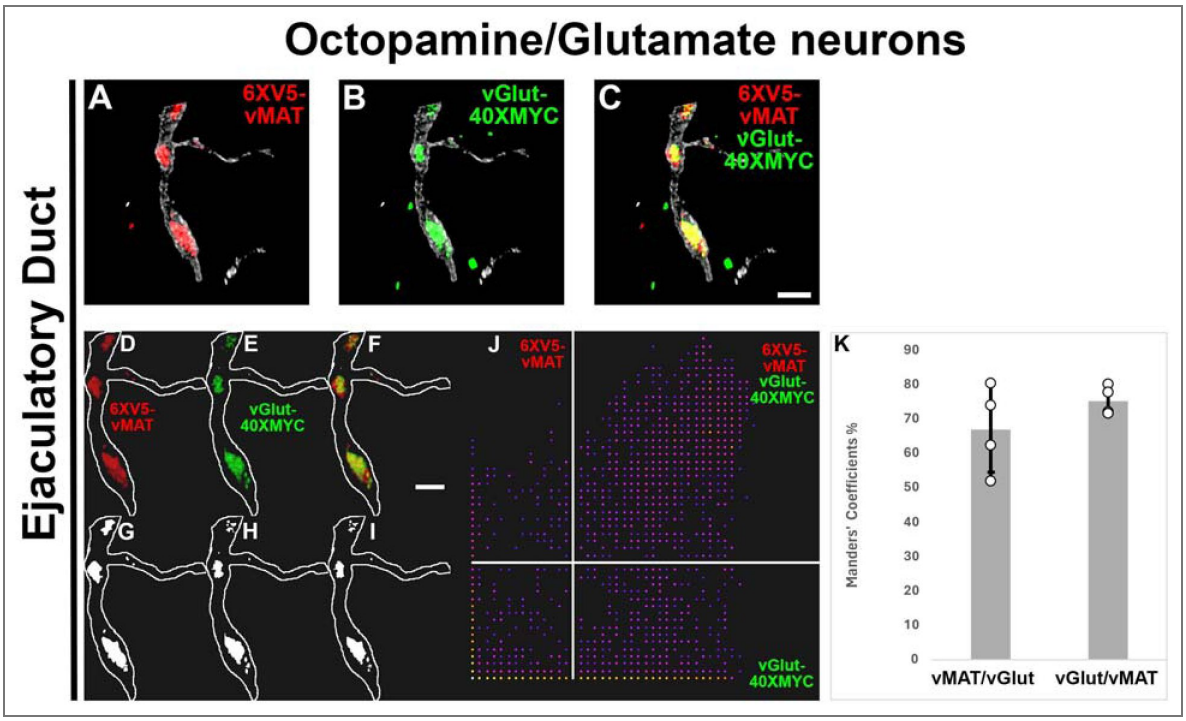

Figure 5S5. Nuclei of unexpanded and expanded EDs.

A) DAPI-stained nuclei from an unexpanded ED. B) DAPI-stained nuclei of an expanded ED. C) Bar graph plot of nuclei area (mean ± SE-black bars). For the experiment shown the calculated expansion factor (post-ExM nuclear area/pre-ExM nuclear area) was 10.47, p-value < 0.00001. Fij/ImageJi open-source software was used to segment images and calculate nuclear area. Scale bars: 25um.

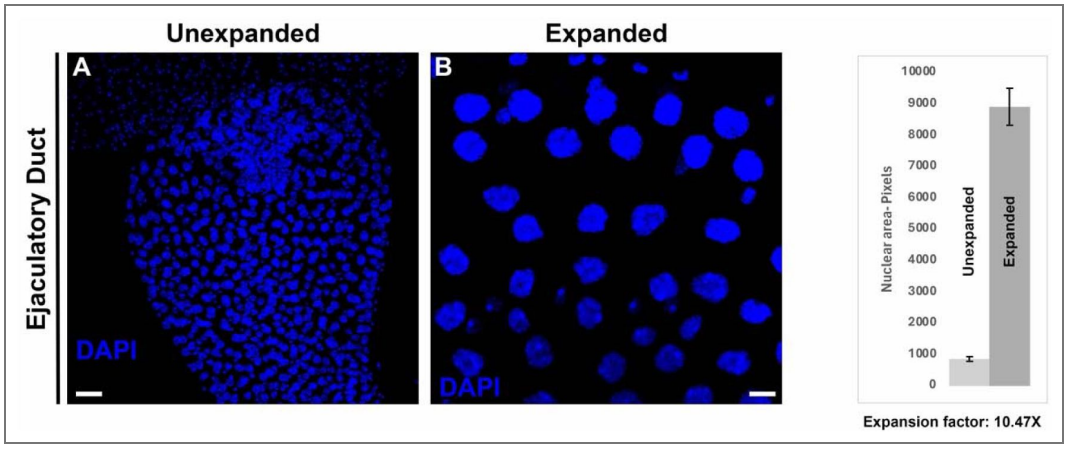

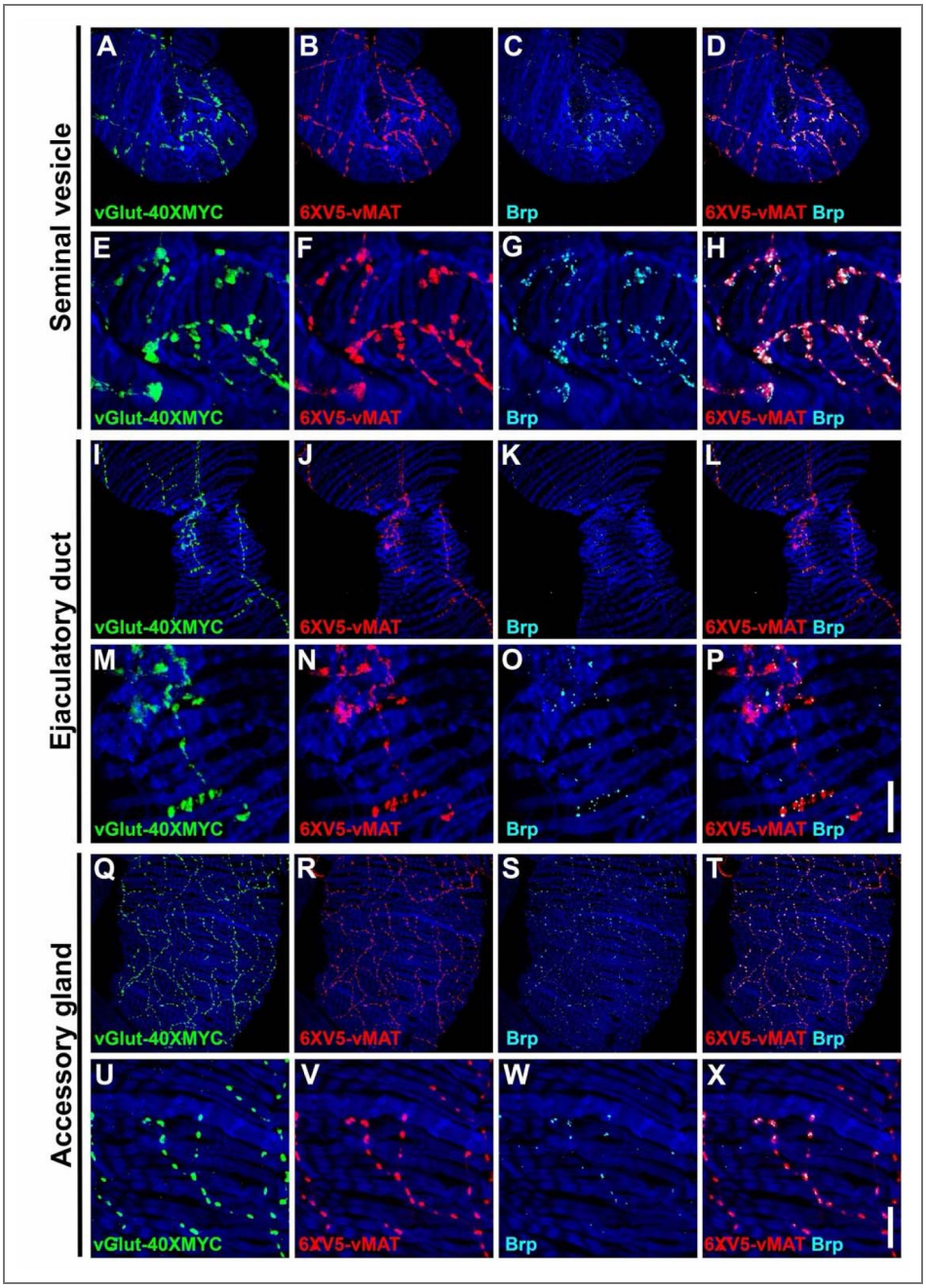

Figure 6S1. Expression of the active zone marker Brp in combination with vGlut-40XMYC and 6XV5-vMAT in the SV, ED, and AG of the Drosophila male reproductive system.

A-H) SV. A) vGlut-40XMYC; B) 6XV5-vMAT; C) Brp; D) 6XV5-vMAT, Brp overlay; E) vGlut-40XMYC; F) 6XV5-vMAT; G) Brp; H) 6XV5-vMAT, Brp overlay. I-P) ED. I) vGlut-40XMYC; J) 6XV5-vMAT; K) Brp; L) 6XV5-vMAT, Brp; M) vGlut-40XMYC; N) 6XV5-vMAT; O) Brp; P) 6XV5-vMAT, Brp overlay. I-P) AG. Q) vGlut-40XMYC; R) 6XV5-vMAT; S) Brp; T) 6XV5-vMAT, Brp; U) vGlut-40XMYC; V) 6XV5-vMAT; W) Brp; X) 6XV5-vMAT, Brp overlay. Scale bars: P-50μm; X-10μm.

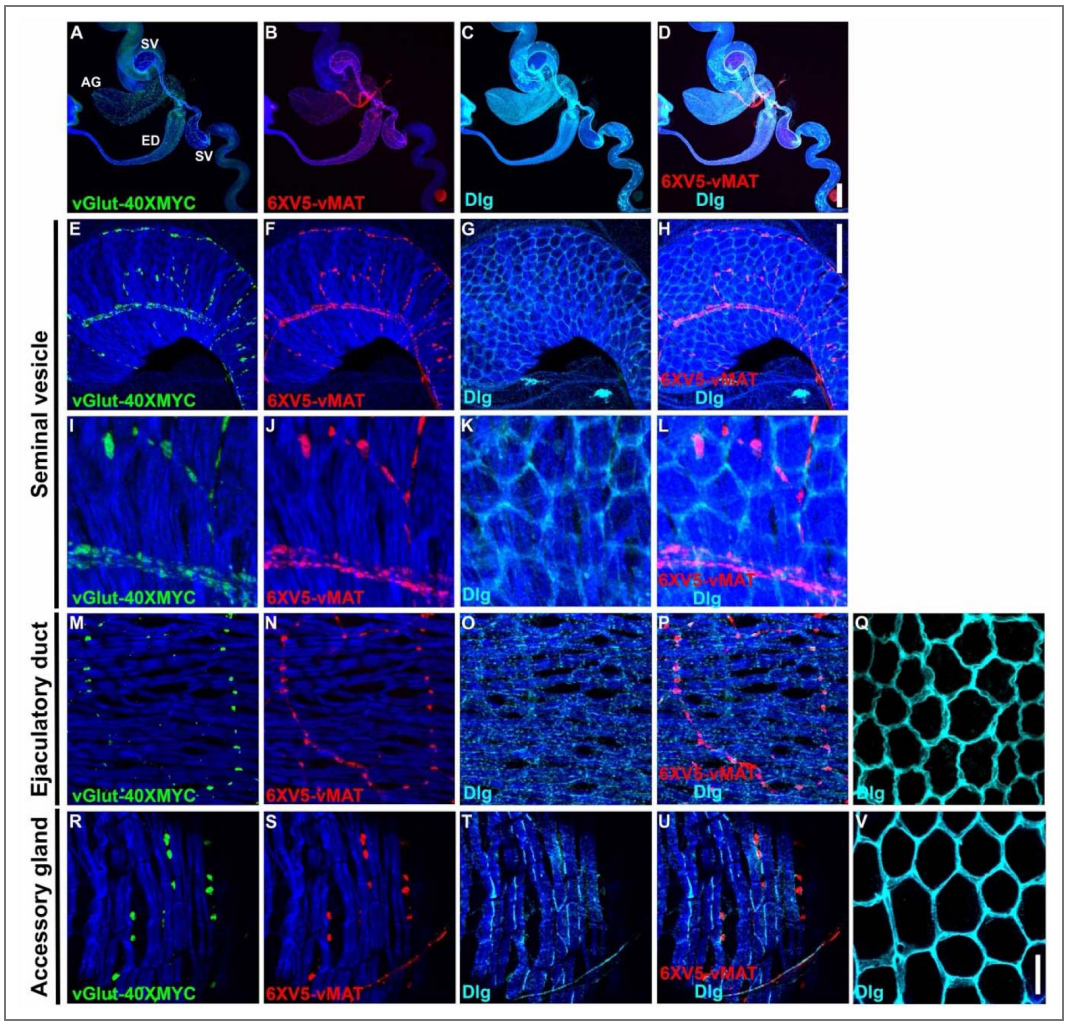

Figure 6S2. Expression of the post-synaptic density marker Dlg in combination with vGlut-40XMYC and 6XV5-vMAT in the SV, ED, and AG of the Drosophila male reproductive system.

A-D) Complete reproductive system. A) vGlut-40XMYC; B) 6XV5-vMAT; C) Dlg; D) 6XV5-vMAT, Dlg overlay; E-L) SV. E) vGlut-40XMYC; F) 6XV5-vMAT; G) Dlg; H) 6XV5-vMAT, Dlg overlay; I) vGlut-40XMYC; J) 6XV5-vMAT; G) Dlg; H) 6XV5-vMAT, Dlg overlay. I-P) ED. I) vGlut-40XMYC; K) 6XV5-vMAT; L) Dlg; M-P) ED muscle surface. M) vGlut-40XMYC; N) 6XV5-vMAT; O) Dlg; P) 6XV5-vMAT, Dlg overlay Q) Dlg in the ED epithelial cells. R-U) AG muscle surface. R) vGlut-40XMYC; S) 6XV5-vMAT; T) Dlg; U) 6XV5-vMAT, Dlg overlay; V) Dlg in AG epithelial cells. Scale bars: D-200µm; H-50µm; V-10µm.

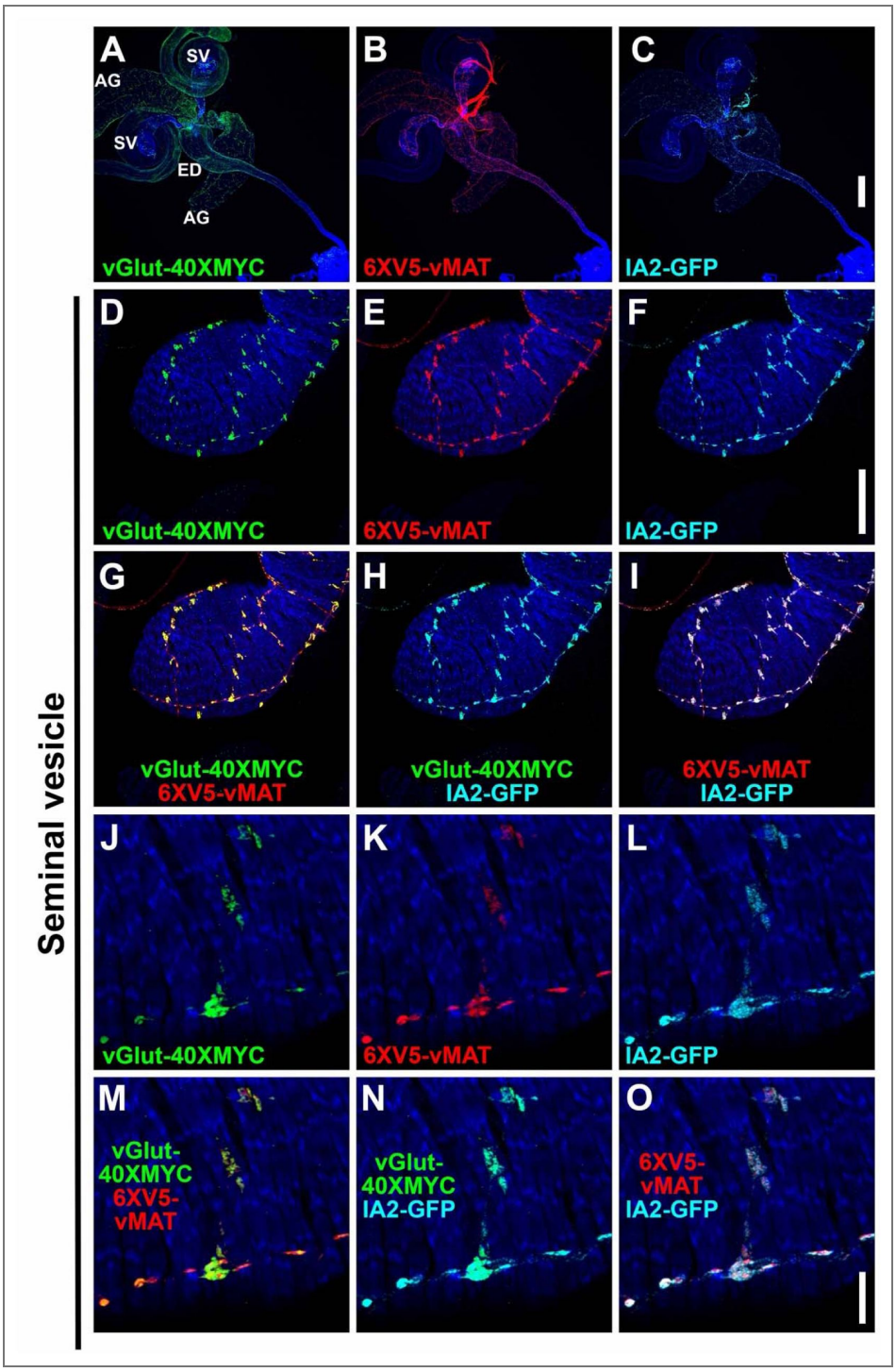

Figure 6S3. Expression of the large core dense vesicle marker IA2-GFP in combination with vGlut-40XMYC and 6XV5-vMAT in the SV of the Drosophila male reproductive system.

A-C) Complete reproductive system. A) vGlut-40XMYC; B) 6XV5-vMAT; C) IA2-GFP; D-O) SV. D, J) vGlut-40XMYC; E, K) 6XV5-vMAT; F, L) IA2-GFP; G, M) vGlut-40XMYC, 6XV5-vMAT overlay; H, N) vGlut-40XMYC, IA2-GFP overlay; I, O) 6XV5-vMAT, IA2 overlay. Scale bars: C-200µm; F-50µm; O-10µm.

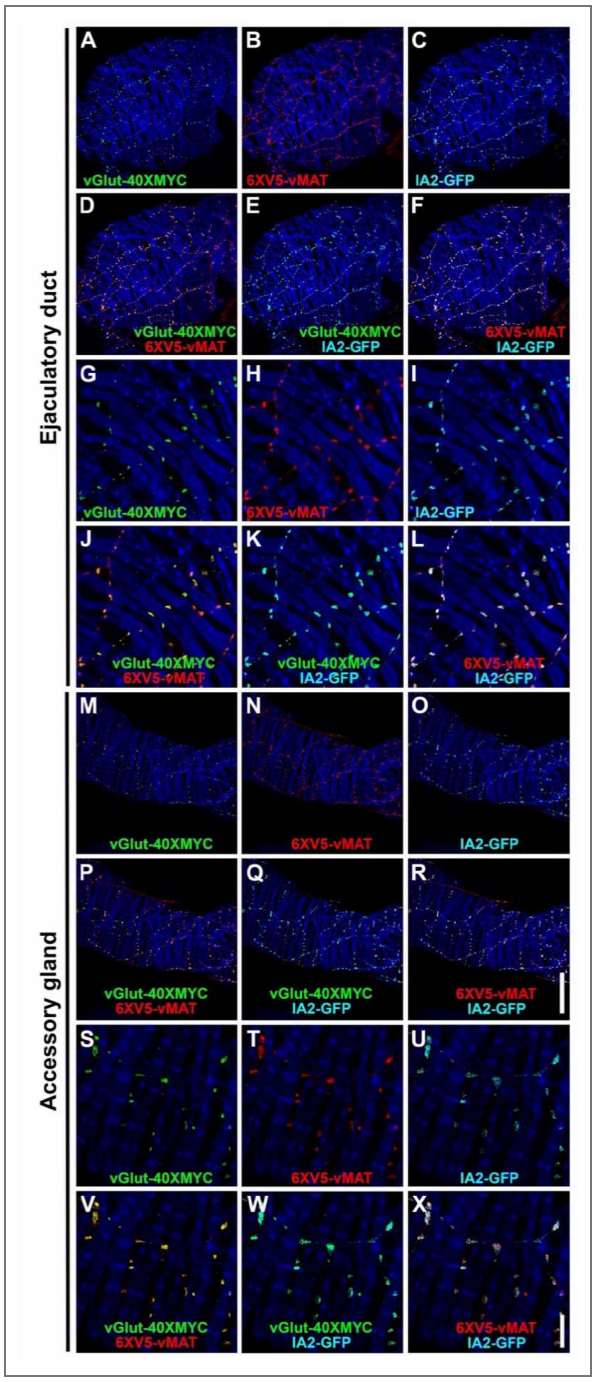

Figure 6S4. Expression of the large core dense vesicle marker IA2-GFP in combination with vGlut-40XMYC and 6XV5-vMAT in the ED and AGs of the Drosophila male reproductive system.

A-L) ED. A, G) vGlut-40XMYC; B, H) 6XV5-vMAT; C, I) IA2-GFP; D, J) vGlut-40XMYC, 6XV5-vMAT overlay; E, K) vGlut-40XMYC, IA2-GFP overlay; F, L) 6XV5-vMAT, IA2 overlay. M-X) AG. M, S) vGlut-40XMYC; N, T) 6XV5-vMAT; O, U) IA2-GFP; P, V) vGlut-40XMYC, 6XV5-vMAT overlay; Q, W) vGlut-40XMYC, IA2-GFP overlay; R, X) 6XV5-vMAT, IA2 overlay. Scale bars: R-50μm; X-10μm.

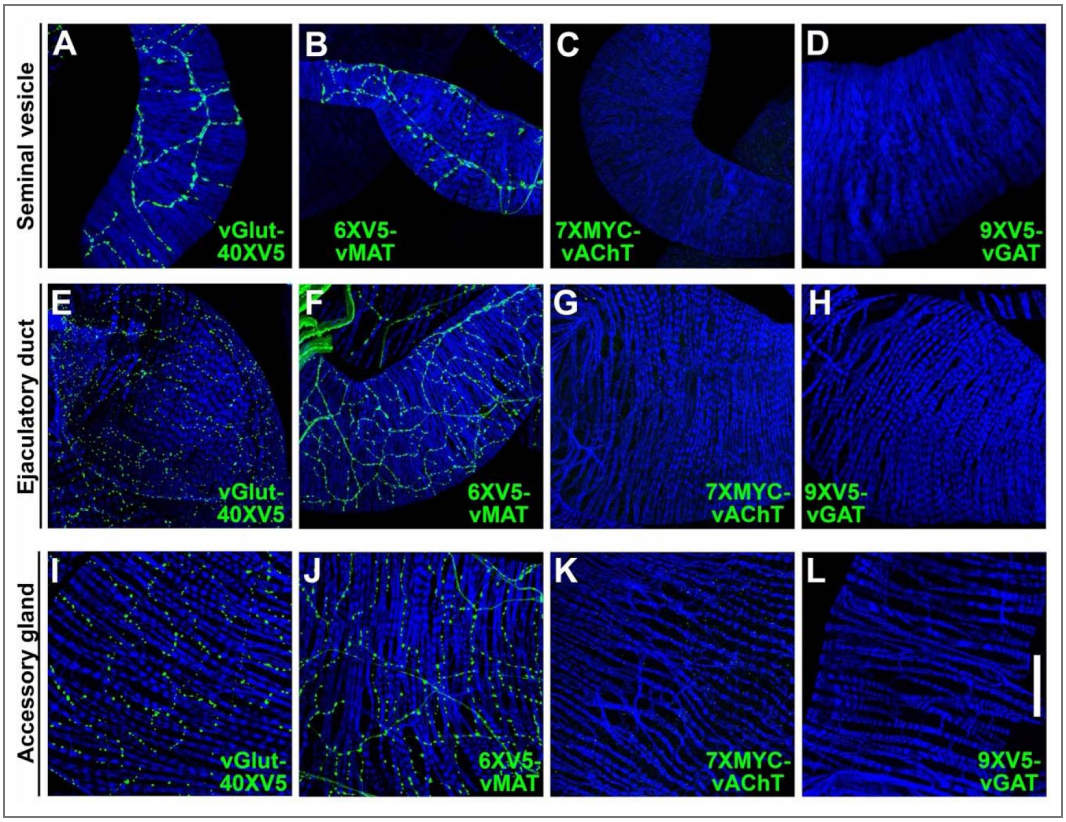

Figure 6S5. Expression of vGlut-40XMYC, 6XV5-vMAT, 7XMYC-vAChT, and 9XV5-vGAT in the SV, ED, and AG of the Drosophila male reproductive system.

A-D) SV. A) vGlut-40XV5; B) 6XV5-vMAT; C) 7XMYC-vAChT; D) 9XV5-vGAT. E-H) ED. E) vGlut-40XV5; F) 6XV5-vMAT; G) 7XMYC-vAChT; H) 9XV5-vGAT. I-L) AG. I) vGlut-40XV5; J) 6XV5-vMAT; K) 7XMYC-vAChT; L) 9XV5-vGAT. Scale bar: 50μm.

Figure 7S1. **OA receptor GAL4 expression patterns in Drosophila male reproductive system.**

A) OAMB; B) OAα2R; C) Oct-TyrR; D) OAβ1R; E) OAβ2R; F) OAβ3R. Scale bar: 200μm.

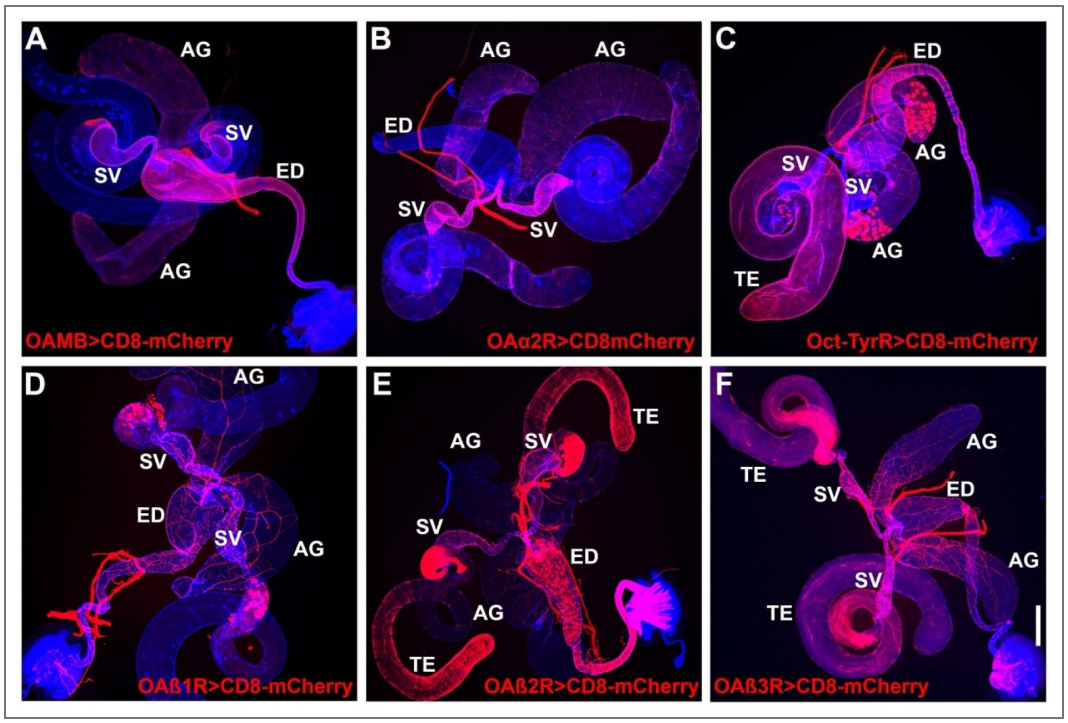

Figure 7S2. **5-HT receptor GAL4 expression patterns in Drosophila male reproductive system.**

A) 5-HT1A; B) 5-HT2A; C) 5-HT1B; D) 5-HT2B; E) 5-HT7. Scale bar: 200μm.

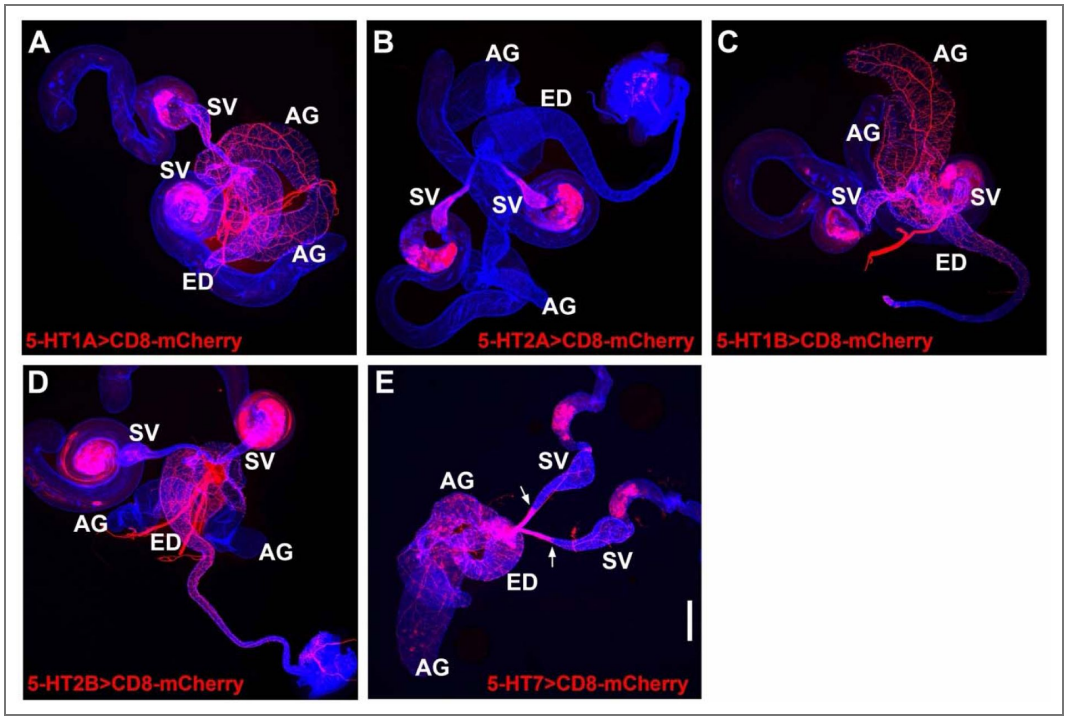

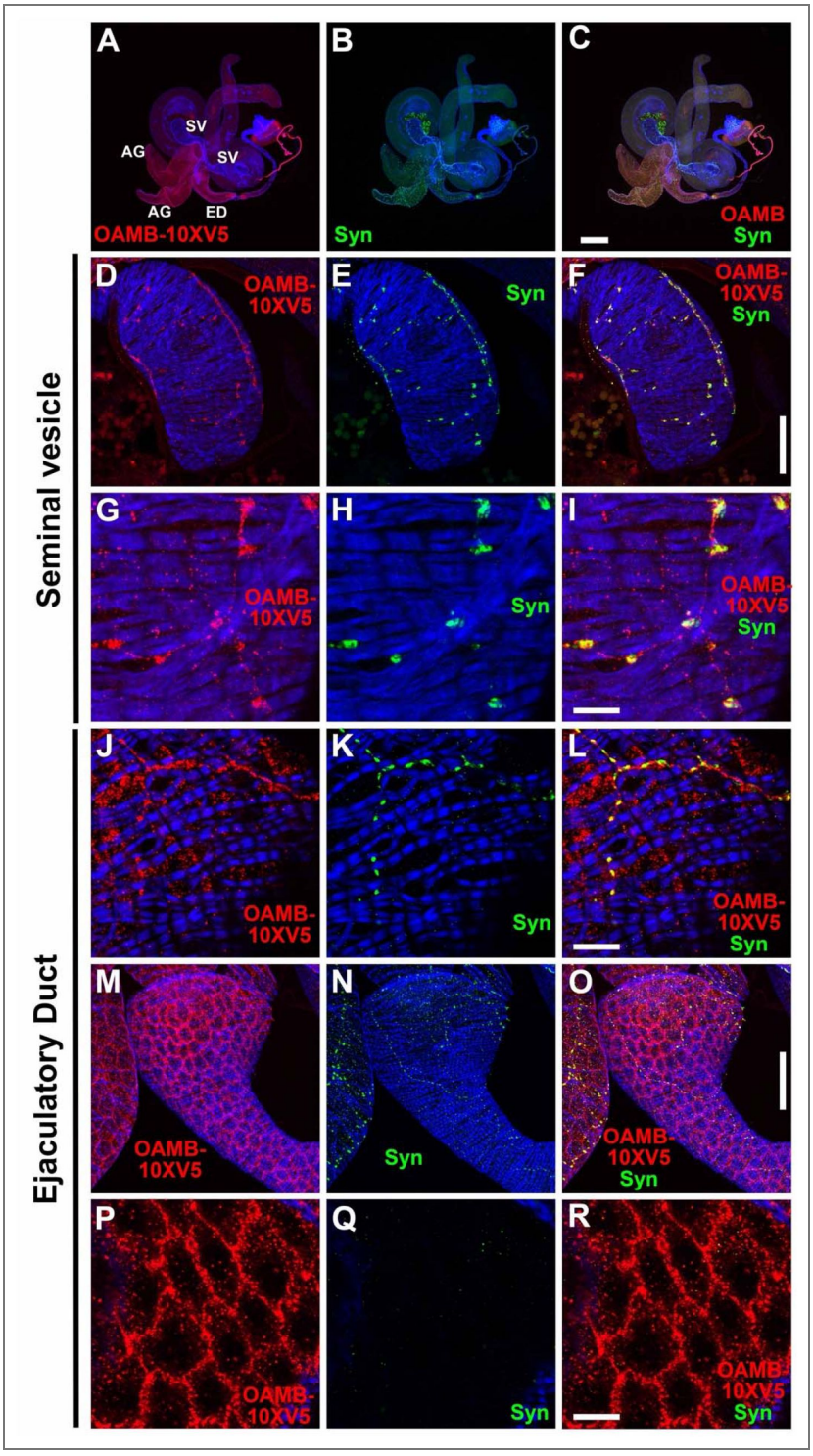

Figure 8S1. OAMB expression in the Drosophila male reproductive system.

A-C) Complete male reproductive system. A) OAMB-10XV5; B) Syn; C) OAMB-10XV5, Syn overlay. D-I) SV. D, G) OAMB-10XV5; E, H) Syn; F, I) OAMB-10XV5, Syn overlay. J-R) ED. J-L) muscle surface. J) OAMB-10XV5; K) Syn; L) OAMB-10XV5, Syn overlay. M-O) muscles and epithelial layers. M) OAMB-10XV5; N) Syn; O) OAMB-10XV5, Syn overlay. P-R) epithelial layer. P) OAMB-10XV5; Q) Syn; R) OAMB-10XV5, Syn overlay. Scale bars: C-200μm; F, O-50μm; I, L, R-10μm.

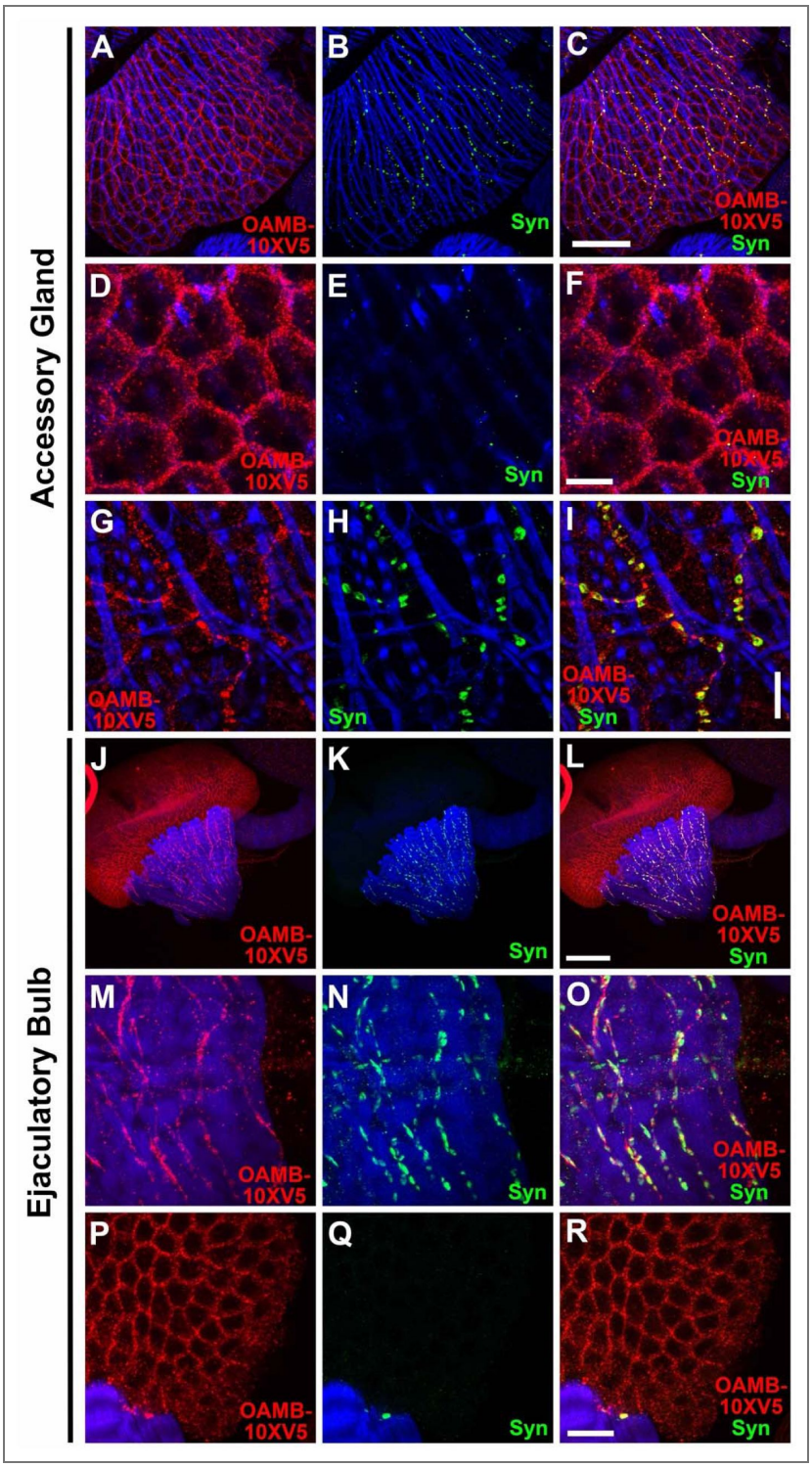

Figure 8S2. OAMB expression in the Drosophila male reproductive system.

A-C) AG. A) OAMB-10XV5; B) Syn; C) OAMB-10XV5, Syn overlay. D-F) Epithelial layer of AG. D) OAMB-10XV5; E) Syn; F) OAMB-10XV5, Syn overlay. G-I) Muscle layer of AG. G) OAMB-10XV5; H) Syn; I) OAMB-10XV5, Syn overlay. J-L) Ejaculatory bulb. J) OAMB-10XV5; K) Syn; L) OAMB-10XV5, Syn overlay. M-O) muscle layer of ejaculatory bulb. M) OAMB-10XV5; N) Syn; O) OAMB-10XV5, Syn overlay. P-Q) Epithelial layer of ejaculatory bulb. P) OAMB-10XV5; Q) Syn; R) OAMB-10XV5, Syn overlay. Scale bars: C, L-50μm; F, I, R-10μm.

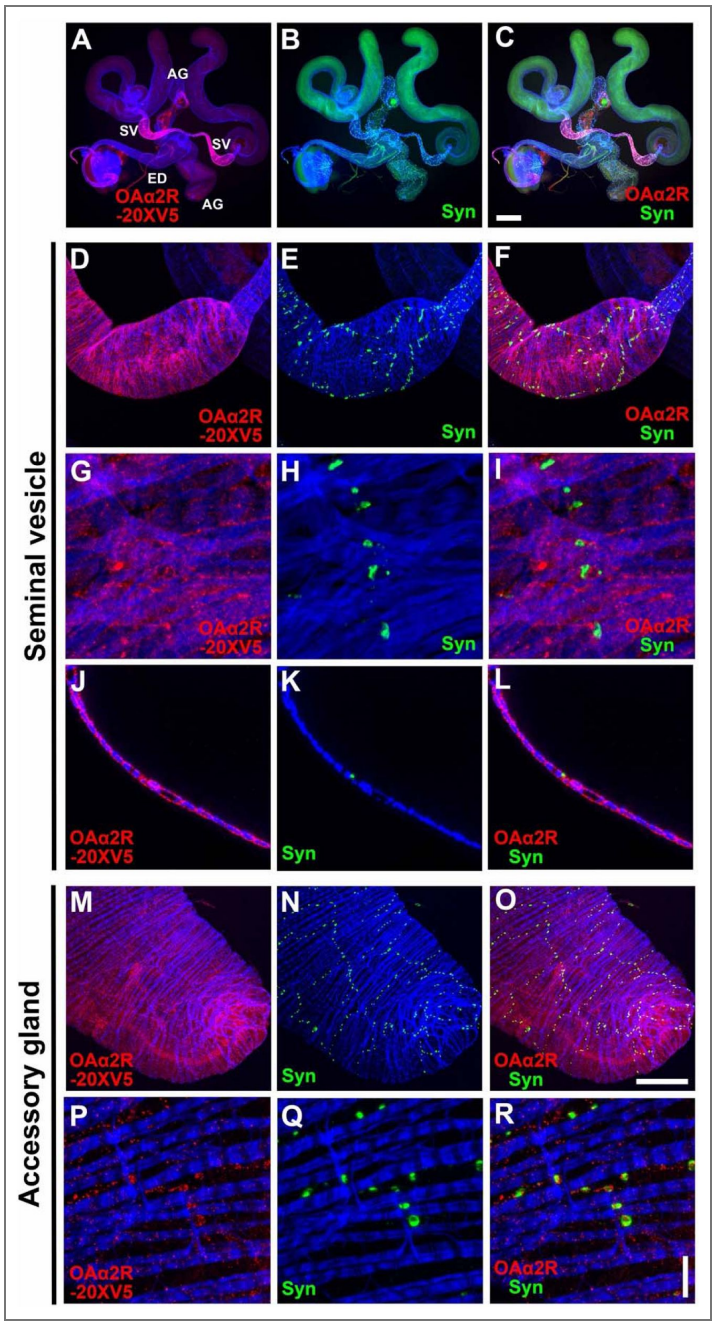

Figure 8S3. OAα2R-20XV5 expression in the Drosophila male reproductive system.

A-C) Complete male reproductive system. A) OAα2R-20XV5; B) Syn; C) OAα2R-20XV5, Syn overlay. D-I) SV. D, G) OAα2R-20XV5; E, H) Syn; F, I) OAα2R-20XV5, Syn overlay. Cross-section of SV. J) OAα2R-20XV5: K) Syn; L) OAα2R-20XV5, Syn overlay. M-R) AG. M, P) OAα2R-20XV5; N, Q) Syn; O, R) OAα2R-20XV5, Syn overlay. Scale bars: C-200μm; O-50μm; R-10μm. distal anterior ejaculatory duct proximal anterior ejaculatory duct seminal vesicle/ ejaculatory duct junction

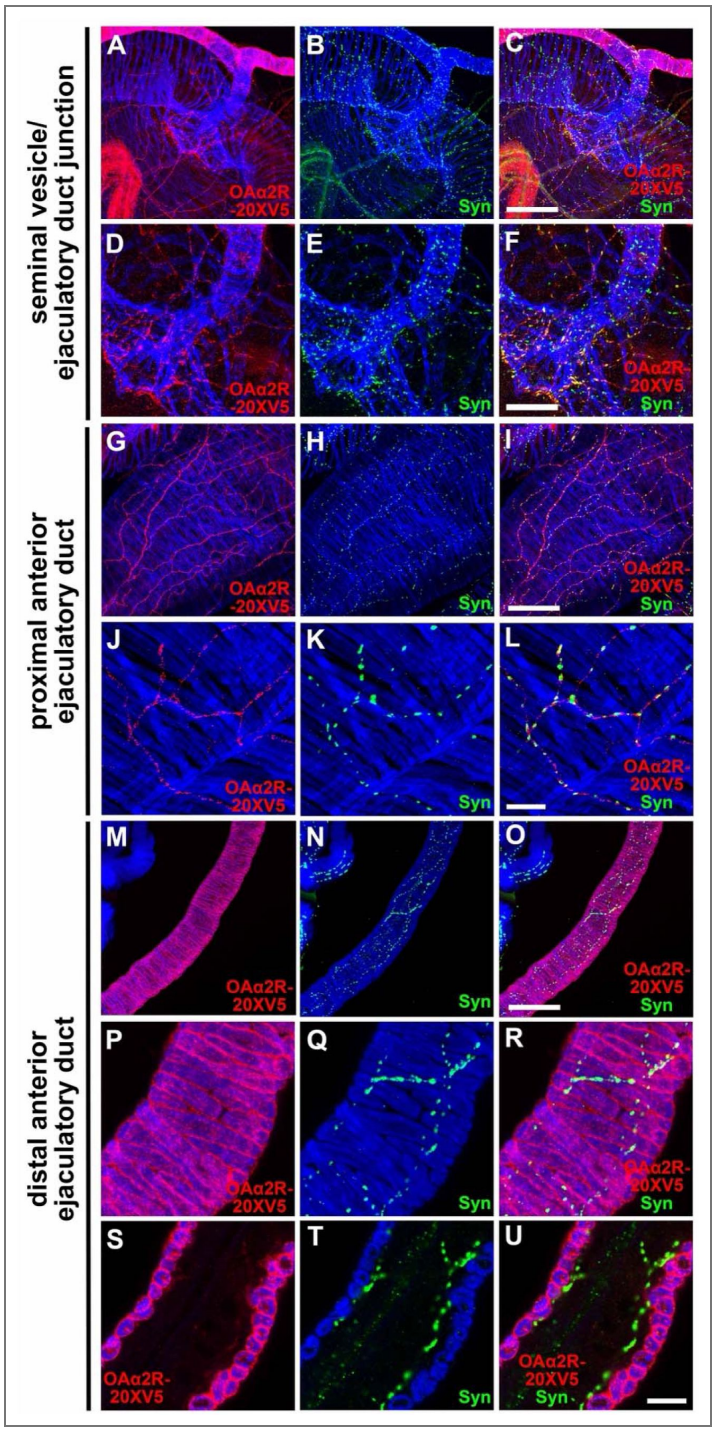

Figure 8S4. OAα2R-20XV5 expression in the Drosophila male reproductive system.

A-C) SV/ED junction. A, D) OAα2R-20XV5; B, E) Syn; C, F) OAα2R-20XV5, Syn overlay. G-L) Proximal anterior ED. G, J) OAα2R-20XV5; H, K) Syn; I, L) OAα2R-20XV5, Syn overlay. M-U) Distal anterior ED. M, P, S) OAα2R-20XV5; N, Q, T) Syn; O, R, U) OAα2R-20XV5, Syn overlay. Scale bars: C, I, O-50μm; F-25μm; L, U-10μm.

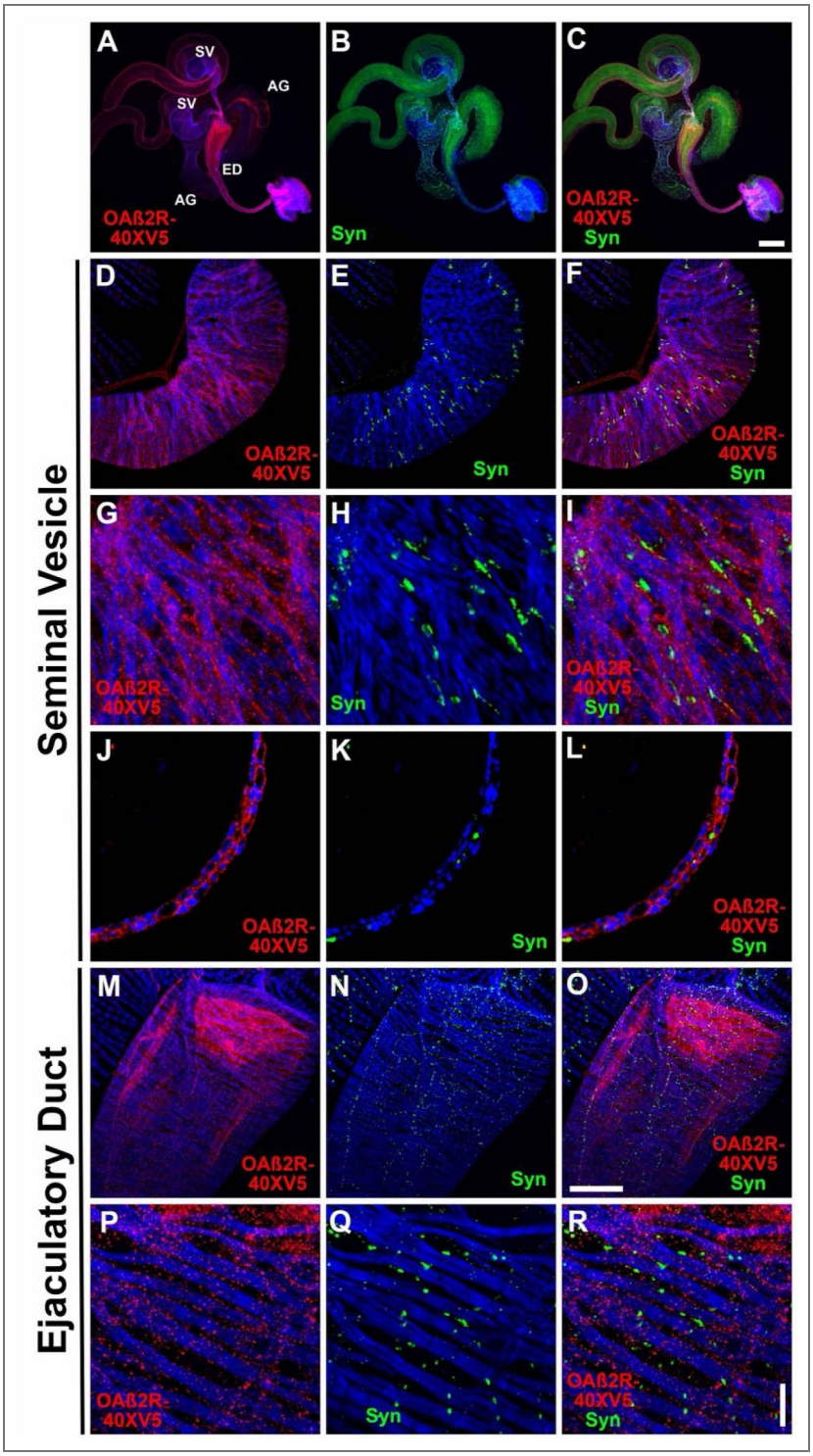

Figure 8S5. OAβ2R-40XV5 expression in the Drosophila male reproductive system.

A-C) Complete male reproductive system. A) OAβ2R-40XV5; B) Syn; C) OAβ2R-40XV5, Syn overlay. D-I) SV. D, G,) OAβ2R; E, H) Syn; F, I) OAβ2R-40XV5, Syn overlay. J-L) Cross section of SV. J) OAβ2R-40XV5; K) Syn; L) OAβ2R-40XV5, Syn overlay. M-R) ED. M, P) OAβ2R; N, Q) Syn; O, R) OAβ2R-40XV5, Syn overlay. Scale bars: C-200μm; O-50μm; R-10μm.

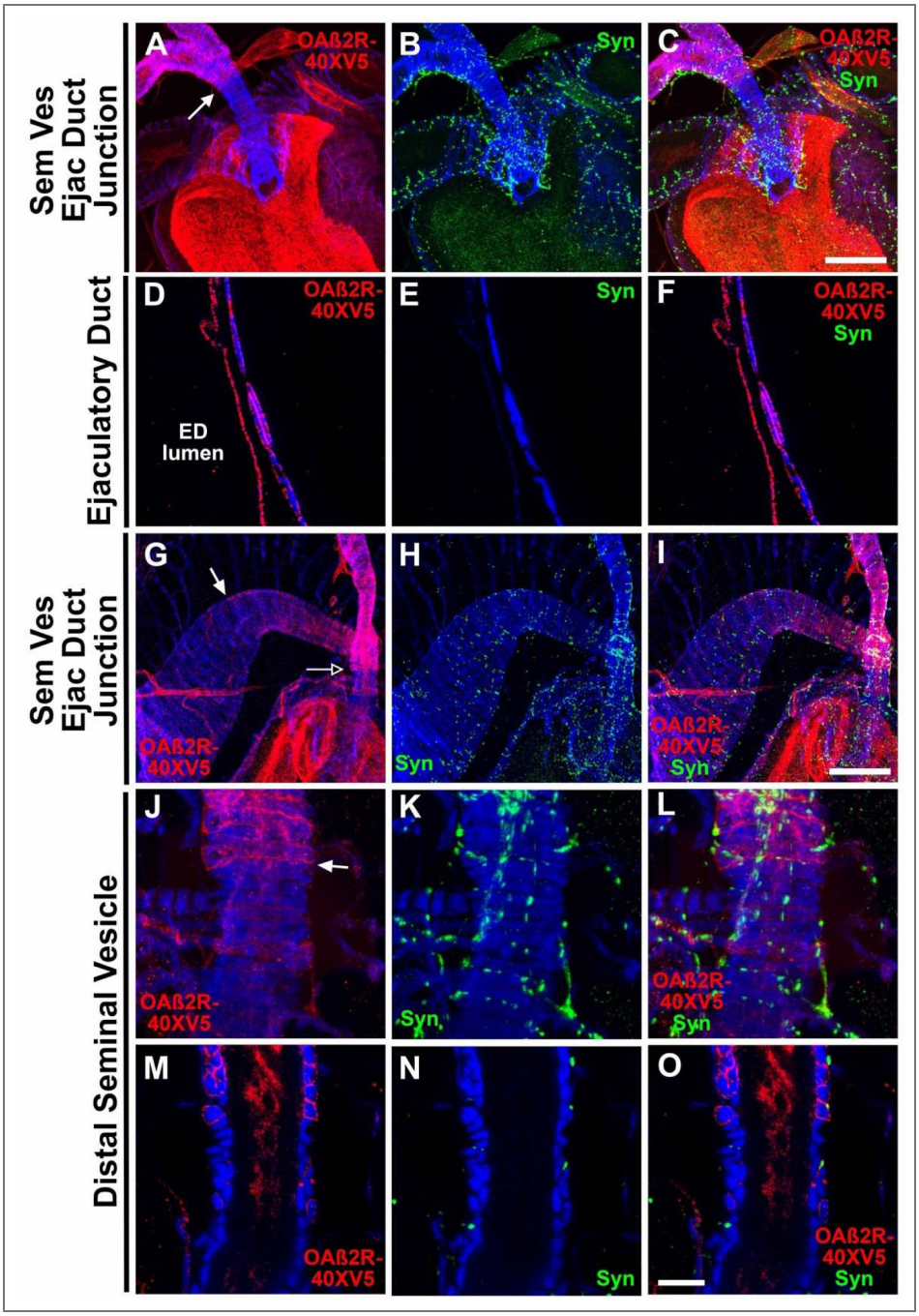

Figure 8S6. OAβ2R-40XV5 expression in the Drosophila male reproductive system.

A-C) Junction of SV and ED. A) OAβ2R-40XV5; B) Syn; C) OAβ2R-40XV5, Syn overlay. D-F) Cross section of ED. D) OAβ2R-40XV5; E) Syn; F) OAβ2R-40XV5, Syn overlay. G-I) Junction of SV and ED. G) OAβ2R-40XV5; H) Syn; I) OAβ2R-40XV5, Syn overlay. J-L) Distal SV. J) OAβ2R-40XV5; E) Syn; F) OAβ2R-40XV5, Syn overlay. M-O) Cross section of distal SV. M) OAβ2R-40XV5; N) Syn; O) OAβ2R-40XV5, Syn overlay. Scale bars: C, I-50μm; O-10μm.

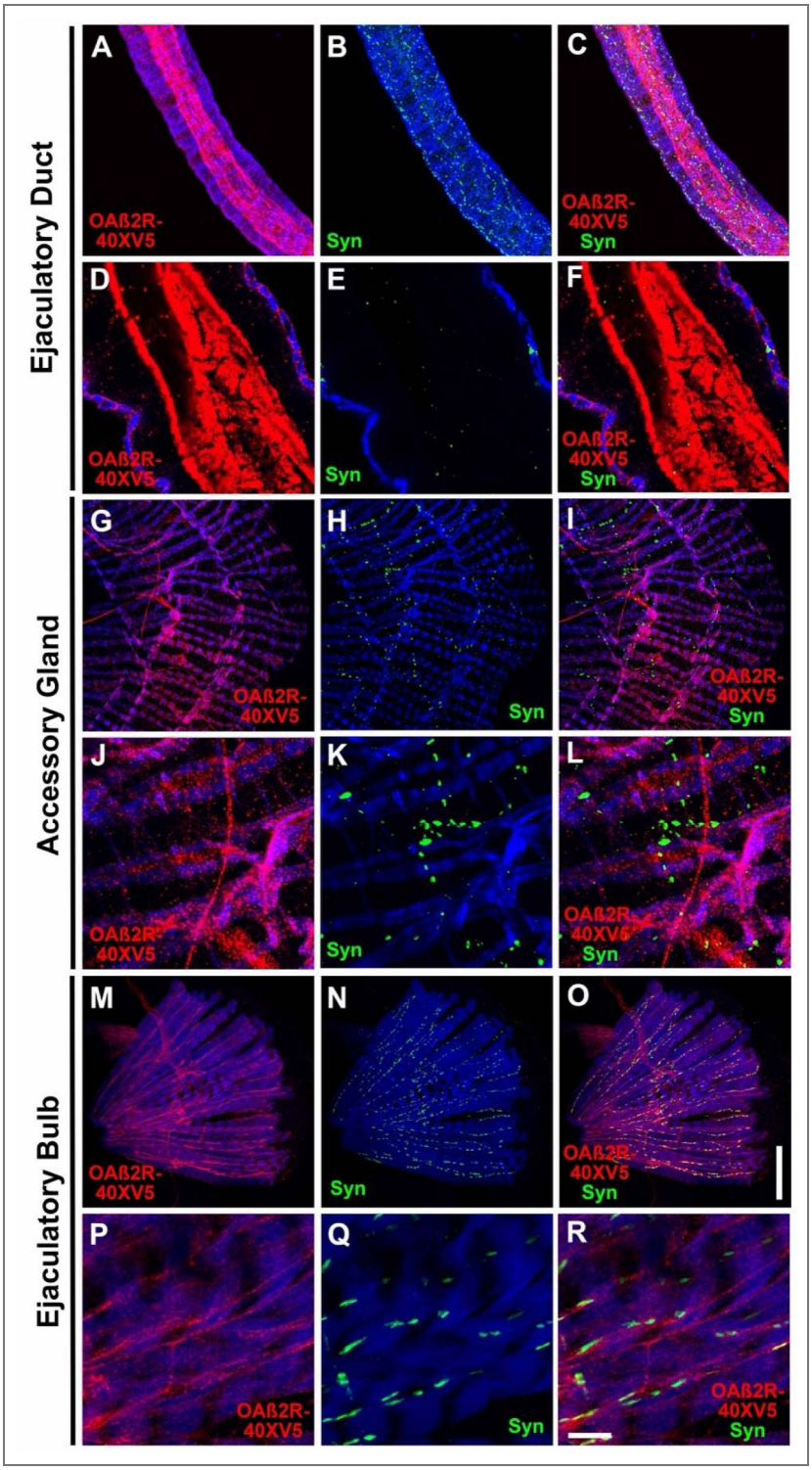

Figure 8S7. OAβ2R-40XV5 expression in the Drosophila male reproductive system.

A-C) Distal anterior ED. A) OAβ2R-40XV5; B) Syn; C) OAβ2R-40XV5, Syn overlay. D-F) Cross section of distal anterior ED. D) OAβ2R-40XV5; E) Syn; F) OAβ2R-40XV5, Syn overlay. G-L) AG. G, J) OAβ2R-40XV5; H, K) Syn; I, L) OAβ2R-40XV5, Syn overlay. M-O) Ejaculatory bulb. M, O) OAβ2R-40XV5; N, Q) Syn; O, R) OAβ2R-40XV5, Syn overlay. Scale bars: O-50μm; R-10μm.

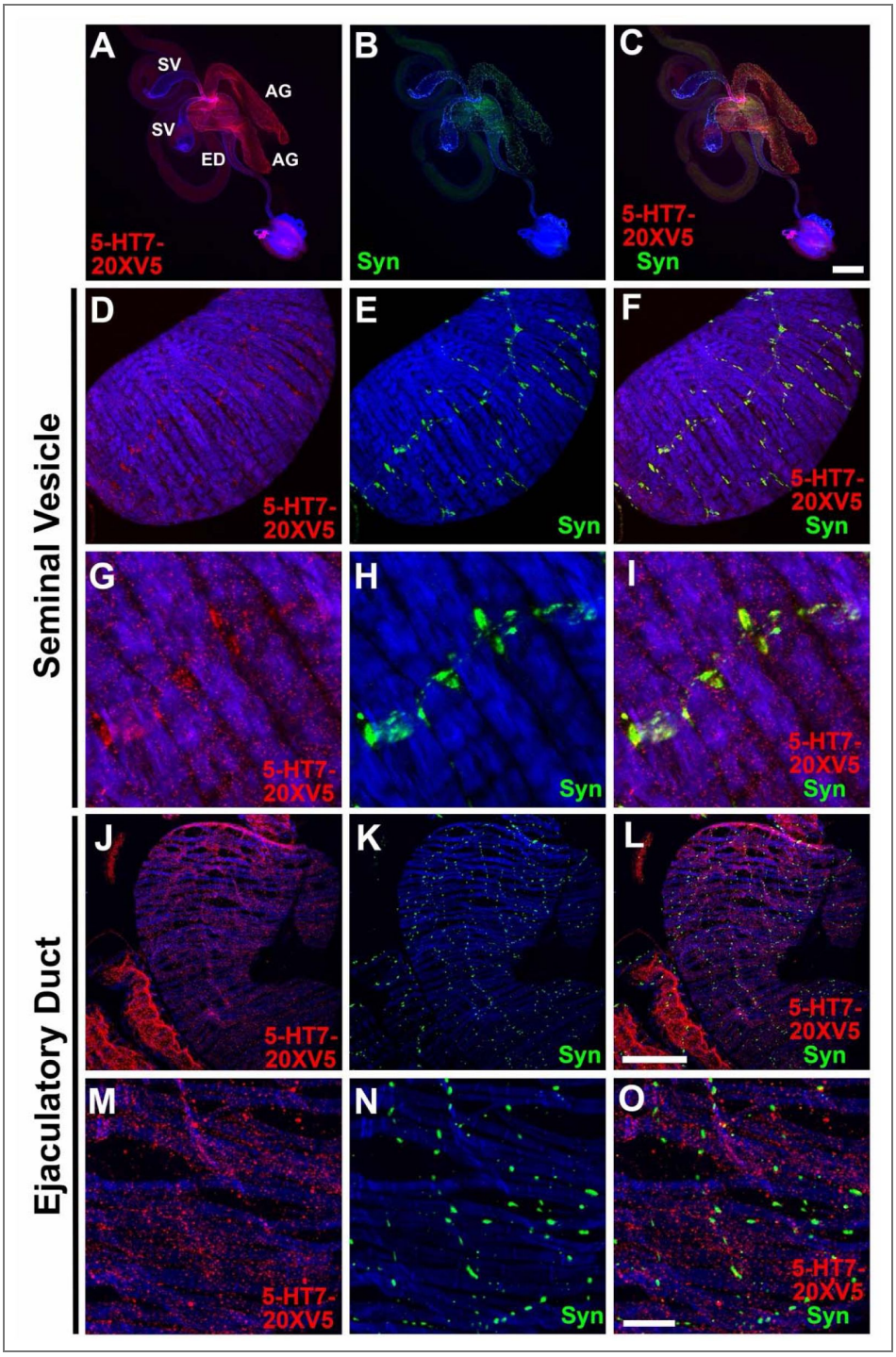

Figure 8S8. 5-HT7-20XV5 expression in the Drosophila male reproductive system.

A-C) Complete male reproductive system. A) 5-HT7-20XV5.; B) Syn; C) 5-HT7-20XV5, Syn overlay. D-I) SV. D, G) 5-HT7-20XV5.; E, H) Syn; F, I) 5-HT7-20XV5, Syn overlay. J-O) ED. J, M) 5-HT7-20XV5.; K, N) Syn; L, O) 5-HT7-20XV5, Syn overlay. Scale bars: C-200μm; L-50μm; O-10μm.

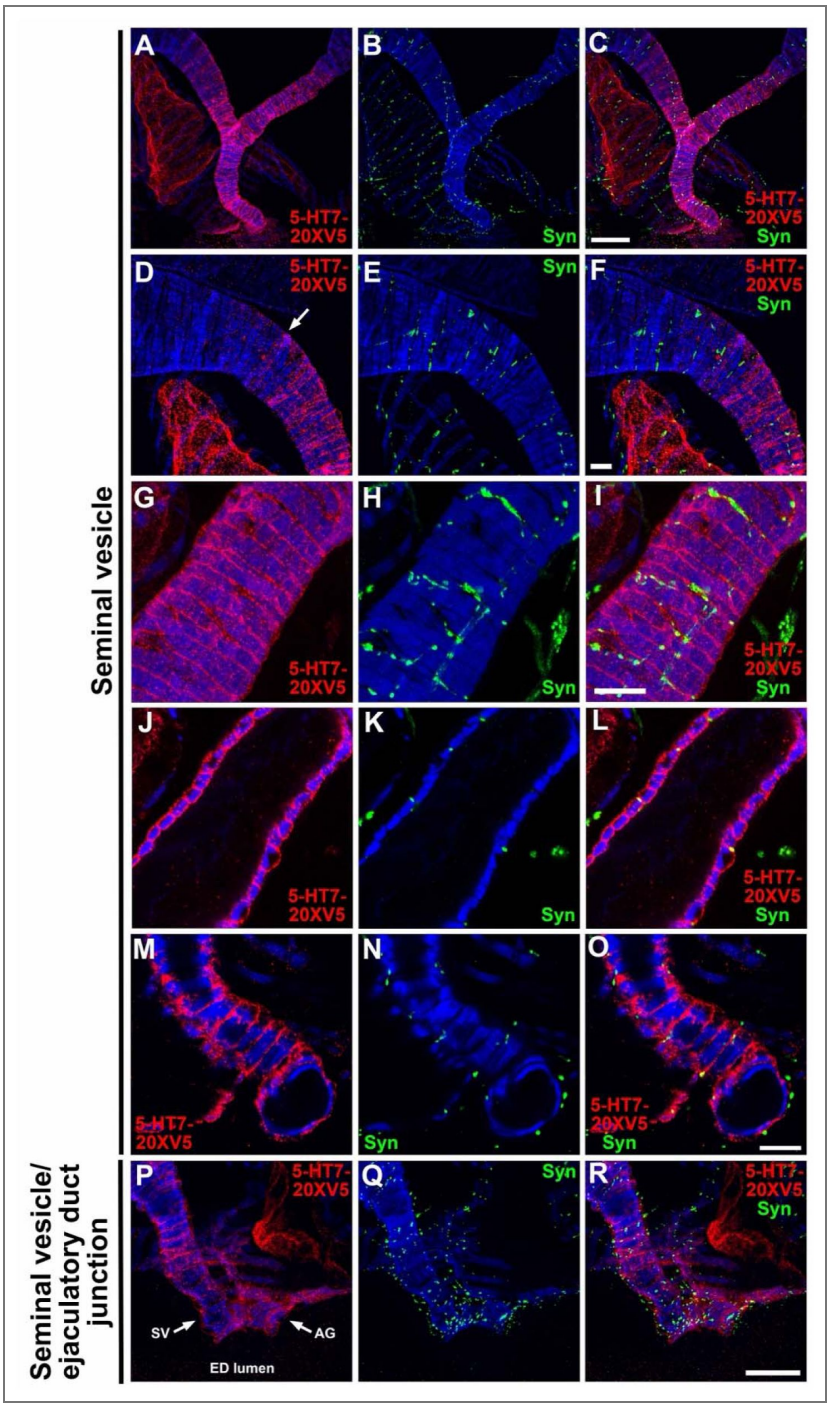

Figure 8S9. 5-HT7-20XV5 expression in the Drosophila male reproductive system.

A-I) SV. A, D, G,) 5-HT7-20XV5.; B, E, H,) Syn; C, F, I,) 5-HT7-20XV5, Syn overlay. J-L) Cross section of SV. J) 5-HT7-20XV5.; K) Syn; L) 5-HT7-20XV5, Syn overlay. M-O) SV terminus. M) 5-HT7-20XV5.; N) Syn; O) 5-HT7-20XV5, Syn overlay. P-R) SV/ED junction. P) 5-HT7-20XV5.; Q) Syn; R) 5-HT7-20XV5, Syn overlay. Scale bars: C, G-50μm; F, O-10μm; R-25μm.

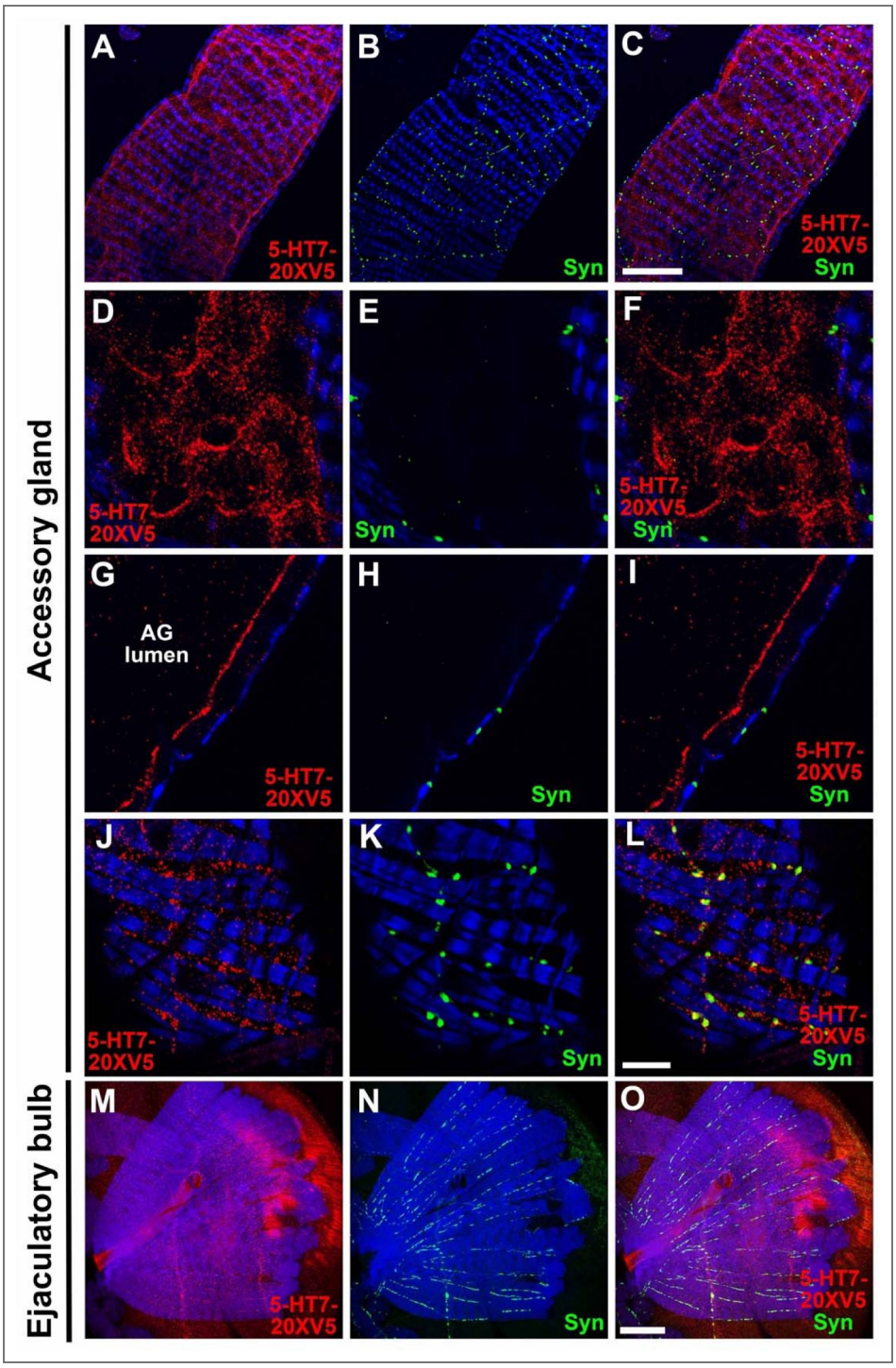

Figure 8S10. 5-HT7-20XV5 expression in the Drosophila male reproductive system.

A-C) AG. A) 5-HT7-20XV5.; B) Syn; C) 5-HT7-20XV5, Syn overlay. D-F) Epithelial layer of AG. D) 5-HT7-20XV5.; E) Syn; F) 5-HT7-20XV5, Syn overlay. G-I) Cross-section of epithelial layer of AG. G) 5-HT7-20XV5.; H) Syn; I) 5-HT7-20XV5, Syn overlay. J-L) Muscle layer of AG. J) 5-HT7-20XV5.; K) Syn; L) 5-HT7-20XV5, Syn overlay. M-O) Ejaculatory bulb. M) 5-HT7-20XV5.; N) Syn; O) 5-HT7-20XV5, Syn overlay. Scale bars: C, O-50μm; L-10μm.

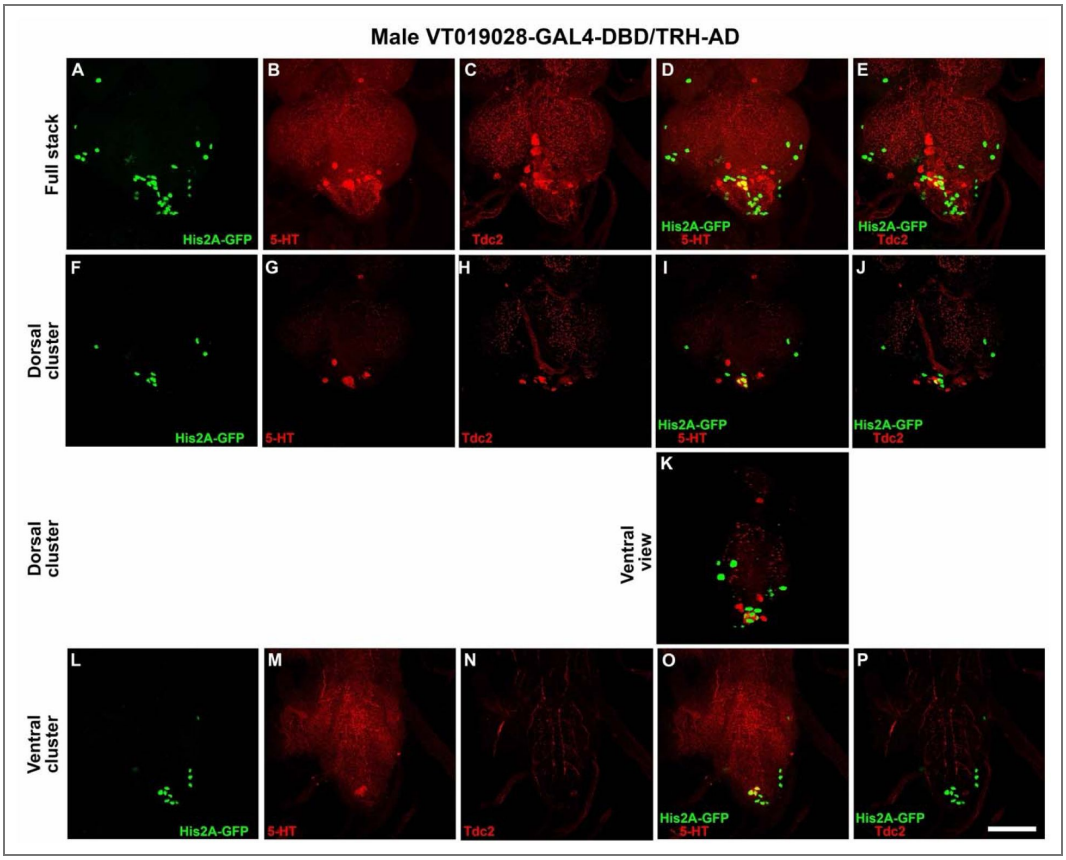

Figure 9S1. High resolution images of nuclear expression of *VT019028-GAL4-DBD* in combination with *TRH-AD* in posterior ventral nerve cord of Drosophila male adult nervous system relative to 5-HT and Tdc2.

A-E) Dorsal view of complete stack of confocal images. A) His2A-GFP; B) 5-HT; C) Tdc2; D) His2A-GFP, 5-HT overlay; E) His2A-GFP, Tdc2 overlay. F) Ventral view of His2A-GFP/5-HT overlay of subset of slices containing the dorsal cluster of 5-HT neurons; G-K) Dorsal view of subset of slices containing the dorsal cluster of 5-HT neurons. G) His2A-GFP; H) 5-HT; I) Tdc2; J) His2A-GFP, 5-HT overlay; K) His2A-GFP, Tdc2 overlay. L-P) Dorsal view of subset of slices containing the ventral cluster of 5-HT neurons. L) His2A-GFP; M) 5-HT; N) Tdc2; O) His2A-GFP, 5-HT overlay; P) His2A-GFP, Tdc2 overlay. Scale bar: 50μm.

Figure 9S2. High resolution images of nuclear expression of *VT019028-GAL4-DBD* in combination with *AbdB-AD* in posterior ventral nerve cord of Drosophila male adult nervous system relative to 5-HT and Tdc2.

A-E) Dorsal view of complete stack of confocal images. A) His2A-GFP; B) 5-HT; C) Tdc2; D) His2A-GFP, 5-HT overlay; E) His2A-GFP, Tdc2 overlay. F-J) Dorsal view of subset of slices containing the dorsal cluster of 5-HT neurons. F) His2A-GFP; G) 5-HT; H) Tdc2; I) His2A-GFP, 5-HT overlay; J) His2A-GFP, Tdc2 overlay. K-O) Dorsal view of subset of slices containing the ventral cluster of 5-HT neurons. K) His2A-GFP; L) 5-HT; M) Tdc2; N) His2A-GFP, 5-HT overlay; O) His2A-GFP, Tdc2 overlay. Scale bar: 50μm.

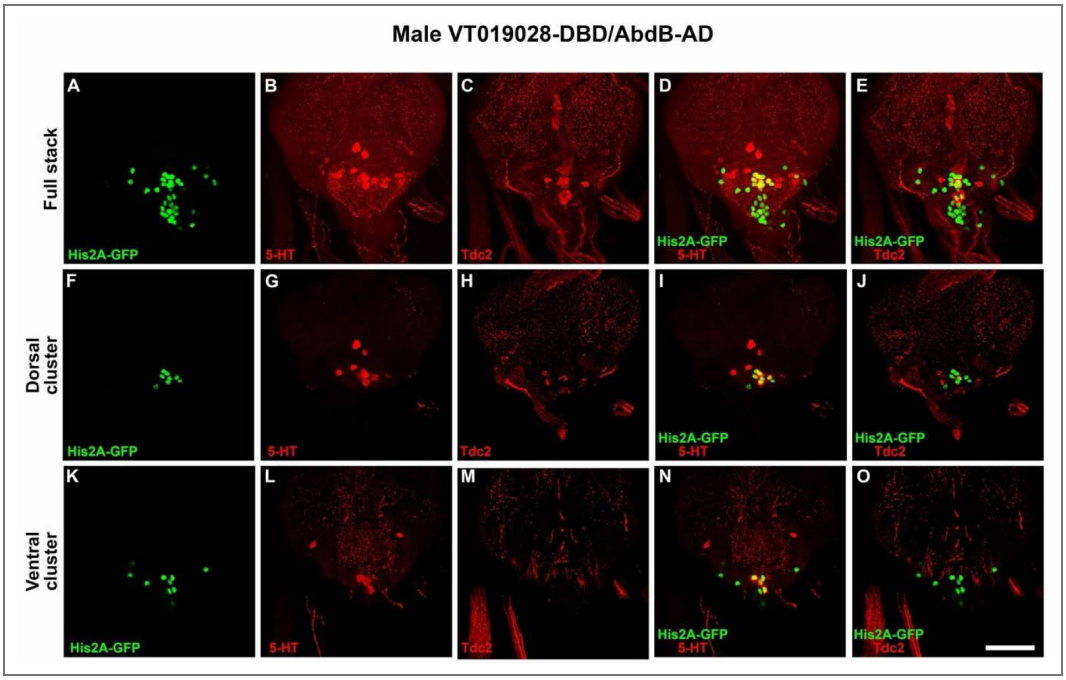

Figure 9S3. Male reproductive system expression of *VT019028-GAL4-DBD* in combination with *TRH-AD* and *AbdB-AD*.

A) *VT019028-GAL4-DBD* ∩ *TRH-AD*; B) *VT019028-GAL4-DBD* ∩ *AbdB-AD*. For both genotypes, there is broad innervation across the SV, AG, and ED. Scale bar: 200μm.

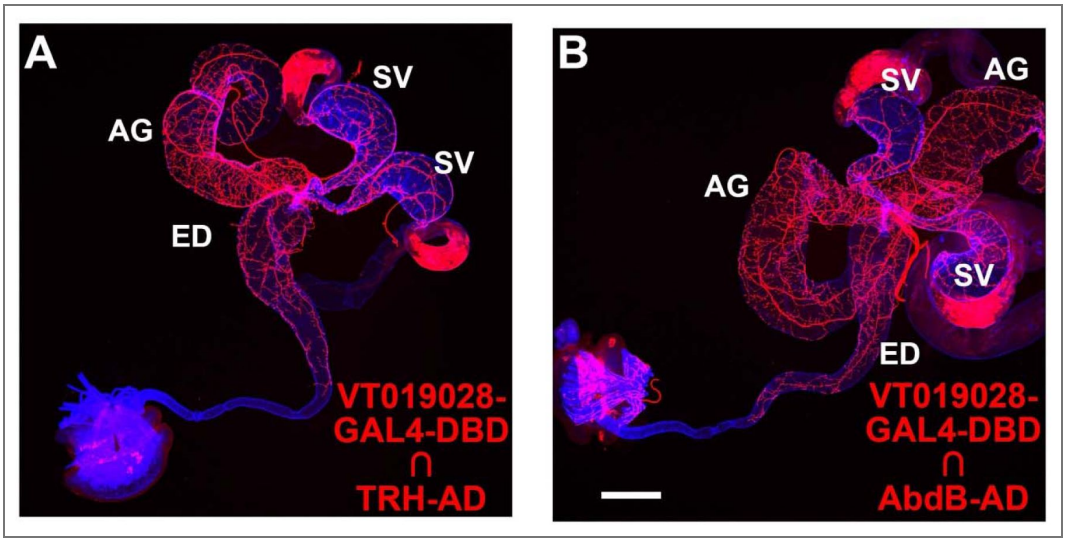

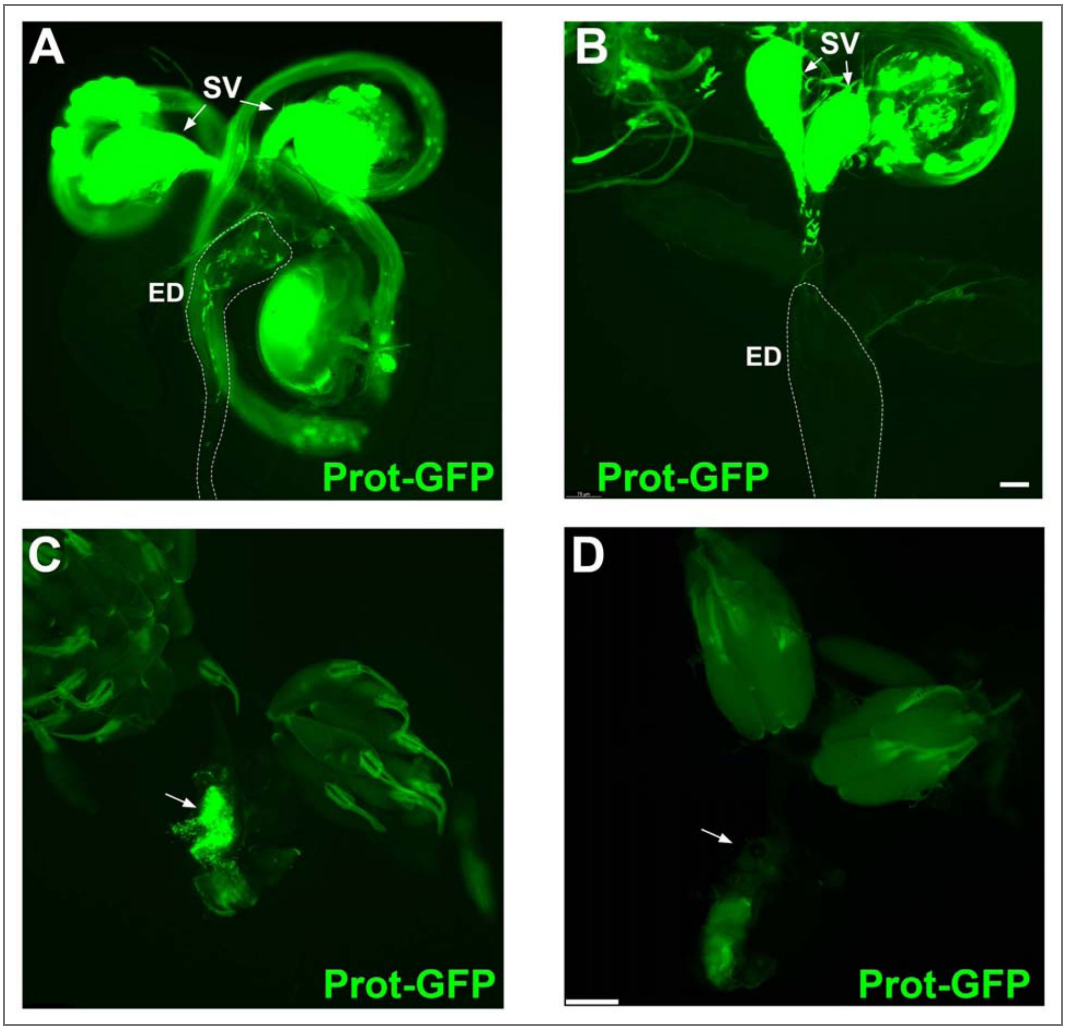

Figure 10S1. Prot-GFP fluorescent marker in male and female reproductive systems in control and *TRH-AD/VT019028-GAL4-DBD* neuron-silenced flies.

A) control. B) *TRH-AD/VT019028-GAL4-DBD* neurons silenced with BONT-C. Matings were interrupted 10 minutes after initiation. No Prot-GFP sperm is observed in the ejaculatory duct of the experimental male. C and D) Wildtype Canton-S female reproductive systems from completed matings to a C) control male; and D) *TRH-AD/VT019028-GAL4-DBD* male whose neurons were silenced with BONT-C. Abundant Prot-GFP sperm are observed in the mating to the control male (arrow), while no Prot-GFP sperm is observed in the female reproductive system after mating to the experimental male (arrow). Prot-GFP-Protamine GFP. SV-SV, ED-ED. Scale bars: A and B-75μm; C and D-200μm.

Figure 10S2. Comparison of male drosophila fecundity between genotypes.

Bar plots show the mean ± SD for each group with individual data points overlaid on each bar. Figure 10S1A males were aged 5 days before copulation. Figure 10S1B males were aged 30 days before copulation. (A) Columns from left to right: TRH ∩ VT019028 → vGlut-: n=34, mean=173.2, SD=24.22. AbdB ∩ TRH, Tdc2 → vGlut-: n=20, mean=175.3, SD=22.92. TRH ∩ VT019028: n=32, mean=149.0, SD=26.10. TRH: n=28, mean=172.8, SD=21.11. VT019028: n=25, mean=148.6, SD=20.81. (B) TRH ∩ VT019028 → vGlut-: n=14, mean=133.9, SD=37.64. TRH ∩ VT019028: n=19, mean=123.7, SD, 25.02. TRH: n=13, mean=106.3, SD=41.93. VT019028: n=9, mean=131.0, SD=38.88.

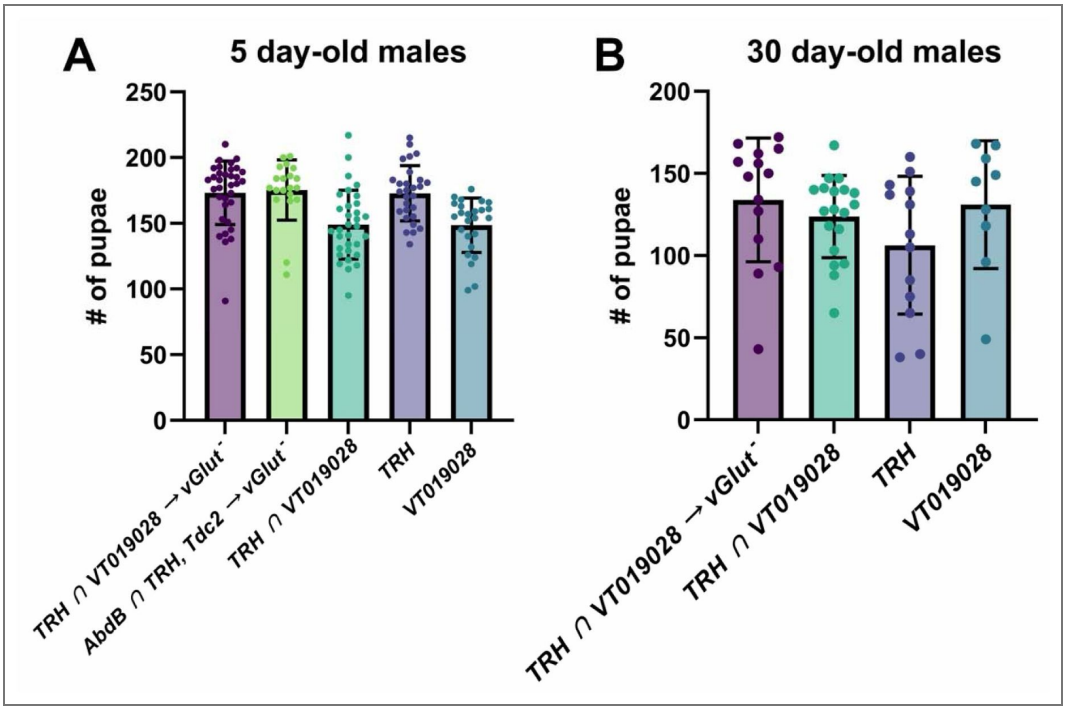

Figure 10S3. vGlut expression in AGs of control and vGlut conditional mutant.

A-C) control male. A) vGlut; B) 6XmCherry; C) overlay. D-F) experimental male conditionally silenced for vGlut in *TRH-AD/VT019028-GAL4* neurons. Scale bar: 50μm.

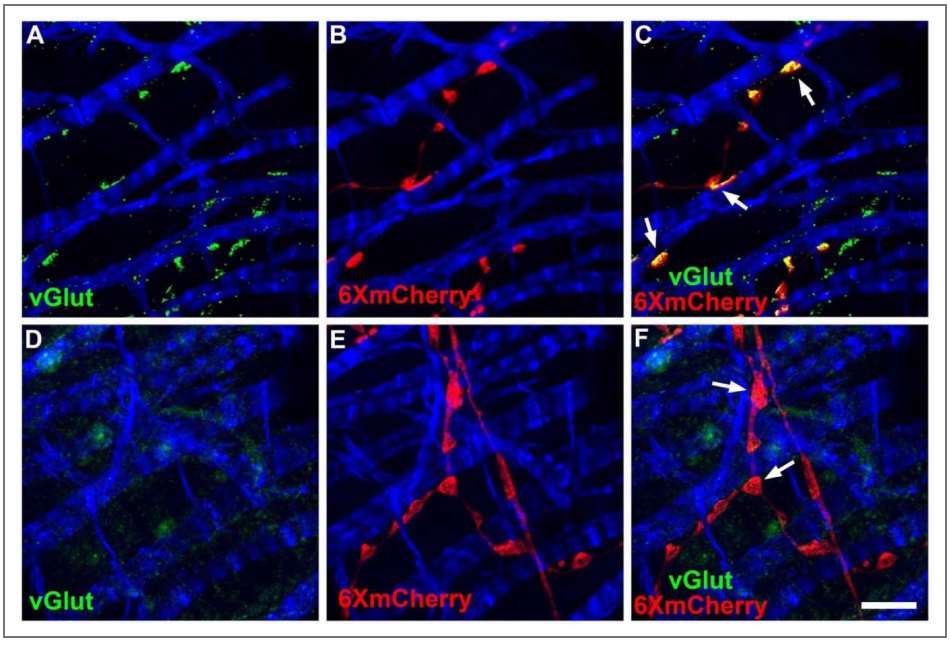

Data availability

All plasmids and their complete sequences are available upon request. Fly strains original to this publication will be deposited at the Bloomington Drosophila Stock Center or made available upon request.

Acknowledgements

Stocks obtained from the Bloomington Drosophila Stock Center (NIH P40OD018537) were used in this study. Antibodies used in this study were obtained from the Developmental Studies Hybridoma Bank created by the NICHD of the NIH and maintained at The University of Iowa, Department of Biology. This work used a Leica Stellaris DMI8 inverted confocal scanning light microscope in the Center for Biofilm Engineering-Bioimaging and Analytical Cores, *RRID:SCR_026519*, which is supported by Montana State University. This work was supported by National Institutes of Health (NIH) grant 2R01GM115510 to SJC and RSS.

Additional files

Video 1. Male reproductive system of a ProtB-GFP control. Sperm with green fluorescent nuclei are visible in the ejaculatory duct of a male subjected to a mid-mating interruption.

Video 2. Male reproductive system of a ProtB-GFP experimental male in which a subset of the *TRH-AD*/*VT019028-GAL4-DBD* subset of serotonergic neurons innervating the male reproductive system have been silenced. Sperm with green fluorescent nuclei are restricted to the seminal vesicle and never enter the ejaculatory duct from a male subjected to a mid-mating interruption.

Video 3. GCAMP8m Ca++ imaging of an ejaculatory duct experiencing spontaneous peristaltic waves of muscle contractions.

Video 4. GCAMP8m Ca++ imaging of the SV/ED junction showing the initiation site of the spontaneous peristaltic waves.

Video 5. GCAMP8m Ca++ imaging of the SV/ED junction showing the subtle variation in the initiation site of spontaneous peristaltic waves as compared to Video 4.

Video 6. GCAMP8m Ca++ imaging of the SV showing spontaneous uncoordinated muscle activity.

Video 7. GCAMP8m Ca++ imaging of an AG showing spontaneous uncoordinated muscle activity.

Video 8. GCAMP8m Ca++ imaging of a testes showing spontaneous uncoordinated muscle activity.

Video 9. GCAMP8m Ca++ imaging of the AG showing strong coordinated muscle activity.

Additional information

Funding

Funder	Grant reference number	Author
HHS | National Institutes of Health (NIH)	2R01GM115510	Sarah J CertelR Steven Stowers

Author ORCID iDs

R Steven Stowers: http://orcid.org/0000-0002-1473-2478

References

Abbe E (1873) Beitrage zur Theorie des microskops und der mikroskopischen Wahrnehmung. *Anatomie IX* 413-468

Acebes A., Grosjean Y., Everaerts C., Ferveur J. F. (2004) Cholinergic control of synchronized seminal emissions in Drosophila. *Curr Biol* **14**:704-710

Allen J. M., Adrian T. E., Tatemoto K., Polak J. M., Hughes J., et al. (1982) Two novel related peptides, neuropeptide Y (NPY) and peptide YY (PYY) inhibit the contraction of the electrically stimulated mouse vas deferens. *Neuropeptides* **3**:71-77

Alwaal A., Breyer B. N., Lue T. F. (2015) Normal male sexual function: emphasis on orgasm and ejaculation. *Fertil Steril* **104**:1051-1060

Bairati A (1968) [The structure and ultrastructure of the male genital apparatus of the Drosophila melanogaster Meig. 2. The genital duct and accessory glands]. *Italian Journal of Zoology* **2**:105-182

Baker C. A., Guan X. J., Choi M., Murthy M. (2024) The role of fruitless in specifying courtship behaviors across divergent Drosophila species. *Sci Adv* **10**:eadk1273

Bakshinska D., Liu W. Y., Schultz R., Stowers R. S., Hoagland A., et al. (2025) Synapse-specific catecholaminergic modulation of neuronal glutamate release. *Proc Natl Acad Sci U S A* **122**:e2420496121

Banerjee S., Vernon S., Jiao W., Choi B. J., Ruchti E., et al. (2021) Miniature neurotransmission is required to maintain Drosophila synaptic structures during ageing. *Nat Commun* **12**:4399

Beckers C. J., Mrestani A., Komma F., Dannhauser S. (2024) Versatile Endogenous Editing of GluRIIA in Drosophila melanogaster. *Cells* **13**

Beguelini M. R., Puga C. C. I., Martins F. F., Betoli A. H. S., Taboga S. R., et al. (2013) Morphological Variation of Primary Reproductive Structures in Males of Five Families of Neotropical Bats. *Anatomical Record-Advances in Integrative Anatomy and Evolutionary Biology* **296**:156-167

Billeter J. C., Goodwin S. F. (2004) Characterization of Drosophila fruitless-gal4 transgenes reveals expression in male-specific fruitless neurons and innervation of male reproductive structures. *J Comp Neurol* **475**:270-287

Billeter J. C., Rideout E. J., Dornan A. J., Goodwin S. F. (2006a) Control of male sexual behavior in Drosophila by the sex determination pathway. *Curr Biol* **16**:R766-776

Billeter J. C., Villella A., Allendorfer J. B., Dornan A. J., Richardson M., et al. (2006b) Isoform-specific control of male neuronal differentiation and behavior in Drosophila by the fruitless gene. *Curr Biol* **16**:1063-1076

Bretman A., Fricke C., Chapman T. (2009) Plastic responses of male Drosophila melanogaster to the level of sperm competition increase male reproductive fitness. *Proc Biol Sci* **276**:1705-1711

Brown G. L., Gillespie J. S. (1957) The output of sympathetic transmitter from the spleen of the cat. *J Physiol* **138**:81-102

Buck S. A., Rubin S. A., Kunkhyen T., Treiber C. D., Xue X., et al. (2023) Sexually dimorphic mechanisms of VGLUT-mediated protection from dopaminergic neurodegeneration. *bioRxiv*

Burnstock G (2009) Purinergic cotransmission. *Exp Physiol* **94**:20-24

Burnstock G (2014) Purinergic signalling in the reproductive system in health and disease. *Purinergic Signal* **10**:157-187

Carro-Juarez M., Cruz S. L., Rodriguez-Manzo G. (2003) Evidence for the involvement of a spinal pattern generator in the control of the genital motor pattern of ejaculation. *Brain Res* **975**:222-228

Carter D., Champney M., Hwang B., Eglen R. M. (1995) Characterization of a postjunctional 5-HT receptor mediating relaxation of guinea-pig isolated ileum. *Eur J Pharmacol* **280**:243-250

Castellanos M. C., Tang J. C., Allan D. W. (2013) Female-biased dimorphism underlies a female-specific role for post-embryonic Ilp7 neurons in Drosophila fertility. *Development* **140**:3915-3926

Certel S. J., McCabe B. D., Stowers R. S. (2022) A conditional GABAergic synaptic vesicle marker for Drosophila. *J Neurosci Methods* **372**:109540

Chan A. K., von der Weid P. Y. (2003) 5-HT decreases contractile and electrical activities in lymphatic vessels of the guinea-pig mesentery: role of 5-HT 7-receptors. *Br J Pharmacol* **139**:243-254

Chang Chien C. C., Hsin L. W., Su M. J. (2015) Activation of serotonin 5-HT(7) receptor induces coronary flow increase in isolated rat heart. *Eur J Pharmacol* **748**:68-75

Chehensse C., Facchinetti P., Bahrami S., Andrey P., Soler J. M., et al. (2017) Human spinal ejaculation generator. *Ann Neurol* **81**:35-45

Cizmar D., Roller L., Pillerova M., Slama K., Zitnan D. (2019) Multiple neuropeptides produced by sex-specific neurons control activity of the male accessory glands and gonoducts in the silkworm Bombyx mori. *Sci Rep* **9**:2253

Cole S. H., Carney G. E., McClung C. A., Willard S. S., Taylor B. J., et al. (2005) Two functional but noncomplementing Drosophila tyrosine decarboxylase genes: distinct roles for neural tyramine and octopamine in female fertility. *J Biol Chem* **280**:14948-14955

Crickmore M. A., Vosshall L. B. (2013) Opposing dopaminergic and GABAergic neurons control the duration and persistence of copulation in Drosophila. *Cell* **155**:881-893

Damstra H. G. J., Mohar B., Eddison M., Akhmanova A., Kapitein L. C., et al. (2023) Ten-fold Robust Expansion Microscopy. *Bio Protoc* **13**:e4698

DeLecce T., Vance G. S., Zeigler-Hill V., Welling L. L. M., Shackelford T. K. (2025) Ejaculate Adjustment in Response to Sperm Competition Risk in Humans. *Arch Sex Behav* **54**:277-287

Demerec M (1950) *Biology of Drosophila*. Wiley. *New York*

Deng B., Li Q., Liu X., Cao Y., Li B., et al. (2019) Chemoconnectomics: Mapping Chemical Transmission in Drosophila. *Neuron* **101**:876-893.

Deshpande S. A., Freyberg Z., Lawal H. O., Krantz D. E. (2020) Vesicular neurotransmitter transporters in Drosophila melanogaster. *Biochim Biophys Acta Biomembr* **1862**:183308

Deshpande S. A., Rohrbach E. W., Asuncion J. D., Harrigan J., Eamani A., et al. (2022) Regulation of Drosophila oviduct muscle contractility by octopamine. *iScience* **25**:104697

DiAntonio A (2006) Glutamate receptors at the Drosophila neuromuscular junction. *Int Rev Neurobiol* **75**:165-179

DiAntonio A., Petersen S. A., Heckmann M., Goodman C. S. (1999) Glutamate receptor expression regulates quantal size and quantal content at the Drosophila neuromuscular junction. *J Neurosci* **19**:3023-3032

Diao F., Ironfield H., Luan H., Diao F., Shropshire W. C., et al. (2015) Plug-and-play genetic access to drosophila cell types using exchangeable exon cassettes. *Cell Rep* **10**:1410-1421

Diao F., Vasudevan D., Heckscher E. S., White B. H. (2024) Hox gene-specific cellular targeting using split intein Trojan exons. *Proc Natl Acad Sci U S A* **121**:e2317083121

Dionne H., Hibbard K. L., Cavallaro A., Kao J. C., Rubin G. M. (2018) Genetic Reagents for Making Split-GAL4 Lines in Drosophila. *Genetics* **209**:31-35

Drobnis E. Z., Nangia A. K. (2017) Cardiovascular/Pulmonary Medications and Male Reproduction. *Adv Exp Med Biol* **1034**:103-130

Dwivedi S., Bautista M., Shrestha S., Elhasasna H., Chaphekar T., et al. (2021) Sympathetic signaling facilitates progression of neuroendocrine prostate cancer. *Cell Death Discov* **7**:364

Eberhard W. G (1985) *Sexual selection and animal genitalia* Cambridge, Mass: Harvard University Press.

Fisher Y. E., Yang H. H., Isaacman-Beck J., Xie M., Gohl D. M., et al. (2017) FlpStop, a tool for conditional gene control in Drosophila. *eLife* **6**

Fromme L., Yogui D. R., Alves M. H., Desbiez A. L. J., Langeheine M., et al. (2021) Morphology of the genital organs of male and female giant anteaters (). *Peerj* **9**

Gage M. J. G., Baker R. R. (1991) Ejaculate Size Varies with Sociosexual Situation in an Insect. *Ecological Entomology* **16**:331-337

Gao S., Takemura S. Y., Ting C. Y., Huang S., Lu Z., et al. (2008) The neural substrate of spectral preference in Drosophila. *Neuron* **60**:328-342

Garbaczewska M., Billeter J. C., Levine J. D. (2013) Drosophila melanogaster males increase the number of sperm in their ejaculate when perceiving rival males. *J Insect Physiol* **59**:306-310

Gilbert D. G (1981) Ejaculate Esterast 6 and Initial Sperm Use by Female Drosophila melanogaster. *Journal of Insect Physiology* **27**:641-650

Gomes L. F., Badke J. P., Zama U., Dolder H., Lino-Neto J. (2012) Morphology of the male reproductive system and spermatozoa in Centris Fabricius, 1804 (Hymenoptera: Apidae, Centridini). *Micron* **43**:695-704

Goulding M., Bourane S., Garcia-Campmany L., Dalet A., Koch S. (2014) Inhibition downunder: an update from the spinal cord. *Curr Opin Neurobiol* **26**:161-166

Gowda S. B. M., Paranjpe P. D., Reddy O. V., Thiagarajan D., Palliyil S., et al. (2018) GABAergic inhibition of leg motoneurons is required for normal walking behavior in freely moving Drosophila. *Proc Natl Acad Sci U S A* **115**:E2115-E2124

Guerrero S. M., Calderón M. L., de Pérez G. R., Pinilla M. P. R. (2004) Morphology of the male reproductive duct system of (Crocodylia, Alligatoridae). . *Annals of Anatomy-Anatomischer Anzeiger* **186**:235-245

Han Y., Chien C., Goel P., He K., Pinales C., et al. (2022) Botulinum neurotoxin accurately separates tonic vs. phasic transmission and reveals heterosynaptic plasticity rules in Drosophila. *eLife* **11**

He K., Dickman D. (2025) Building and modifying diverse synaptic properties: Insights from Drosophila. *Curr Opin Neurobiol* **92**:102995

Hiramoto A., Jonaitis J., Niki S., Kohsaka H., Fetter R. D., et al. (2021) Regulation of coordinated muscular relaxation in Drosophila larvae by a pattern-regulating intersegmental circuit. *Nat Commun* **12**:2943

Honda K., Miyata-Osawa A., Takenaka T. (1985) alpha 1-Adrenoceptor subtype mediating contraction of the smooth muscle in the lower urinary tract and prostate of rabbits. *Naunyn Schmiedebergs Arch Pharmacol* **330**:16-21

Hopkins B. R., Sepil I., Thezenas M. L., Craig J. F., Miller T., et al. (2019) Divergent allocation of sperm and the seminal proteome along a competition gradient in Drosophila melanogaster. *Proc Natl Acad Sci U S A* **116**:17925-17933

Inoue M., Kitazawa T., Cao J., Taneike T. (2003) 5-HT7 receptor-mediated relaxation of the oviduct in nonpregnant proestrus pigs. *Eur J Pharmacol* **461**:207-218

Jois S., Chan Y. B., Fernandez M. P., Leung A. K. (2018) Characterization of the Sexually Dimorphic fruitless Neurons That Regulate Copulation Duration. *Front Physiol* **9**:780

Kaufman B. P., Demerec M. (1942) Utilization of sperm by Female Drosophila Melanogaster. *The American Naturalist* **76**:445-469

Klagges B. R., Heimbeck G., Godenschwege T. A., Hofbauer A., Pflugfelder G. O., et al. (1996) Invertebrate synapsins: a single gene codes for several isoforms in Drosophila. *J Neurosci* **16**:3154-3165

Kreiner T., Sossin W., Scheller R. H. (1986) Localization of Aplysia neurosecretory peptides to multiple populations of dense core vesicles. *J Cell Biol* **102**:769-782

Lange A. B., Kisana A., Leyria J., Orchard I. (2023) The Male Reproductive System of the Kissing Bug, Rhodnius prolixus Stal, 1859 (Hemiptera: Reduviidae: Triatominae): Arrangements of the Muscles and the Myoactivity of the Selected Neuropeptides. *Insects* 14

Lee G., Hall J. C. (2001) Abnormalities of male-specific FRU protein and serotonin expression in the CNS of fruitless mutants in Drosophila. *J Neurosci* **21**:513-526

Lee P. T., Zirin J., Kanca O., Lin W. W., Schulze K. L., et al. (2018) A gene-specific T2A-GAL4 library for Drosophila. *eLife* **7**

Leung E., Walsh L. K., Pulido-Rios M. T., Eglen R. M. (1996) Characterization of putative 5-ht7 receptors mediating direct relaxation in Cynomolgus monkey isolated jugular vein. *Br J Pharmacol* **117**:926-930

Li-Kroeger D., Kanca O., Lee P. T., Cowan S., Lee M. T., et al. (2018) An expanded toolkit for gene tagging based on MiMIC and scarless CRISPR tagging in Drosophila. *eLife* **7**

Liao A., Cavigliasso F., Savary L., Kawecki T. J. (2024) Effects of an entomopathogenic fungus on the reproductive potential of Drosophila males. *Ecol Evol* **14**:e11242

Macartney E. L., Zeender V., Meena A., De Nardo A. N., Bonduriansky R., et al. (2021) Sperm depletion in relation to developmental nutrition and genotype in Drosophila melanogaster. *Evolution* **75**:2830-2841

Maciel E. D. S., Zieri R., de Almeida-Santos S. M. (2024) Male genital system of Ameiva ameiva (Squamata: Teiidae). *Anat Rec* **307**:3596-3605

Magnon C., Hall S. J., Lin J., Xue X., Gerber L., et al. (2013) Autonomic nerve development contributes to prostate cancer progression. *Science* **341**:1236361

Majane A. C., Cridland J. M., Begun D. J. (2022) Single-nucleus transcriptomes reveal evolutionary and functional properties of cell types in the Drosophila accessory gland. *Genetics* **220**

Manier M. K., Belote J. M., Berben K. S., Novikov D., Stuart W. T., et al. (2010) Resolving mechanisms of competitive fertilization success in Drosophila melanogaster. *Science* **328**:354-357

Marciniak P., Urbanski A., Kudlewska M., Szymczak M., Rosinski G. (2017) Peptide hormones regulate the physiological functions of reproductive organs in Tenebrio molitor males. *Peptides* **98**:35-42

Matsumoto-Miyai K., Yoshizumi M., Kawatani M. (2015) Regulatory Effects of 5-Hydroxytryptamine Receptors on Voiding Function. *Adv Ther* **32**:3-15

McCullough E. L., Whittington E., Singh A., Pitnick S., Wolfner M. F., et al. (2022) The life history of Drosophila sperm involves molecular continuity between male and female reproductive tracts. *Proc Natl Acad Sci U S A* **119**:e2119899119

McKinney H. M., Sherer L. M., Williams J. L., Certel S. J., Stowers R. S. (2020) Characterization of Drosophila octopamine receptor neuronal expression using MiMIC-converted Gal4 lines. *J Comp Neurol* **528**:2174-2194

Michel M. C., Vrydag W. (2006) Alpha1-, alpha2- and beta-adrenoceptors in the urinary bladder, urethra and prostate. *Br J Pharmacol* **147**:S88-119

Miyazaki T., Kobayashi H., Tosaka T. (1998) Presynaptic inhibition by noradrenaline of the EPSC evoked in neonatal rat sympathetic preganglionic neurons. *Brain Res* **790**:170-177

Moatt J. P., Dytham C., Thom M. D. (2014) Sperm production responds to perceived sperm competition risk in male Drosophila melanogaster. *Physiol Behav* **131**:111-114

Monastirioti M., Linn C. E., White K. (1996) Characterization of Drosophila tyramine beta-hydroxylase gene and isolation of mutant flies lacking octopamine. *J Neurosci* **16**:3900-3911

Norville K., Sweeney S. T., Elliott C. J. (2010) Postmating change in physiology of male Drosophila mediated by serotonin (5-HT). *J Neurogenet* **24**:27-32

O'Connor S. C., Brain K. L., Bennett M. R. (1999) Individual sympathetic varicosities possess different sensitivities to alpha 2 and P2 receptor agonists and antagonists in mouse vas deferens. *Br J Pharmacol* **128**:1739-1753

Oliveira M. S., Serrao J. E., Dias G., Martins L. C. B., Araújo V. A. (2021) Anatomy and histology of the male reproductive tractof Machtima crucigera (Fabricius, 1775) (Heteroptera: Coreidae). *Zoologischer Anzeiger* **293**:156-162

Parnas D., Haghighi A. P., Fetter R. D., Kim S. W., Goodman C. S. (2001) Regulation of postsynaptic structure and protein localization by the Rho-type guanine nucleotide exchange factor dPix. *Neuron* **32**:415-424

Pauls D., Blechschmidt C., Frantzmann F., El Jundi B., Selcho M. (2018) A comprehensive anatomical map of the peripheral octopaminergic/tyraminergic system of Drosophila melanogaster. *Sci Rep* **8**:15314

Pavlou H. J., Lin A. C., Neville M. C., Nojima T., Diao F., et al. (2016) Neural circuitry coordinating male copulation. *eLife* **5**

Pelletier G., Leclerc R. (1979) Localization of Leu-enkephalin in dense core vesicles of axon terminals. *Neurosci Lett* **12**:159-163

Petersen L. K., Stowers R. S. (2011) A Gateway MultiSite recombination cloning toolkit. *PLoS One* **6**:e24531

Pizzari T., Cornwallis C. K., Lovlie H., Jakobsson S., Birkhead T. R. (2003) Sophisticated sperm allocation in male fowl. *Nature* **426**:70-74

Port F., Chen H. M., Lee T., Bullock S. L. (2014) Optimized CRISPR/Cas tools for efficient germline and somatic genome engineering in Drosophila. *Proc Natl Acad Sci U S A* **111**:E2967-2976

Pound N., Gage M. J. G. (2004) Prudent sperm allocation in Norway rats, :: a mammalian model of adaptive ejaculate adjustment. *Animal Behaviour* **68**:819-823

Prins N. H., Briejer M. R., Van Bergen P. J., Akkermans L. M., Schuurkes J. A. (1999) Evidence for 5-HT7 receptors mediating relaxation of human colonic circular smooth muscle. *Br J Pharmacol* **128**:849-852

Qi Y. X., Xu G., Gu G. X., Mao F., Ye G. Y., et al. (2017) A new Drosophila octopamine receptor responds to serotonin. *Insect Biochem Mol Biol* **90**:61-70

Recio P., Barahona M. V., Orensanz L. M., Bustamante S., Martinez A. C., et al. (2009) 5-hydroxytryptamine induced relaxation in the pig urinary bladder neck. *Br J Pharmacol* **157**:271-280

Rohrbach E. W., Asuncion J. D., Meera P., Kralovec M., Deshpande S. A., et al. (2024a) Heterogeneity in the projections and excitability of tyraminergic/octopaminergic neurons that innervate the Drosophila reproductive tract. *Front Mol Neurosci* **17**:1374896

Rohrbach E. W., Knapp E. M., Deshpande S. A., Krantz D. E. (2024b) Expression and potential regulatory functions of Drosophila octopamine receptors in the female reproductive tract. *G3 (Bethesda)* 14

Scheibner J., Trendelenburg A. U., Hein L., Starke K. (2001) Stimulation frequency-noradrenaline release relationships examined in alpha2A-, alpha2B-and alpha2C-adrenoceptor-deficient mice. *Naunyn Schmiedebergs Arch Pharmacol* **364**:321-328

Schindelin J., Arganda-Carreras I., Frise E., Kaynig V., Longair M., et al. (2012) Fiji: an open-source platform for biological-image analysis. *Nat Methods* **9**:676-682

Segawa T., Murakami H., Ogawa H., Yajima H. (1978) Effect of enkephalin and substance P on sympathetic nerve transmission in mouse vas deferens. *Jpn J Pharmacol* **28**:13-19

Sepil I., Hopkins B. R., Dean R., Thezenas M. L., Charles P. D., et al. (2019) Quantitative Proteomics Identification of Seminal Fluid Proteins in Male Drosophila melanogaster. *Mol Cell Proteomics* **18**:S46-S58

Shearin H. K., Dvarishkis A. R., Kozeluh C. D., Stowers R. S. (2013) Expansion of the gateway multisite recombination cloning toolkit. *PLoS One* **8**:e77724

Shearin H. K., Macdonald I. S., Spector L. P., Stowers R. S. (2014) Hexameric GFP and mCherry reporters for the Drosophila GAL4, Q, and LexA transcription systems. *Genetics* **196**:951-960

Shen H., Marino R. A. M., McDevitt R. A., Bi G. H., Chen K., et al. (2018) Genetic deletion of vesicular glutamate transporter in dopamine neurons increases vulnerability to MPTP-induced neurotoxicity in mice. *Proc Natl Acad Sci U S A* **115**:E11532-E11541

Sherer L. M., Catudio Garrett E., Morgan H. R., Brewer E. D., Sirrs L. A., et al. (2020) Octopamine neuron dependent aggression requires dVGLUT from dual-transmitting neurons. *PLoS Genet* **16**:e1008609

Shirangi T. R., Wong A. M., Truman J. W., Stern D. L. (2016) Doublesex Regulates the Connectivity of a Neural Circuit Controlling Drosophila Male Courtship Song. *Dev Cell* **37**:533-544

Siwicki K. K., Kravitz E. A. (2009) Fruitless, doublesex and the genetics of social behavior in Drosophila melanogaster. *Curr Opin Neurobiol* **19**:200-206

Somogyi G. T., de Groat W. C. (1990) Modulation of the release of [3H]norepinephrine from the base and body of the rat urinary bladder by endogenous adrenergic and cholinergic mechanisms. *J Pharmacol Exp Ther* **255**:204-210

Soni K. K., Jeong H. S., Jang S. (2022) Neurons for Ejaculation and Factors Affecting Ejaculation. *Biology* **11**

Starke K (1972) Alpha sympathomimetic inhibition of adrenergic and cholinergic transmission in the rabbit heart. *Naunyn Schmiedebergs Arch Pharmacol* **274**:18-45

Stowers R. S (2025) Multimerized Epitope Tags for High Sensitivity Protein Detection. *G3 (Bethesda)*

Susic-Jung L., Hornbruch-Freitag C., Kuckwa J., Rexer K. H., Lammel U., et al. (2012) Multinucleated smooth muscles and mononucleated as well as multinucleated striated muscles develop during establishment of the male reproductive organs of Drosophila melanogaster. *Dev Biol* **370**:86-97

Tainio H (1995) Peptidergic innervation of the human prostate, seminal vesicle and vas deferens. *Acta Histochem* **97**:113-119

Tayler T. D., Pacheco D. A., Hergarden A. C., Murthy M., Anderson D. J. (2012) A neuropeptide circuit that coordinates sperm transfer and copulation duration in Drosophila. *Proc Natl Acad Sci U S A* **109**:20697-20702

Tison K. V., McKinney H. M., Stowers R. S. (2020) Demonstration of a Simple Epitope Tag Multimerization Strategy for Enhancing the Sensitivity of Protein Detection Using Drosophila vAChT. *G3 (Bethesda)* 10

Tomas A. L., Bento M. A. G., Mutti L. D., Zara F. J., Greco L. S. L. (2019) New insights in the male anatomy, spermatophore formation, and sperm structure in Atyidae: The red cherry shrimp. *Invertebrate Biology* **138**:17-28

Trendelenburg A. U., Meyer A., Klebroff W., Guimaraes S., Starke K. (2003) Crosstalk between presynaptic angiotensin receptors, bradykinin receptors and alpha 2-autoreceptors in sympathetic neurons: a study in alpha 2-adrenoceptor-deficient mice. *Br J Pharmacol* **138**:1389-1402

Trendelenburg A. U., Starke K., Limberger N. (1994) Presynaptic alpha 2A-adrenoceptors inhibit the release of endogenous dopamine in rabbit caudate nucleus slices. *Naunyn Schmiedebergs Arch Pharmacol* **350**:473-481

Truitt W. A., Coolen L. M. (2002) Identification of a potential ejaculation generator in the spinal cord. *Science* **297**:1566-1569

Verhulst E. C., van de Zande L. (2015) Double nexus--Doublesex is the connecting element in sex determination. *Brief Funct Genomics* **14**:396-406

Villella A., Hall J. C. (2008) Neurogenetics of courtship and mating in Drosophila. *Adv Genet* **62**:67-184

Wedell N., Cook P. A. (1999) Butterflies tailor their ejaculate in response to sperm competition risk and intensity. *Proceedings of the Royal Society B-Biological Sciences* **266**:1033-1039

Wigby S., Brown N. C., Allen S. E., Misra S., Sitnik J. L., et al. (2020) The Drosophila seminal proteome and its role in postcopulatory sexual selection. *Philos Trans R Soc Lond B Biol Sci* **375**:20200072

Williams J. L., Shearin H. K., Stowers R. S. (2019) Conditional Synaptic Vesicle Markers for Drosophila. *G3 (Bethesda)* **9**:737-748

Wolfner M. F (1997) Tokens of love: functions and regulation of Drosophila male accessory gland products. *Insect Biochem Mol Biol* **27**:179-192

Wong R., Lange A. B. (2014) Octopamine modulates a central pattern generator associated with egg-laying in the locust, Locusta migratoria. *J Insect Physiol* **63**:1-8

Wuest M., Eichhorn B., Grimm M. O., Wirth M. P., Ravens U., et al. (2009) Catecholamines relax detrusor through beta 2-adrenoceptors in mouse and beta 3-adrenoceptors in man. *J Pharmacol Exp Ther* **328**:213-222

Yamamoto D (2007) The neural and genetic substrates of sexual behavior in Drosophila. *Adv Genet* **59**:39-66

Yartsev V. V., Evseeva S. S. (2021) The Male Urogenital System of a Salamander (Amphibia, Caudata). *Current Herpetology* **40**:10-21

Yu J., Zhang Y., Clements K., Chen N., Griffith L. C. (2025) Genetically-encoded markers for confocal visualization of single dense core vesicles. *Commun Biol* **8**:383

Zhang Y., Rozsa M., Liang Y., Bushey D., Wei Z., et al. (2023) Fast and sensitive GCaMP calcium indicators for imaging neural populations. *Nature* **615**:884-891

Peer reviews

Reviewer #1 (Public review):

Summary:

This very thorough anatomical study addresses the innervation of the Drosophila male reproductive tract. Two distinct glutamatergic neuron types were classified: serotonergic (SGNs) and octopaminergic (OGNs). By expansion microscopy, it was established that glutamate and serotonin /octopamine are co-released. The expression of different receptors for 5-HT and OA in muscles and epithelial cells of the innervation target organs was characterized. The pattern of neurotransmitter receptor expression in the target organs suggests that seminal fluid and sperm transport and emission are subjected to complex regulation. While silencing of abdominal SGNs leads to male infertility and prevents sperm from entering the ejaculatory duct, silencing of OGNs does not render males infertile.

Strengths:

The studied neurons were analysed with different transgenes and methods, as well as antibodies against neurotransmitter synthesis enzymes, building a consistent picture of their neurotransmitter identity. The careful anatomical description of innervation patterns together with receptor expression patterns if the target organs provides a solid basis for advancing the understanding how seminal fluid and sperm transport and emission are subjected to complex regulation. The functional data showing that SGNs are required for male fertility and for the release of sperm from the seminal vesicle into the ejaculatory duct is convincing.

Weaknesses:

The functional analysis of the characterized neurons is not as comprehensive as the anatomical description and phenotypic characterization was limited to simple fertility assays. It is understandable that a full functional dissection is beyond the scope of the present work. The paper contains experiments showing neuron-independent peristaltic waves in the reproductive tract muscles, which are thematically not very well integrated into the paper. Although very interesting, one wonders if these experiments would not fit better into a future work that also explores these peristaltic waves and their interrelation with neuromodulation mechanistically.

Comments on revisions:

The manuscript has improved after fixing many small issues/errors. The new sections in the discussion are likewise adding to the quality of the manuscript.

https://doi.org/10.7554/eLife.108225.2.sa3

Reviewer #2 (Public review):

Summary:

Cheverra et al. present a comprehensive anatomical and functional analysis of the motor neurons innervating the male reproductive tract in Drosophila melanogaster, addressing a gap in our understanding of the peripheral circuits underlying ejaculation and male fertility. They identify two classes of multi-transmitter motor neurons-OGNs (octopamine/glutamate) and SGNs (serotonin/glutamate)-with distinct innervation patterns across reproductive organs. The authors further characterize the differential expression of glutamate, octopamine, and serotonin receptors in both epithelial and muscular tissues of these organs. Behavioral assays reveal that SGNs are essential for male fertility, whereas OGNs and glutamatergic transmission are dispensable. This work provides a high-resolution map linking neuromodulatory identity to organ-specific motor control, offering a valuable framework to explore the neural basis of male reproductive function.

Strengths:

Through the use of an extensive set of GAL4 drivers and antibodies, this work successfully and precisely defines the neurons that innervate the male reproductive tract, identifying the specific organs they target and the nature of the neurotransmitters they release. It also characterizes the expression patterns and localization of the corresponding neurotransmitter receptors across different tissues. The authors describe two distinct groups of dual-identity neurons innervating the male reproductive tract: OGNs, which co-express octopamine and glutamate, and SGNs, which co-express serotonin and glutamate. They further demonstrate that the various organs within the male reproductive system differentially express receptors for these neurotransmitters. Based on these findings, the authors propose that a single neuron capable of co-releasing a fast-acting neurotransmitter along side a slower-acting one may more effectively synchronize and stagger events that require precise timing. This, together with the differential expression of ionotropic glutamate receptors and metabotropic aminergic receptors in postsynaptic muscle tissue, adds an additional layer of complexity to the coordinated regulation of fluid secretion, organ contractility, and directional sperm movement-all contributing to the optimization of male fertility.

Weaknesses:

One potential limitation of the study is the absence of information regarding the number of individuals examined for the various characterizations, which may weaken the strength of the conclusions. Another limitation may be the lack of quantitative analyses in the colocalization and morphological differentiation experiments. Nevertheless, the authors have indicated that such quantifications will be provided in a forthcoming publication; therefore, this should be considered only a partial limitation, as it is expected to be addressed in the near future.

Wider context:

This study delivers the first detailed anatomical map connecting multi-transmitter motor neurons with specific male reproductive structures. It highlights a previously unrecognized functional specialization between serotonergic and octopaminergic pathways and lays the groundwork for exploring fundamental neural mechanisms that regulate ejaculation and fertility in males. The principles uncovered here may help explain how males of Drosophila and other organisms adjust reproductive behaviors in response to environmental changes. Furthermore, by shedding light on how multi-transmitter systems operate in reproductive control, this model could provide insights into therapeutic targets for conditions such as male infertility and prostate cancer-where similar neuronal populations are involved in humans. Ultimately, this genetically accessible system serves as a powerful tool for uncovering how

multi-transmitter neurons orchestrate coordinated physiological actions necessary for the functioning of complex organs.

https://doi.org/10.7554/eLife.108225.2.sa2

Reviewer #3 (Public review):

Summary:

This work provides an overview of the motor neuron landscape in the male reproductive system. Some work had been done to elucidate the circuits of ejaculation in the spine, as well as, the cord but this work fills a gap of knowledge at the level of the reproductive organs. Using complementary approaches the authors show that there are two types of motor neurons that are mutually exclusive: neurons that co-express octopamine and glutamate and neurons that co-express serotonin and glutamate. They also show evidence that both types of neurons express large dense core vesicles indicating that neuropeptides play a role in male fertility. This paper provides a thorough characterization of expression of the different glutamate, octopamine and serotonin receptors in the different organs and tissues of the male reproductive system. The differential expression in different tissues and organs allows building initial theories on the control of emission and expulsion. Additionally, the authors characterize the expression of synaptic proteins and the neuromuscular junction sites. On a mechanistic level, the authors show that neither octopamine/glutamate neuron transmission nor glutamate transmission in serotonin/glutamate neurons are required for male fertility. This final result is quite surprising and opens up many questions on how ejaculation is coordinated.

Strengths:

This work fills an important gap on characterization of innervation of the male reproductive system by providing an extensive characterization of the motor neurons and the potential receptors of motor neuron release.The authors show convincing evidence of glutamate/monoamine co-release and of mutual exclusivity of serotonin/glutamate and octopamine/glutamate neurons.

Weaknesses:

The experiment looking at peristaltic waves in the male organs is missing labeling of the different regions and quantification of the observed waves.

https://doi.org/10.7554/eLife.108225.2.sa1

Author response:

The following is the authors' response to the original reviews.

> ***Reviewer #1 (Public review):***
>
> *Summary:*
>
> *This very thorough anatomical study addresses the innervation of the Drosophila male reproductive tract. Two distinct glutamatergic neuron types were classified: serotonergic (SGNs) and octopaminergic (OGNs). By expansion microscopy, it was established that glutamate and serotonin /octopamine are co-released. The expression of different receptors for 5-HT and OA in muscles and epithelial cells of the innervation target organs was characterized. The pattern of neurotransmitter receptor expression in the target organs suggests that seminal fluid and sperm transport and emission are subjected to complex regulation. While silencing of abdominal SGNs leads to male infertility and*

prevents sperm from entering the ejaculatory duct, silencing of OGNs does not render males infertile.

Strengths:

The studied neurons were analysed with different transgenes and methods, as well as antibodies against neurotransmitter synthesis enzymes, building a consistent picture of their neurotransmitter identity. The careful anatomical description of innervation patterns together with receptor expression patterns of the target organs provides a solid basis for advancing the understanding of how seminal fluid and sperm transport and emission are subjected to complex regulation. The functional data showing that SGNs are required for male fertility and for the release of sperm from the seminal vesicle into the ejaculatory duct is convincing.

Weaknesses:

The functional analysis of the characterized neurons is not as comprehensive as the anatomical description, and phenotypic characterization was limited to simple fertility assays. It is understandable that a full functional dissection is beyond the scope of the present work. The paper contains experiments showing neuron-independent peristaltic waves in the reproductive tract muscles, which are thematically not very well integrated into the paper. Although very interesting, one wonders if these experiments would not fit better into a future work that also explores these peristaltic waves and their interrelation with neuromodulation mechanistically.

Reviewer #2 (Public review):

Summary:

Cheverra et al. present a comprehensive anatomical and functional analysis of the motor neurons innervating the male reproductive tract in Drosophila melanogaster, addressing a gap in our understanding of the peripheral circuits underlying ejaculation and male fertility. They identify two classes of multi-transmitter motor neurons-OGNs (octopamine/glutamate) and SGNs (serotonin/glutamate)-with distinct innervation patterns across reproductive organs. The authors further characterize the differential expression of glutamate, octopamine, and serotonin receptors in both epithelial and muscular tissues of these organs. Behavioral assays reveal that SGNs are essential for male fertility, whereas OGNs and glutamatergic transmission are dispensable. This work provides a high-resolution map linking neuromodulatory identity to organ-specific motor control, offering a valuable framework to explore the neural basis of male reproductive function.

Strengths:

Through the use of an extensive set of GAL4 drivers and antibodies, this work successfully and precisely defines the neurons that innervate the male reproductive tract, identifying the specific organs they target and the nature of the neurotransmitters they release. It also characterizes the expression patterns and localization of the corresponding neurotransmitter receptors across different tissues. The authors describe two distinct groups of dual-identity neurons innervating the male reproductive tract: OGNs, which co-express octopamine and glutamate, and SGNs, which co-express serotonin and glutamate. They further demonstrate that the various organs within the male reproductive system differentially express receptors for these neurotransmitters. Based on these findings, the authors propose that a single neuron capable of co-releasing a fast-acting neurotransmitter alongside a slower-acting one may more effectively synchronize and stagger events that require precise timing. This, together with the differential expression of ionotropic glutamate receptors and metabotropic aminergic

receptors in postsynaptic muscle tissue, adds an additional layer of complexity to the coordinated regulation of fluid secretion, organ contractility, and directional sperm movement-all contributing to the optimization of male fertility.

Weaknesses:

The main weakness of the manuscript is the lack of detail in the presentation of the results. Specifically, all microscopy image figures are missing information about the number of samples (N), and in the case of colocalization experiments, quantitative analyses are not provided. Additionally, in the first behavioral section, it would be beneficial to complement the data table with figures similar to those presented later in the manuscript for consistency and clarity.

Wider context:

This study delivers the first detailed anatomical map connecting multi-transmitter motor neurons with specific male reproductive structures. It highlights a previously unrecognized functional specialization between serotonergic and octopaminergic pathways and lays the groundwork for exploring fundamental neural mechanisms that regulate ejaculation and fertility in males. The principles uncovered here may help explain how males of Drosophila and other organisms adjust reproductive behaviors in response to environmental changes. Furthermore, by shedding light on how multi-transmitter systems operate in reproductive control, this model could provide insights into therapeutic targets for conditions such as male infertility and prostate cancer, where similar neuronal populations are involved in humans. Ultimately, this genetically accessible system serves as a powerful tool for uncovering how multi-transmitter neurons orchestrate coordinated physiological actions necessary for the functioning of complex organs.

Reviewer #3 (Public review):

Summary:

This work provides an overview of the motor neuron landscape in the male reproductive system. Some work had been done to elucidate the circuits of ejaculation in the spine, as well as the cord, but this work fills a gap in knowledge at the level of the reproductive organs. Using complementary approaches, the authors show that there are two types of motor neurons that are mutually exclusive: neurons that co-express octopamine and glutamate and neurons that co-express serotonin and glutamate. They also show evidence that both types of neurons express large dense core vesicles, indicating that neuropeptides play a role in male fertility. This paper provides a thorough characterization of the expression of the different glutamate, octopamine, and serotonin receptors in the different organs and tissues of the male reproductive system. The differential expression in different tissues and organs allows building initial theories on the control of emission and expulsion. Additionally, the authors characterize the expression of synaptic proteins and the neuromuscular junction sites. On a mechanistic level, the authors show that neither octopamine/glutamate neuron transmission nor glutamate transmission in serotonin/glutamate neurons is required for male fertility. This final result is quite surprising and opens up many questions on how ejaculation is coordinated.

Strengths:

This work fills an important gap in the characterization of innervation of the male reproductive system by providing an extensive characterization of the motor neurons and the potential receptors of motor neuron release. The authors show convincing

> *evidence of glutamate/monoamine co-release and of mutual exclusivity of serotonin/glutamate and octopamine/glutamate neurons.*
>
> *Weaknesses:*
>
> *(1) Often, it is mentioned that the expression is higher or lower or regional without quantification or an indication of the number of samples analysed.*
>
> *(2) The experiment aimed at tracking sperm in the male reproductive system is difficult to interpret when it is not assessed whether ejaculation has occurred.*
>
> *(3) The experiment looking at peristaltic waves in the male organs is missing labeling of the different regions and quantification of the observed waves.*
>
> ***Recommendations for the authors:***
>
> ***Reviewer #1 (Recommendations for the authors):***
>
> *(1) While the peripheral innervations are very carefully described, it is not clear to which SGNs and OGNs (i.e., cell bodies in the central nervous system) these innervations belong. Are SV, AG, and ED innervated by branches of one neuron or by separate neurons? Multi-color flip-out experiments could provide an answer to this.*

We agree this is important and are planning these experiments for follow-up study.

> *(2) In contrast, for the analysis of the VT19028 split line (Figure 9), only vnc and cell body images are shown. How do the arborisations of these split combinations look in the periphery? Are the same reproductive organs innervated as shown in Figure 2?*

Figure 9S3 was inadvertently omitted from the initial submission. That figure is now included and shows that the VT019028 split broadly innervates the SV, AG, and ED.

> *(3) In the discussion, I think it would be helpful to offer some potential explanations for the role of octopaminergic and glutamatergic signaling. If not required for basic fertility, they probably have some other role.*

Thank you, we have included speculation in the Discussion section "Potential for adaptation to environment".

> *(4) Line 543: Figure 8S4 E, (not 8E).*

Correction made.

> ***Reviewer #2 (Recommendations for the authors):***
>
> *(1) Line 213-217*
>
> *Comment:*
>
> *The use of "significantly less expression" may be misleading, as no quantification or statistical analysis is provided to support this comparison.*
>
> *Suggestion:*
>
> *Consider using a more neutral term, such as "markedly less" or "noticeably less," unless quantitative data and statistical analysis are included to substantiate the claim.*

Good recommendation.This suggestion has been incorporated.

> *(2) Line 264-267*

> *Comment:*
>
> *The observation regarding the distinct morphology of SGNs and OGNs is interesting and could strengthen the argument regarding functional differences.*
>
> *Suggestion:*
>
> *Consider including a quantification of morphological complexity (e.g., branching) to support the claim. A method such as Sholl analysis (Sholl, 1953), as adapted in Fernández et al., 2008, could be applied.*

This is a good suggestion, and we will consider it as part of a follow-up study.

> *(3) Line 269-271*
>
> *Comment:*
>
> *The anatomical context of the observation is not explicitly stated.*
>
> *Suggestion:*
>
> *Add "in the ED" for clarity: "With the TRH-GAL4 experiment in the ED, vGlut-40XMYC (Figure 5S1, A and E) and 6XV5-vMAT (Figure 5S1, B and F) were both present with a highly overlapping distribution (Figure 5S1, I)."*

Suggestion has been incorporated.

> *(4) Line 275-276*
>
> *Comment:*
>
> *The claim about the reduced ability to distinguish SGNs and OGNs in the ED would benefit from quantitative support.*
>
> *Suggestion:*
>
> *Include a morphological comparison or quantification between SGNs and OGNs in the ED and SV to reinforce this point.*

Certain information on morphological comparison can be inferred within the images themselves, and we will include quantitation in a follow-up study.

> *(5) Line 277-279*
>
> *Comment:*
>
> *As with line 269, the anatomical site could be specified more clearly.*
>
> *Suggestion:*
>
> *Rephrase as: "With the Tdc2-GAL4 experiment in the ED, vGlut-40XMYC (Figure 5S1, M and Q) and 6XV5-vMAT (Figure 5S1, N and R) were both observed in a highly overlapping distribution (Figure 5S1, U)."*

Suggestion has been incorporated.

> *(6) Line 348-350*
>
> *Comment:*

> *The phrase "significantly higher density" implies a statistical comparison that is not shown.*
>
> *Suggestion:*
>
> *If no quantification is provided, replace with a qualitative term such as "visibly higher" or "notably more dense." Alternatively, add a quantitative analysis with statistical testing to justify the use of "significantly."*

Suggestion has been incorporated.

> *(7) Lines 415-458 (Section comment)*
>
> *Comment:*
>
> *There appears to be differential localization of neurotransmitter receptor expression (glutamate in muscle vs. 5-HT in epithelium or neurons), which could have functional implications.*
>
> *Suggestion:*
>
> *Expand this section to briefly discuss the differential localization patterns of these receptors and potential implications for signal transduction in male reproductive tissues.*
>
> *(8) Lines 638-682 (Section comment)*
>
> *Comment:*
>
> *The table summarizing fertility phenotypes would be more informative with additional detail on experimental outcomes.*
>
> *Suggestion:*
>
> *Add a column showing the number of fertile males over the total tested (e.g., "n fertile / n total"). Also, clarify whether the fertility assays are identical to those reported in Figure 10S2, and whether similar analyses were conducted for females. Consider including a figure summarizing fertility results for all genotypes listed in the table, similar to Figure 10S2.*

The fertility tests reported in Table 1 were separate from those reported in Figure 10S2. For these tests, the results were clear-cut with 100% of males and females reported as infertile exhibiting the infertile phenotype. For the males and females reported as fertile, it was also clear-cut with nearly 100% showing fertility at a high level. In subsequent figures we attempted to assess degrees of fertility.

> *(9) Line 724-727*
>
> *Comment:*
>
> *There seems to be a mistake in the identification of the driver lines used to silence OA neurons. Also, figure references might be incorrect.*
>
> *Suggestion:*
>
> *The OA neuron driver line should be corrected to "Tdc2-GAL4-DBD ∩ AbdB-AD" instead of TRH-GAL4. Additionally, the figure references should be verified; specifically, the letter "B" (in "Figure 10B, D" and "10B, E") appears to be unnecessary or misplaced.*

Thanks for catching this, the corrections have been made.

> *(10) Line 872-877*
>
> *Comment:*
>
> *The discussion on the co-release of fast-acting glutamate and slower aminergic neurotransmitters is interesting and well-articulated. However, it remains somewhat disconnected from the behavioral findings.*
>
> *Suggestion:*
>
> *Consider linking this proposed mechanism to the results observed in the mating duration assays. For instance, the sequential action of neurotransmitters described here could potentially underlie the prolonged mating observed when specific neuromodulators are active, helping to functionally integrate molecular and behavioral data.*
>
> *(11) Line 926-928*
>
> *Comment:*
>
> *The interpretation of 5-HT7 receptor expression in the sphincter is compelling, suggesting a role in regulating its function. However, this anatomical observation could be further contextualized with the functional data.*
>
> *Suggestion:*
>
> *It may strengthen the interpretation to explicitly connect this finding with the fertility assays, where SGNs - presumably acting via serotonergic signaling - are shown to be necessary for male fertility. This would support a functional role for 5-HT7 in reproductive success via sphincter regulation.*

This has been added.

> *(12) Figure 1*
>
> *Comment:*
>
> *The figure legend is generally clear, but could benefit from more consistency and precision in the color-coded labeling. Additionally, the naming of some structures could be more explicit.*
>
> *Suggestion:*
>
> *Revise the figure and the legend as follows:*
>
> *Figure 1. The Drosophila male reproductive system. A) Schematic diagram showing paired testes (colour), SVs (green), AGs (purple), Sph (red), ED (gray), and EB (colour). B) Actual male reproductive system. Te - testes, SV - seminal vesicle, AG - accessory gland, Sph - singular sphincter, ED - ejaculatory duct, EB - ejaculatory bulb. Scale bar: 200 μm.*

This suggestion has been incorporated.

> *(13) Figure 3S2*
>
> *Comment:*
>
> *There appears to be a typographical error in the description of the genotypes, which may lead to confusion.*
>
> *Suggestion:*

> *Correct the legend to reflect the appropriate genotypes:*
>
> *Figure 3S2. Expression of vGlut-LexA and Tdc2-GAL4 in the Drosophila male reproductive system. A, D, G, J, M, P) vGlut-LexA, LexAop-6XmCherry; B, E, H, K, N, Q) Tdc2-GAL4, UAS-6XGFP; C, F, I, L, O, R) Overlay. Scale bars: O - 50 μm; R - 10 μm.*

The corrections have been made.

> *(14) Figure 3S3*
>
> *Comment:*
>
> *The genotypes for panels D and E appear to be incomplete; the DBD component of the split-GAL4 drivers is missing.*
>
> *Suggestion:*
>
> *Update the figure legend to:*
>
> *Figure 3S3. Fruitless and Doublesex expression in the Drosophila male reproductive system. A) fru-GAL4, UAS-6XGFP; B) vGlut-LexA, LexAop-6XmCherry; C) Overlay; D) Tdc2-AD ∩ dsx-GAL4-DBD; E) TRH-AD ∩ dsx-GAL4-DBD. Scale bar: 200 μm.*

The corrections have been made.

> *(15) Figure 4S4*
>
> *Comment:*
>
> *There is a repeated segment in the figure legend, which makes it unclear and redundant.*
>
> *Suggestion:*
>
> *Edit the legend to remove the duplicated lines:*
>
> *Figure 4S4. Expression of vGlut, TβH-GFP, and 5-HT at the junction of the SV and AGs with the ED of the Drosophila male reproductive system. A) vGlut-40XV5; B) TβH-GFP; C) 5-HT; D) vGlut-40XV5, TβH-GFP overlay; E) vGlut-40XV5, 5-HT overlay; F) TβH-GFP, 5-HT overlay. Scale bar: 50 μm.*

The correction has been made.

> *(16) Figure 6S5*
>
> *Comment:*
>
> *Within this figure, the orientation and/or scale of the tissue varies noticeably between individual panels, making it difficult to directly compare the different experimental conditions.*
>
> *Suggestion:*
>
> *For improved clarity and interpretability, consider standardizing the orientation and size of the tissue shown across all panels within the figure. Consistent presentation will facilitate direct comparisons between treatments or genotypes.*

There is often variation in the size of the male reproductive organs. They were all acquired at the same magnification. The only point of this figure is there is no vGAT or vAChT at these NMJs and the result is unambiguously negative.

> *(17) Figure 10*
>
> *Comment:*
>
> *Panel A appears redundant, as it shows the same information as the other panels but without indicating statistical significance.*
>
> *Suggestion:*
>
> *Consider removing panel A and keeping only the remaining four graphs, which include relevant statistical comparisons and clearly show significant differences.*

We realize there is some redundancy of panel A with the other panels, but we feel there is value in having all the genotypes in a single panel for comparison.

> ***Reviewer #3 (Recommendations for the authors):***
>
> *Here are some suggestions to improve the manuscript:*
>
> *(1) Prot B GFP experiment: the authors should explain better the time chosen to look at the sperm content of the male reproductive system. At 10 minutes, it is expected that the male has already ejaculated, and therefore, a failure to ejaculate would result in more sperm in the reproductive system, not less. Since we are not certain when the male ejaculates, it would be important to do the analysis at different time points.*

In the Prot-GFP experiments, the 10-minute time point was chosen because we nearly always observe sperm in the ejaculatory duct of control males. In the experimental males, we never observed sperm in the ejaculatory duct at this time point. Also, no Prot-GFP sperm were observed in the reproductive tract of females mated to experimental males even when mating was allowed to go to completion, while abundant sperm were found in females mated to Prot-GFP controls. Figure 10S1 has been updated to include Images of these female reproductive systems. The results showing the absence of Prot-GFP sperm in the female reproductive tract mated to experimental males indicates sperm transfer in these males isn't occurring earlier during the copulation process than in control males and that we didn't miss it by only examining at the ejaculatory duct.

> *(2) Discuss what may be the role of the octopamine/glutamate neurons and glutamate transmission in serotonin/glutamate neurons in the male reproductive system, given that they are not required for fertility (at least under the context in which it was tested). It is quite a striking result that deserves some attention.*

We agree it is a surprising result and have included speculation on the role of glutamate and octopamine in male reproduction in the Discussion section "Potential for adaptation to environment".

> *(3) Very important:*
>
> *(a) Figure 3 is present in the Word document but not the PDF.*
>
> *(b) Figure 9S3 is not present*
>
> *(c) In Figure 5 X), the legend does not correspond to the panel.*

All of these corrections have been made.

> *(4) Other suggestions:*
>
> *(a) A summary schematic (or several) of the findings would make it an easier read.*

(b) Explain why the ejaculatory bulb was left out of the analysis.

(c) Explain in the main text some of the tools, such as, BONT-C and the conditional vGlut mutation.

https://doi.org/10.7554/eLife.108225.2.sa0